DIFFERENTIAL GAME GUIDANCE VERSUS PROPORTIONAL NAVIGATION FOR AN AIR-TO-AIR MISSILE

Robin A. Poulter

Air Force Institute of Technology
Wright-Patterson Air Force Base, Ohio

December 1975

DIFFERENTIAL GAME GUIDANCE VERSUS PROPORTIONAL NAVIGATION FOR AN AIR-TO-AIR MISSILE

Thesis

GA/MC/75-5

Robin A. Poulter
Flt. Lt. RAF

Approved for public release; distribution unlimited.

Unclassified
SECURITY CLASSIFICATION OF THIS PAGE (When Data Entered)

REPORT DOCUMENTATION PAGE		READ INSTRUCTIONS BEFORE COMPLETING FORM
1. REPORT NUMBER GA/MC/75-5	2. GOVT ACCESSION NO.	3. RECIPIENT'S CATALOG NUMBER
4. TITLE (and Subtitle) DIFFERENTIAL GAME GUIDANCE VERSUS PROPORTIONAL NAVIGATION FOR AN AIR-TO-AIR MISSILE		5. TYPE OF REPORT & PERIOD COVERED AFIT Thesis 6. PERFORMING ORG. REPORT NUMBER
7. AUTHOR(s) Robin A. Poulter Flt. Lt RAF		8. CONTRACT OR GRANT NUMBER(s)
9. PERFORMING ORGANIZATION NAME AND ADDRESS Air Force Institute of Technology (AU) Wright-Patterson AFB, OH 45433		10. PROGRAM ELEMENT, PROJECT, TASK AREA & WORK UNIT NUMBERS
11. CONTROLLING OFFICE NAME AND ADDRESS		12. REPORT DATE December 1975 13. NUMBER OF PAGES 114
14. MONITORING AGENCY NAME & ADDRESS(if different from Controlling Office)		15. SECURITY CLASS. (of this report) 15a. DECLASSIFICATION/DOWNGRADING SCHEDULE

16. DISTRIBUTION STATEMENT (of this Report)

Approved for public release; distribution unlimited.

17. DISTRIBUTION STATEMENT (of the abstract entered in Block 20, if different from Report)

18. SUPPLEMENTARY NOTES

Approved for public release; IAW AFR 190-17

JERRY C. HIX, Captain, USAF
Director of Information

19. KEY WORDS (Continue on reverse side if necessary and identify by block number)

Game Theory
Differential Games
Air-to-Air Missiles
Missile Control

20. ABSTRACT (Continue on reverse side if necessary and identify by block number)

Proportional navigation is a closed loop optimal control for the case of a linear dynamic model of the air-to-air missile intercept problem and a quadratic cost function (Ref 6).

This paper presents a differential game model of the intercept problem using nonlinear realistic dynamics, free final time and a terminal cost function related to probability of kill. With this model proportional navigation is no longer optimal and

DD FORM 1 JAN 73 1473 EDITION OF 1 NOV 65 IS OBSOLETE

Unclassified
SECURITY CLASSIFICATION OF THIS PAGE (When Data Entered)

the extent of its nonoptimality is indicated for a range of saddle point solutions.

A guidance concept based on differential game theory is discussed and is compared to proportional navigation in an off line simulation. The considerable gains made by this scheme over proportional navigation provide the incentive to develop a real time version.

DIFFERENTIAL GAME GUIDANCE VERSUS PROPORTIONAL NAVIGATION FOR AN AIR-TO-AIR MISSILE

THESIS

Presented to the Faculty of the School of Engineering
of the Air Force Institute of Technology
Air University
in Partial Fulfillment of the
Requirements for the Degree of
Master of Science

by

Robin A. Poulter, B.Sc.(Hons)
Flight Lieutenant Royal Air Force
Graduate Astronautical Engineering

December 1975

Preface

Differential game models of realistic problems rarely lead to closed loop laws. Major G. M. Anderson of the Department of Mechanics has proposed a means of approximating the closed loop law based on updating the open loop law. This thesis is a result of my work investigating the applicability of his method to the air-to-air missile intercept problem using nonlinear dynamics.

I wish to acknowledge the assistance of Major Anderson both in the work on this thesis and in his sequences on Optimal Control. I would also like to thank Squadron Leader F. D. Reddyhof for his assistance with the missile model and the proportional navigation scheme.

Lastly, I wish to acknowledge the support of my family throughout my trials and tribulations.

Robin A. Poulter

Contents

List of Figures

List of Tables

Abstract

Proportional navigation is a closed loop optimal control for the case of a linear dynamic model of the air-to-air missile intercept problem and a quadratic cost function (Ref 6).

This paper presents a differential game model of the intercept problem using nonlinear realistic dynamics, free final time and a terminal cost function related to probability of kill. With this model proportional navigation is no longer optimal and the extent of its nonoptimality is indicated for a range of saddle point solutions.

A guidance concept based on differential game theory is discussed and is compared to proportional navigation in an off line simulation. The considerable gains made by this scheme over proportional navigation provide the incentive to develop a real time version.

DIFFERENTIAL GAME GUIDANCE VERSUS PROPORTIONAL NAVIGATION FOR AN AIR-TO-AIR MISSILE

I. Introduction

Background

Proportional navigation has been a major guidance law for some considerable time and at present there does not appear to be any viable replacement from either optimal control theory or differential game theory. Bryson and Ho (Ref 6:267) show that proportional navigation is an optimum guidance law for the simple case of linear dynamics and quadratic cost function where the evader is not maneuvering. Over the years fighter pilots have adopted tactis, based on experience, that capitalize on the shortcomings of proportional navigation.

Attempts have been made to devise closed loop control laws based on optimal control theory. Two such examples (Refs 5 and 7) use linear dynamics and a quadratic cost function and produced laws that require knowledge of the future tactics of the evader. However no allowance is made for the evaders desire to capitalize on the limitations of the missile and the errors in its prediction of the evaders controls.

Using differential game theory it is possible to include in the optimal control problem the evaders desire and possible capacity to escape interception. In theory, therefore, an optimum guidance law could be devised such that for given

launch conditions the probability of kill was some minimum value for the case of the optimum evader. Any nonoptimal tactics on the part of the evader could be converted into a higher predicted probability of kill by the closed loop optimal control.

The optimal controls, for a saddle point solution of a differential game model of the intercept problem, are defined in terms of a two point boundary value problem. For nonlinear dynamics the result is invariably an open loop control law based on the initial states. The only means of updating the optimal control scheme is by solving the two point boundary value problem at each instant to account for the nonoptimal play by the pursuer. A near optimal scheme may be possible by linearizing the dynamics of the states and costates about the nominal saddle point solution and periodically updating the costates. This was proposed by Anderson (Refs 1, 2, and 4) and has been shown to be near-optimal and real time for some simple problems where closed loop laws existed for comparison.

The principle drawback to the scheme at present is the computational burden in that numerical integration is required firstly to go forward to the predicted final range generating the nominal trajectory and then backwards from final time generating an "update" matrix until the backward integration meets current real time at which point the update is made. This procedure needs to be repeated often enough to keep the linearization assumption valid.

Unfortunately, for a realistic model not only is the dimension of the equations, that need to be integrated, quite high but also the amount of computation at each step is extensive.

Statement of the Problem

This scheme is not capable of being used real time at present on a small air-to-air missile but could be used in an off line simulation to indicate the possible performance of such a control scheme as compared with proportional navigation.

The aim of this thesis was to model the intercept problem in differential game theory as a zero sum, free final time, minimax range game with realistic dynamics and a cost function based on the final states. The saddle point optimality of differential games is valid for the case where at least one player has a continuously optimal control. Where both players play their open loop controls this condition is met but where either one deviates the open loop control is no longer optimal. By means of a Fortran subroutine (Ref 10) that solves a set of n nonlinear equations in n unknowns a program was to be developed to provide updates to the open loop controls by solving the two point boundary value problem at intervals throughout the interception. The continuously optimal controls of either pursuer or evader could then be approximated for the purposes of evaluating the performance of proportional navigation.

The following cases could then be studied:

(a) Optimal pursuer against optimal evader

(b) Proportional navigation against the open loop optimal evader of (a)

(c) Proportional navigation against updated optimal evader of (a)

(d) Updated optimal pursuer against nonoptimal evader

(e) Proportional navigation against the nonoptimal evader in (d).

Summary

The air-to-air missile interception of an aircraft is modelled as a two person, zero sum, minimax range differential game. Chapter II presents a brief discussion of game theory. Chapter III presents the model used for the intercept problem, based on a typical infrared seeking missile and a F4 type aircraft, and derives the optimal controls in terms of the states and costates together with the two point boundary value problem. Chapter III also presents the model used for proportional navigation. The results are presented in Chapter IV with examples of each of the cases discussed above.

II. Differential Game Theory

Problem Formulation

The mathematical elements of differential game theory comprise the state equations, a cost function, control or path constraints and a terminal surface. The vector differential equation describing the motion of the two vehicles is

$$\dot{x} = f(x,u,v,t) \quad x(t_0) = x_0 \tag{2-1}$$

where u is the control vector of the pursuer and v the control vector of the evader. The cost function in its general form is

$$J = \phi(x,t)\Big|_{t_f} + \int_{t_0}^{t_f} L \, dt \tag{2-2}$$

For a zero-sum game the pursuer attempts to minimize J whilst the evader attempts to maximize J, using their respective control vectors. These controls may be subject to inequality constraints of the form

$$\begin{aligned} C(x_p,u) &\leq 0 \\ C(x_e,v) &\leq 0 \end{aligned} \tag{2-3}$$

where x_p, x_e are the components of the state vector x associated with the pursuer's and the evader's position and velocity.

The game being considered is a free final time problem with no terminal constraints and "minimax" range as the cost

function. The "minimax" range cost function may include terms associated with the velocity vector.

An augmented cost function is formed

$$\tilde{J} = J + \int_{t_0}^{t_f} [\lambda^T(f-x) + \mu C]dt \qquad (2-4)$$

where

λ = costate vector

μ = Lagrange multiplier vector

$= 0$ for $C < 0$

$\neq 0$ for $C = 0$

A saddle point solution is presumed to exist such that

$$J(u^*,v) \leq J(u^*,v^*) \leq J(u,v^*) \qquad (2-5)$$

where

u^*,v^* = optimal controls

u,v = any other admissible control

The necessary conditions for the saddle point solution to the game for a Hamiltonian that is separable in u and v, where the Hamiltonian, H, is given by

$$H = \lambda^T f + L = H_e(x,v) + H_p(x,u) \qquad (2-6)$$

is as follows (Ref 6:277)

$$\dot{\lambda}^T = - H_x$$

$$\lambda^T(t_f) = \phi_x\Big|_{t_f}$$

$$H_u = 0$$

$$H_v = 0$$

$$H(t_f) = -\phi_t\Big|_{t_f} \tag{2-7}$$

These conditions are for interior controls and should the controls be constrained then the conditions become

$$\dot{\lambda}^T = -H_x - \mu C_x$$

$$\lambda^T(t_f) = \phi_x(t_f)$$

$$H_u = -\mu C_u$$

$$H_v = -\mu C_v$$

$$H(t_f) = -\phi_t\Big|_{t_f} \tag{2-8}$$

These conditions together with the state dynamics are a two point boundary value problem (TPBVP) of the form

$$\dot{x} = f(x,\lambda,t) \qquad x(t_0) = x_0$$

$$\dot{\lambda} = g(x,\lambda,t) \qquad \lambda(t_f) = \phi_x^T\Big|_{t_f}$$

$$H(t_f) = -\phi_t\Big|_{t_f} \qquad t_f \text{ free} \tag{2-9}$$

The solution of this TPBVP provides $\lambda(t_0)$, t_f such that the necessary conditions are met. The controls that

need to be applied to optimize the cost function can be found from

$$\dot{x} = f(x,\lambda,t) \quad x(t_0) = x_0$$

$$\dot{\lambda} = g(x,\lambda,t) \quad \lambda(t_0) = \lambda_0 \tag{2-10}$$

and by integrating these state and costate equations forward to t_f the trajectories of the saddle point solution to the game are given.

The controls defined in Eq (2-10) are valid for the case where both the players use the saddle point controls. Should one player use nonoptimal controls then the value of the cost function may change in his opponent's favor provided his opponent can adjust his controls to capitalize on the non-optimal play.

Where the optimal controls are determined from Eq (2-10) in the form

$$u(t) = u(x_0,\lambda_0,t)$$

$$v(t) = v(x_0,\lambda_0,t) \tag{2-11}$$

the controls are known as open loop controls and will not automatically adapt to changes in the game. In order to capitalize on nonoptimal play the values of $\lambda(t_1)$ must be amended by some amount $\delta\lambda(t_1)$ based on the difference between the value of $x(t_1)$ from the saddle point solution and the actual value of $x(t_1)$ as a result of some nonoptimal play.

Pseudo Closed-Loop Scheme

In some neighborhood of the saddle point trajectory the expressions of Eq (2-10) can be expanded about this nominal trajectory ignoring terms of second order and higher to give

$$\delta\dot{x} = f_x(x,\lambda,t)\delta x + f_\lambda(x,\lambda,t)\delta\lambda$$

$$\delta\dot{\lambda} = g_x(x,\lambda,t)\delta x + g_\lambda(x,\lambda,t)\delta\lambda \qquad (2\text{-}12)$$

By similar reasoning the transversality conditions can be considered as linear functions of $\delta x(t_f)$, $\delta\lambda(t_f)$ and dtf. Anderson in Ref 1 shows that for any set of transversality conditions the small change in the costates can be represented by

$$\delta\lambda(t_f) = A\delta x(t_f) \qquad (2\text{-}13)$$

The matrix A is evaluated at the nominal terminal states, costates and final time.

The corresponding change in the state at some prior time, t_1, due to small changes in the terminal states can be expressed as

$$\delta x(t_1) = \Phi_{xx}(t_1,t_f)\delta x(t_f) + \Phi_{x\lambda}(t_1,t_f)\delta\lambda(t_f) \qquad (2\text{-}14)$$

where

Φ_{xx}, $\Phi_{x\lambda}$ are state transition matrices.

The changes in the costates are then

$$\delta\lambda(t_1) = \Phi_{\lambda x}(t_1,t_f)\delta x(t_f) + \Phi_{\lambda\lambda}(t_1,t_f)\delta\lambda(t_f) \qquad (2\text{-}15)$$

Hence for a small deviation from an open loop optimal trajectory due to sub-optimal play on the part of one player the change $\delta x(t_1)$ can be used to predict a change in costates $\delta\lambda(t_1)$ that updates the costates, and hence the open loop controls, to account for the small divergence from the previous saddle point solution.

The relationship between $\delta\lambda(t_1)$ and $\delta x(t_1)$ is found by integrating back from the expected terminal state either a matrix ricatti equation or the time derivatives of the transition matrices of Eq (2-14) and similarly for the costates. This integration backwards from the expected final time is terminated as it reaches the current real time state. The difference between the states at that time if both players had played optimally and the actual states provides the vector $\delta x(t_1)$. This small change in state is then used to update the costates to convert the suboptimal play of one player into a gain for the other.

Anderson (Refs 1, 2, and 4) has proposed such a means of updating the saddle point solution to capitalize on non-optimal play and the references give comparisons with closed loop laws for some simple problems. The updating is done in real time and is shown to be near optimal.

III. Intercept Problem

The particular game considered is a zero sum differential game between an air-to-air missile and an aircraft with final time free.

Game Scenario

The game scenario is as follows:

(a) The aircraft model is based on the F4, with altitude and velocity dependent stall limits, thrust and drag.

(b) The missile is based on typical boost-coast air-to-air missile with an infra-red seeker. The missile guidance scheme begins at the end of the boost phase and, as for the aircraft, has altitude and velocity dependent drag.

(c) The vehicles are represented as point masses flying co-ordinated turns in 3 dimensions.

(d) Gravity is included but taken to be constant in direction and magnitude.

(e) Final time is left free.

(f) The game ends when $\frac{d}{dt}(J) = 0$.

Aircraft Model

The F4 has been the basis for the aircraft model with polynomials used to represent the variations in stall limits and maximum thrust with velocity and altitude. The vehicle dynamics are

$$\dot{x} = v \cos\gamma \cos\sigma$$

$$\dot{y} = v \cos\gamma \sin\sigma$$

$$\dot{z} = v \sin\gamma$$

$$\dot{v} = [T \cos\alpha - D]\frac{1}{m} - g \sin\gamma$$

$$\dot{\gamma} = [L + T \sin\alpha]\frac{\cos\mu}{mv} - \frac{g \cos\gamma}{v}$$

$$\dot{\sigma} = [L + T \sin\alpha]\frac{\sin\mu}{mv \cos\gamma} \qquad (3\text{-}1)$$

where

x = distance north

y = distance west

z = height

v = velocity magnitude

γ = angle velocity vector makes with the horizontal

σ = angle between the velocity vector projected into the horizontal plane and the x axis.

α = angle of attack

$\alpha \triangleq$ angle between thrust and velocity vectors

μ = bank angle

D = drag force

L = lift perpendicular to wing plan form and perpendicular to velocity vector

g = gravity

T = thrust, along a/c centerline.

The controls are load factor and bank angle. Bank angle is unconstrained and for this problem max throttle

has been specified, with thrust then dependent upon altitude and speed. The constraints on the load factor are taken to be a function of altitude and speed below the corner velocity and a structural limit above the corner speed of 6 g's.

Finally the drag force is taken to be

$$D = C_D \, QS \tag{3-2}$$

where

$$C_D = C_{DO} + kC_L^2$$

$$Q = \frac{1}{2} \rho_0 \, e^{-\beta z} \, V^2$$

S = reference area

Missile Model

The missile model is similar to the aircraft model but has the following differences.

(a) Thrust = 0

(b) No aerodynamic constraint on load factor.

The missile is considered in the coast phase only. The load factor constraint is taken at 15 g's independent of speed and altitude.

Cost Function

The cost function for the game, which the evader wishes to maximize and the pursuer to minimize, is

$$J = AR^2 - B \cos (TCA) \tag{3-3}$$

where

R = distance between the a/c and the missile

TCA = angle between their respective velocity vectors (Track Crossing Angle)

A,B = positive weighting factors

The justification for using "R^2" is that, although it produces large values of some of the costates at t_f through the transversality conditions, the effectiveness of the missile warhead will probably be inversely proportional to R^2. The justification for using "-cos (TCA)" is that the cost function should in some way represent the problems associated with fuzing a warhead. By and large, to achieve a high probability of kill, a missile should fly a parallel flight path with the a/c at the final time. The term in TCA represents a minimum cost of -B for a tail-on chase in the final stages. The cost varies slightly for small values of TCA but increases rapidly for angles above 45°. It will also penalize the pursuer for a head-on attack on the basis that the relative range rate is very high, which makes fuzing very difficult.

At a later stage, when investigating the behavior of the game where the missile had more than sufficient control necessary to intercept the aircraft, the cost function was changed slightly. In order to provide a cost function that was capable of directing the missile to choose between non-unique optimal controls, a small penalty related to final time was added. Its magnitude was such that if the missile

could not intercept the aircraft at all, or if the missile could intercept the aircraft but not at an acceptable track crossing angle then the time penalty was insignificant. However for situations where the missile could bring the original cost function to its absolute minima then the time penalty became significant.

The cost function used was therefore

$$J = AR^2 - B \cos (TCA) + C\, t_f \qquad (3\text{-}4)$$

with

$A = 1$

$B = 10$

$C = 1/6$

These values were chosen to make the TCA term significant below 10 ft and the t_f term significant near the minimum value of the TCA term when $R(t_f) \rightarrow 0$.

Differential Game Guidance

By application of the necessary conditions for a saddle point solution the controls can be expressed as functions of the states and costates.

The costate dynamics are found from the partial derivative of the Hamiltonian with respect to the corresponding state e.g.

$$\dot{\lambda}_x = - \frac{\partial H}{\partial x} \qquad (3\text{-}5)$$

producing the following

$$\dot{\lambda}_x = \dot{\lambda}_y = 0 \tag{3-6}$$

$$\dot{\lambda}_z = -\frac{\lambda_v}{m}\left[\frac{\partial T}{\partial z}\cos\alpha - T\sin\alpha\,\frac{\partial \alpha}{\partial z} - \frac{\partial D}{\partial z}\right]$$

$$-\left[\frac{\lambda_\gamma \cos\mu}{mv} + \frac{\lambda_\sigma \sin\mu}{mv\cos\gamma}\right]\times$$

$$\left[\frac{\partial L}{\partial z} + \frac{\partial T}{\partial z}\sin\alpha + T\cos\alpha\,\frac{\partial \alpha}{\partial z}\right] \tag{3-7}$$

$$\dot{\lambda}_v = -\lambda_x[\cos\gamma\cos\sigma] - \lambda_y[\cos\gamma\sin\sigma] - \lambda_z[\sin\gamma]$$

$$-\frac{\lambda_v}{m}\left[\frac{\partial T}{\partial v}\cos\alpha - T\sin\alpha\,\frac{\partial \alpha}{\partial v} - \frac{\partial D}{\partial v}\right]$$

$$+\lambda_\gamma\frac{\dot{\gamma}}{v} + \lambda_\sigma\frac{\dot{\sigma}}{v}$$

$$-\left[\frac{\lambda_\gamma \cos\mu}{mv} + \frac{\lambda_\sigma \sin\mu}{mv\cos\gamma}\right]\times$$

$$\left[\frac{\partial L}{\partial v} + \frac{\partial T}{\partial v}\sin\alpha + T\cos\alpha\,\frac{\partial \alpha}{\partial v}\right] \tag{3-8}$$

$$\dot{\lambda}_\gamma = -\lambda_x[-v\sin\gamma\cos\sigma]$$

$$-\lambda_y[-v\sin\gamma\sin\sigma]$$

$$-\lambda_z[v\cos\gamma]$$

$$-\lambda_v[-g\cos\gamma]$$

$$-\lambda_\gamma\left[\frac{g\sin\gamma}{v}\right]$$

$$-\lambda_\sigma[\dot{\sigma}\tan\gamma] \tag{3-9}$$

$$\dot{\lambda}_\sigma = -\lambda_x[-v \cos\gamma \sin\sigma]$$

$$-\lambda_y[v \cos\gamma \cos\sigma] \qquad (3\text{-}10)$$

The controls used are n, the load factor and μ the bank angle. The evader's thrust is set to max throttle and is then state dependent while the pursuer's thrust is zero.

Hence the unexpanded partial derivatives above become with

$$L = nW \qquad (3\text{-}11)$$

$$\frac{\partial L}{\partial z} = \frac{\partial L}{\partial v} = 0 \qquad (3\text{-}12)$$

with

$$T_{max} = A + Bz + Cv \qquad (3\text{-}13)$$

$$\frac{\partial T}{\partial z} = B, \quad \frac{\partial T}{\partial v} = C \qquad (3\text{-}14)$$

with

$$D = \frac{1}{2}\rho_0 e^{-\beta z} v^2 s(C_{D_0} + kC_L^2) \qquad (3\text{-}15)$$

$$\frac{\partial D}{\partial z} = -\beta D + \frac{1}{2}\rho_0 e^{-\beta z} v^2 s\, 2kC_L \frac{\partial C_L}{\partial z}$$

$$= -\beta \frac{1}{2}\rho_0 e^{-\beta z} v^2 s[C_{D_0} - kC_L^2] \qquad (3\text{-}16)$$

with

$$\alpha = KC_L \qquad (3\text{-}17)$$

$$\frac{\partial \alpha}{\partial v} = K \frac{\partial C_L}{\partial v} \quad \text{etc.} \tag{3-18}$$

with

$$C_L = \frac{nW}{\frac{1}{2} \rho_0 e^{-\beta z_v} {}^2 s} \tag{3-19}$$

$$\frac{\partial C_L}{\partial v} = - \frac{C_L}{v} \tag{3-20}$$

$$\frac{\partial C_L}{\partial z} = \beta C_L \tag{3-21}$$

The load factor control is constrained and so account must be taken of the effect of the constraint on the costate equation.

$$C_1(n,z,v) \geq 0 \tag{3-22}$$

$$C_2(n) \geq 0 \tag{3-23}$$

where C_1 is the constraint below the corner speed and C_2 the constraint above the corner speed and,

$$C_1 = n_1(z,v) - n \geq 0 \tag{3-24}$$

$$C_2 = 6 - n \geq 0 \tag{3-25}$$

Where the control is constrained

$$\dot{\lambda}_z = - H_z - \mu C_z \tag{3-26}$$

$$\dot{\lambda}_v = - H_v - \mu C_v \tag{3-27}$$

$$\mu = - \frac{H_n}{C_n} = H_n \tag{3-28}$$

Hence

$$\dot{\lambda}_z = - H_z - H_n C_z \tag{3-29}$$

$$\dot{\lambda}_v = - H_v - H_n C_v \tag{3-30}$$

for constrained load factor below the corner speed and since the constraint above the corner speed is state independent

$$\dot{\lambda}_z = - H_z \tag{3-31}$$

$$\dot{\lambda}_v = - H_v \tag{3-32}$$

as before. In the case of the pursuer the missile is considered to have sufficient control at all speeds of interest that only the state independent constraint is in force.

For numerical purposes a Fortran integer variable "mu" was used to switch the additional terms on and off as necessary in the costate equations so that as the load factor selected by the control algorithm was constrained to the state dependent limit "mu" was set to 1, otherwise it was left at 0.

Optimal Controls

For an unconstrained control such as the bank angle the first order necessary conditions for an optimal control require that

$$H_u = 0 \tag{3-33}$$

Hence

$$H_\mu = -\frac{\lambda_\gamma}{mv}\,[L + T \sin\alpha]\,\sin\mu \tag{3-34}$$

$$+\frac{\lambda_\sigma}{mv\cos\gamma}\,[L + T \sin\alpha]\,\cos\mu \tag{3-35}$$

The second order necessary conditions require that

$$H_{\mu\mu} \leq 0 \tag{3-36}$$

for a maximizing player. Combining these two equations we are able to define

$$\sin\mu_e = \frac{\lambda_{\sigma_e}}{\sqrt{(\lambda_{\gamma_e}\cos\gamma_e)^2 + \lambda_{\sigma_e}^2}} \tag{3-37}$$

$$\cos\mu_e = \frac{\lambda_{\gamma_e}\cos\gamma_e}{\sqrt{(\lambda_{\gamma_e}\cos\gamma_e)^2 + \lambda_{\sigma_e}^2}} \tag{3-38}$$

For the minimizing player we find

$$\sin\mu_p = \frac{-\lambda_{\sigma_p}}{\sqrt{(\lambda_{\gamma_p}\cos\gamma_p)^2 + \lambda_{\sigma_p}^2}} \tag{3-39}$$

$$\cos\mu_p = \frac{-\lambda_{\gamma_p}\cos\gamma_p}{\sqrt{(\lambda_{\gamma_p}\cos\gamma_p)^2 + \lambda_{\sigma_p}^2}} \tag{3-40}$$

In the case of the load factors we solve for the unconstrained load factor that is a stationary control of the Hamiltonian. Should there be an interior control that optimizes the Hamiltonian we check the sufficient conditions to ensure maximization or minimization as the case may be. Where however there is no interior control that is a stationary control with respect to H we choose either maximum or minimum load factor to achieve constrained optimization.

For the evader then we consider the first order necessary conditions

$$H_n = 0 \tag{3-41}$$

$$H_n = \frac{\lambda_V}{m}\left[-T \sin\alpha \frac{\partial\alpha}{\partial n} - \frac{\partial D}{\partial n}\right] + \frac{\lambda_\gamma}{mv}\left[\frac{\partial L}{\partial n} + T\cos\alpha\frac{\partial\alpha}{\partial n}\right]\cos\mu + \frac{\lambda_\sigma}{mv\cos\gamma}\left[\frac{\partial L}{\partial n} + T\cos\alpha\frac{\partial\alpha}{\partial n}\right]\sin\mu \tag{3-42}$$

where

$$\frac{\partial\alpha}{\partial n} = \frac{\partial(KC_L)}{\partial n} = \frac{\partial(KnW/QS)}{\partial n} = \frac{KW}{QS} \tag{3-43}$$

$$\frac{\partial D}{\partial n} = \frac{\partial}{\partial n}(C_{D0}+kC_L^2)QS = \frac{2knW^2}{QS} \tag{3-44}$$

and

$$\frac{\partial L}{\partial n} = W \tag{3-45}$$

Thus

$$H_n = 0 = \lambda_v \left[- T \sin \alpha \frac{KW}{QS} - \frac{2knW^2}{QS} \right]$$

$$+ \left[\frac{\lambda_\gamma \cos \mu}{mv} + \frac{\lambda_\sigma \sin \mu}{mv \cos \gamma} \right] x \left[W + T \cos \alpha \frac{KW}{QS} \right] \tag{3-46}$$

Substituting for cos μ etc and making small angle approximations

$$0 = \frac{\lambda_v}{m} \left[- \frac{TK^2 nW^2}{Q^2 S^2} - \frac{2knW^2}{QS} \right]$$

$$+ \left[W + \frac{TKW}{QS} \right] x \left[\sqrt{\lambda_\gamma^2 + \frac{\lambda_\sigma^2}{\cos(\gamma)^2}} \right] x \frac{1}{mv} \tag{3-47}$$

$$n = \frac{\sqrt{\lambda_\gamma^2 + \frac{\lambda_\sigma^2}{(\cos \gamma)^2}} \quad [QS+TK]QS}{Wv\lambda_v [TK^2 + 2kQS]} \tag{3-48}$$

For an interior control the second order conditions are

$$H_{nn} = - \frac{\lambda_v}{m} \left[\frac{TK^2 W^2}{Q^2 S^2} + \frac{2kW^2}{QS} \right] \leq 0 \tag{3-49}$$

i.e., $\lambda_v > 0$ for n, above, to be a maximizing control.

For a constrained load factor the choice is either max or min load factor. The Hamiltonian terms that contain load factor dependent terms are

$$H_1 = \frac{\lambda_V}{m}(T\cos\alpha - D) + \frac{\lambda_\gamma}{mV}(L + T\sin\alpha)\cos\mu$$

$$+ \frac{\lambda_\sigma}{mV\cos\gamma}(L + T\sin\alpha)\sin\mu$$

$$= \frac{\lambda_V}{m}(T\cos\alpha - D) + \frac{(L + T\sin\alpha)}{mV}\sqrt{\lambda_\gamma^2 + \frac{\lambda_\sigma^2}{(\cos\gamma)^2}} \qquad (3\text{-}50)$$

For $\lambda_V > 0$ we can look for an interior control and if n so defined is too large we choose n = n max. For $\lambda_V \leq 0$ we find that our sufficient condition predicts a minimization of H in some region of negative load factor. In order to maximize the Hamiltonian we select n = n max for $\lambda_V \leq 0$.

The exact opposite arguments are used to select the optimum load factor for the missile. Thus, for interior controls

$$n = -QS\sqrt{\lambda_{\gamma_p}^2 + \frac{\lambda_{\sigma_p}^2}{(\cos\gamma_p)^2}}\;\frac{1}{Wv\lambda_{V_p}{}^{2k_p}} \qquad (3\text{-}51)$$

which requires $\lambda_{V_p} < 0$ for an interior control to be possible. Sufficient conditions for a minimum with respect to the Hamiltonian are

$$H_{nn} \geq 0 \qquad (3\text{-}52)$$

$$H_{nn} = - \frac{2kW^2}{mQS} \lambda_v \qquad (3\text{-}53)$$

Hence $\lambda_v < 0$ for minima and following similar arguments for the pursuer as for the evader we choose the constrained load factor to be

$$n = n_{max} \text{ for } \lambda_v \geq 0 \qquad (3\text{-}54)$$

and

$$n = n_{max} \text{ for } \lambda_v < 0 \qquad (3\text{-}55)$$

Proportional Navigation Scheme

In order to check the validity of the results a proportional navigation algorithm was produced for the missile and used against an open loop optimal evasion scheme.

We expected to find that the proportional navigation scheme (PN) would fly a similar course to the open loop optimal missile but would not get as close to the evader.

For the purposes of the test the PN scheme was allowed to use the exact current values of the vehicle velocities and positions to measure the spin rates of the line of sight. The line of sight was defined by two angles, one an azimuth angle and the other the angle out of the horizontal plane. For the Cartesian frame centered on the missile as in Fig. 1 the two angles are respectively θ, ψ.

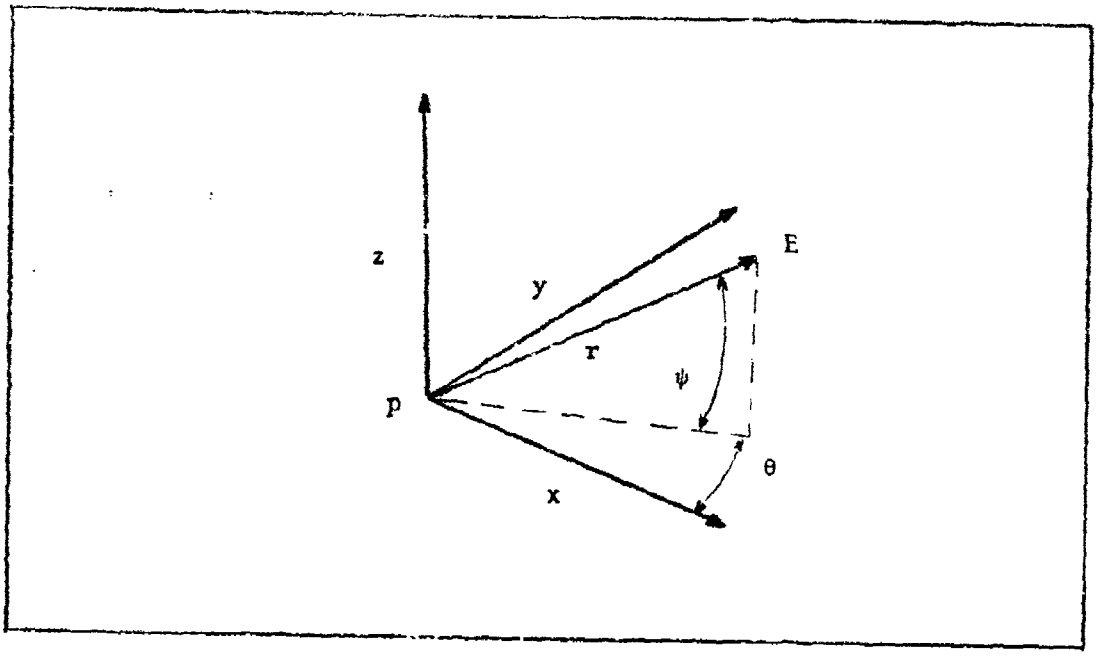

Fig. 1. Line of Sight Angles.

$$\tan \psi = \frac{z}{\sqrt{x^2 + y^2}} \tag{3-56}$$

$$\dot{\psi} = \frac{1}{\left(1 + \frac{z^2}{x^2+y^2}\right)} \left\{ \frac{\dot{z}}{\sqrt{x^2 + y^2}} - \frac{z(x\dot{x}-y\dot{y})}{\sqrt{(x^2+y^2)^3}} \right\} \tag{3-57}$$

Similarly

$$\tan \theta = \frac{y}{x} \tag{3-58}$$

$$\dot{\theta} = \frac{1}{\left(1 + \frac{y^2}{x^2}\right)} \left\{ \frac{\dot{y}}{x} - \frac{y\dot{x}}{x^2} \right\} \tag{3-59}$$

We wish to fly the missile so that $\dot{\gamma}_p$, and $\dot{\sigma}_p$ are some multiple of $\dot{\psi}$ and $\dot{\theta}$.

$$\dot{\gamma} = RK1\ \dot{\psi} = \frac{L}{mv} \cos \mu - \frac{g \cos \gamma}{v} \tag{3-60}$$

$$\dot{\sigma} = RK2\ \dot{\theta} = \frac{L \sin \mu}{mv \cos \gamma} \tag{3-61}$$

Hence

$$\tan \mu = \frac{RK2\ \dot{\theta}}{RK1\ \dot{\psi} + \frac{g \cos \gamma}{v}} \tag{3-62}$$

and then

$$L = \frac{RK2\dot{\theta}\, mv \cos \gamma}{\sin \mu} = nW \tag{3-63}$$

If n so defined exceeded 15 it was set at 15.

These values of μ, n were then used in Eq (3-60) and Eq (3-61) to give the time rate of change of γ and σ for the missile.

In the case where $\dot{\theta}$ is very small or zero the evaluation of the load factor in Eq (3-63) leads to numerical inaccuracies. In this case Eq (3-60) is used

$$n = \frac{v}{g \cos \mu} \left[RK1\ \dot{\psi} + \frac{g \cos \gamma}{v} \right] \tag{3-64}$$

IV. Results

TPBVP Solution Method

The results can be divided into two phases namely

(a) nominal saddle point solutions

(b) variations about the nominal solution.

Subroutine NSOIA was utilized in both phases. Firstly, it was used to provide a one dimensional search for a point on the terminal surface, and secondly it was used to solve two point boundary value problems, both in the refining of the nominal saddle point solution so as to minimize the errors resulting from numerical integration and in the updating schemes to solve the two point boundary value problem (TPBVP) at each update point. Appendix B presents a short discussion on the principles of the subroutine and on an aspect of the numerical integration of the state and costate equations that is the probable cause of variations in a Hamiltonian which should be constant.

Saddle Point Solutions

In order to produce a large number of saddle point solutions covering a wide range of terminal conditions, points on the terminal surface were found by selecting eleven out of twelve of the terminal states and varying the remaining state until the transversality condition on $H(t_f)$ was met. Reference 3 provides justification for this approach since it is shown that barriers do not occur in the game formulation.

By integrating backwards from the terminal surface it was possible to construct saddle point solutions to games which ended at 30,000, 20,000 and 10,000 ft with final miss distances from 0 to 200 ft and with a variety of track crossing angles (TCA). TCA was defined as the angle between the missile and aircraft velocity vectors at t_f. By integrating forward again to t_f it was found that there were errors, due to the numerical integration scheme, and the transversality conditions were not met exactly. These could be reduced by letting NSOIA vary the initial costates slightly until these errors in the transversality conditions were reduced to some acceptable level.

The measure of convergence for the TPBVP was the sum of the squares of these errors, namely

$$\varepsilon = \left[\lambda(t_f) - \left.\frac{\partial \phi}{\partial x}\right|_{t_f}\right]^T \left[\lambda(t_f) - \left.\frac{\partial \phi}{\partial x}\right|_{t_f}\right] + \left[H(t_f) + \left.\frac{\partial \phi}{\partial t}\right|_{t_f}\right]^T \left[H(t_f) + \left.\frac{\partial \phi}{\partial t}\right|_{t_f}\right] \qquad (4\text{-}1)$$

Because of the dynamics and the cost function it was possible to reduce the TPBVP to eleven states by removing λ_{xp} and λ_{yp}. Hence for a value of $\varepsilon = 121$ the average error in the transversality conditions would be 1. With the program coded in ft, ft/sec etc. this represents an error of 1 ft in the final range. For values of ε less than 100 the trajectories showed little change as ε was decreased and it

was possible to keep NSOIA searching until ε was less than .001 at which point the terminal miss distance was fixed to within a fraction of an inch. ε was therefore used to define acceptable convergence in the solution of TPBVP's. For refining nominal solutions ε was set at 20 and for the updating scheme ε was set at 400 so as to reduce computer time. In a typical updating scheme approximately 25 TPBVP's were solved and it was necessary to sacrifice some accuracy to keep total running time to a minimum.

Open Loop Controls

With final time free and with the cost function used the open loop optimal trajectories looked realistic. The optimal evader normally turns across the missile's path and in most instances descends. The aircraft was kept subsonic because polynomials representing load factor limit, maximum thrust and drag as functions of height and velocity were only valid subsonic. As a result the aircraft was usually below its corner speed in the cases considered and by descending it was able to turn faster. The aircraft also gained thrust and load limit advantages by descending. Both missile and aircraft used maximum load factor along smooth arcs to the terminal surface. This was, for nonzero final range ,the point at which each had the same radius of turn and the aircraft was on the inside of the missile. The missile paid a large drag penalty using maximum load

factor and would typically give up 1500 ft/sec in velocity during the 6 second engagement.

The initial relative position of the two vehicles 6 seconds away from termination varied from a beam attack at 5000 ft range for a final range of 0. ft to 12,000 ft with the missile about 40° off the front of the aircraft for final ranges of 200 ft.

In all the cases studied interior controls were never used and despite attempts to force interior controls by utilizing zero final range and a TCA of zero and forcing interior controls at t_f when integrating backwards, interior control solutions were never found.

The justification for free final time is not only that it is more realistic but also for terminal pay off it is essential for valid results as the following example shows. The work of Ref 9 uses a comparable game model as the model of this thesis and it presents one solution for an air-to-air missile using fixed final time. The cost functions are different but the small difference should not affect the game significantly. In the problem of Ref 9 a beam attack at 30,000 ft results in the aircraft turning away from the missile and both missile and aircraft use interior controls. At t_f = 5 secs the missile is 1300 ft astern of the aircraft flying a parallel trajectory. It appears that in about 2 secs at most the missile will achieve a maximum hit. The same problem under a free final time formulation is shown in Figs. 2 and 3. The 3D trajectory is given in

Fig. 2 with the ground tracks of the two vehicles plotted on the bottom of the box containing the trajectories. The bank angle selected in the saddle point solution is plotted along with the proportional navigation (PN) choice of bank angle. The PN plot represents the choice of bank angle based on line of sight (LOS) considerations as the missile flies along the optimal trajectory. The aircraft flies across the path of the missile and dives. The missile is then forced into a maneuver whereby it begins to fly to the right of the initial position of the evader and then continues to climb above the evader for an approach with the minimum TCA it can achieve. Both vehicles use maximum load factor throughout the 5.108 secs.

It appears that the fixed final time problem guarantees the aircraft's safety provided $R(t_f)$ is nonzero. It also does not prevent range going to zero at some intermediate stage. The trajectory in Fig. 2 has a smaller final range than that of Ref 9 in similar times and yet ultimately the result of Ref 9 will be more in the missile's favor than that of Fig. 2.

A selection of open loop saddle point trajectories are shown in Figs. 4 through 15. For comparison purposes plots are made of the bank angle selected by the missile on the basis of optimal control and proportional navigation. Since the missile flies along only one of these paths the bank angle selection of the alternate scheme is not accurate. In the very early stages the inaccuracies will be small and

comparisons can be made between the two schemes. The plot of bank angle immediately following an optimum pursuit trajectory plot is made along the optimum pursuit path.

Proportional Navigation Versus Optimal Control

The variations of optimal control (OPT), nonoptimal control (NONOPT), and proportional navigation (PN) considered are:

(a) saddle point solution

(b) open loop OPT evasion versus PN pursuit

(c) updated OPT evasion versus PN pursuit

(d) updated OPT pursuit versus NONOPT evasion

(e) PN pursuit versus NONOPT evasion.

The open loop optimal evader results demonstrated that for all but a few cases the open loop optimal evader gained against proportional navigation. The few cases were the problems where the saddle point solution lay in a plane of constant X or Y and hence bank angle was predetermined. Since PN used maximum load factor in these cases the outcome was the same as for the saddle point solution. Figures 12 and 13 are two such cases. Figures 16 through 23 present two cases for comparison of open loop optimal control versus proportional navigation for an open loop optimal evader. In each case the open loop optimal evader gains against proportional navigation. In this group of figures the bank angle selection of the two schemes when flown along the proportional navigation path is given after the proportional

navigation pursuit trajectory plot. Plots are also given of the rotation rates of the line of sight (LOS) whilst guided by the proportional navigation scheme.

Tables II and III give the initial conditions for the two cases presented in Figs. 16 through 23. Table I gives the final ranges for the two cases for the optimal control and proportional control missile against open loop optimal evader.

Table I

Final Ranges for OPT and PN

Fig. No.	Final Range
16	182
17	440
20	1.76
22	11

Tuned Proportional Navigation

An incidental result, on which little time was spent, is mentioned here because it greatly improved the performance of the PN scheme. For a given set of initial conditions and for an evader playing the open loop optimal control the PN scheme could be "tuned" to improve its performance. The two navigation gain constants for PN had previously been set to the same value. By introducing a ratio between these gain constants considerable improvement in the performance was achieved.

The case considered was the problem in Fig. 16. The PN scheme used maximum load factor throughout the flight and only the bank angle differed between PN and OPT guidanc . The bank angle selected by PN had similar characteristics and so the initial bank angle of the PN scheme was brought closer to the initial bank angle for the OPT guidance. The means of varying the PN bank angle was to select some ratio for RK1:RK2, the vertical and horizontal gain constants. For a ratio 1:2 the final range had been brought down from 440 feet to 207 feet which compared very favorably with the OPT scheme result of 182 feet.

An example of the advantages of the tuned navigation scheme is given in Figs. 24 through 27. The ratio used for RK1:RK2 was 1:2 and this ratio was not optimized. It was merely a first estimate of an improvement and since ratios of 1:1.7 and 1:2.3 gave similar improvements 1:2 was used to present the results. Figures 24 and 25 are the open loop saddle point solution with the "tuned" proportional navigation bank angle plotted whilst flying the optimal trajectory. Normal proportional navigation achieved a 478 ft miss and with "tuned" proportional navigation the result was 191 ft against the 173 ft for the saddle point solution. Table IV presents the initial conditions.

Pseudo Closed Loop Guidance

For an open loop solution to be useful the evader must play optimally or the open loop solution must be updated.

The open loop scheme was updated at approximately .3 sec intervals throughout the attack by solving the associated two point boundary value problem. The solution was considered acceptable when the sum of the squares of the errors in the transversality conditions was less than 400. The new solution could then be used to update the optimal missile attacking a nonoptimal evader or an optimal evader escaping a PN missile. This was an expensive process in terms of computer resources and is completely out of the question for real time guidance. It does however provide valuable information as to the magnitude of the changes in the costates and demonstrates what gain could be made in the "cost" for whichever player was being updated.

The motivation for this approach is that a proposed real time pseudo-closed loop scheme (Ref 1, 2, and 4) will probably have to give up some of the realism of the model for the advantages of a better behaved two point boundary value problem. In order to test simpler models for their ability to provide sufficient advantages over proportional navigation, or in fact any other scheme, to warrant implementation, then some means of comparison is required. The work of this thesis is therefore intended to provide a reference performance standard. Table V and Fig. 20 provide a saddle point solution as the basis for the various comparisons that can be made. These are:

(a) open loop optimal evasion versus proportional navigation

(b) updated optimal evasion versus proportional navigation

(c) updated optimal pursuit versus nonoptimal evasion

(d) proportional navigation versus nonoptimal evasion.

These cases are presented in the same order in the following sections.

Open Loop Optimal Evasion

The saddle point optimality condition for differential games requires that at least one of the players uses an optimal control. The open loop solution for the evader against proportional navigation has neither player playing optimally. However the result does indicate that the evasive maneuver capitalizes on the nonoptimality of proportional navigation. Figures 30 through 32 present the trajectories, the bank angle of the proportional navigation missile and the optimal guided missile whilst flying the proportional navigation trajectory and the line of sight rates resulting from the proportional navigation scheme. The result is a 20 ft miss with a TCA of 1.1 radians.

Updated Optimal Evader

Where the optimal evader, pursued by the proportional navigation missile, is allowed to update its controls at intervals to capitalize on the nonoptimal play of the pursuer considerable gains are made. The predicted final

range, track crossing angle and the cost function assuming the missile reverts to optimal control given by the TPBVP solution at each update are given in Table VI. The range R is in feet and the track crossing angle TCA is in radians. The cost function and the degree of convergence are also given. τ is the predicted time to go, again assuming both players play optimally, and the column τ_0 - t gives a comparison with the column τ to show how the game is extended by the updating optimal evader to gain further advantage. The entry at line 22 in the table is the final range (180 ft). Figures 33 and 34 present the results for the updated optimal evader. The bank angle selected by the optimal missile is actually perturbed by being forced along the PN trajectory in Fig. 34. It does show, however, that the PN scheme is near optimal and that the solution to the TPBVP at the update points was realistic.

For the case of the updated optimal evader the costates are presented in tabular form in Tables VIII and IX. At each update point the current values of the costates are given in the "in" column. The values of the costates after the return from NSOIA are given in column "out". The game is then integrated forward to the next update point and the current values of the costates are used as guesses and appear in the "in" column. The change in costates between updates is therefore the difference between the costates in the "out" column at one update point and the "in" column at the next update.

The close similarity between proportional navigation bank angle and optimal control bank angle in Fig. 34 suggests that "tuned" proportional navigation may well have made considerable improvements. Unfortunately, no time was available to consider this case.

Updated Pursuer

These cases are those where the missile is allowed an update at .3 second intervals against a nonoptimal evader. The evader flies max g load at a bank angle of 90° as a nonoptimal evasion.

Flying optimally the evader could only achieve a final range of 1.5 feet. The final time was 6.004 secs. During the updating computer run a less accurate solution was taken to be acceptable. The first call to N3O1A solves the initial two point boundary value problem and the time to go was set at 6 sec. The answer was acceptable within the new accuracy requirements but the small change in time alone of 4/1000 secs changed the terminal miss to 4.4 feet with a sum of squares of the transversality errors at 240. The results in Table V represent a solution with an error of 14.

Table IX gives the results from the computer run. The overriding factor in determining the number of updates, the acceptable accuracy and the maximum allowable number of iterations in the solution of the TPBVP was the central memory time requirements. These results are therefore not ideal in that the trade offs between accuracy and central

memory time have not allowed convergence in many instances. The instability of the resulting controls reflect this lack of convergence but at intervals the solution converges and the missile promptly makes up lost ground. However, in the last time period the missile is flying open loop against a nonoptimal evader who is able to double his miss distance during this last critical stage.

An interesting aspect was the fact that at updates 12, 13, 14 the 11th update open loop solution remained acceptable. With no update made the evader gained ground against the missile. Figures 35 and 36 represent the trajectory and the optimal bank angle respectively.

Proportional Navigation with Nonoptimal Evasion

In this case the nonoptimal evasion maneuver is used against a proportional navigation missile. The result is a 20 ft miss with a TCA of 2.02 radians which is more in the evader's favor than the open loop optimal evasion. Where neither player plays a game optimal strategy the saddle point optimality is not meaningful. It does suggest that only a poor estimate of the open loop evasion strategy makes reasonable gains against proportional navigation. The updated evader however makes considerable gains for this problem. That the updated optimal evader cannot always make such startling gains can be seen in Tables X and XI. These two problems are based on saddle point solutions that end in similar ranges but different TCA's. In the first

case the saddle point solution is given in Table III and Fig. 20. The bank angle plot of Fig. 21 indicates the near-optimal nature of proportional navigation. As a consequence the updated evader can only extend the range to 22 ft. However for the case of Table XI the updated evader makes considerable gains against proportional navigation. The saddle point solution is given by Fig. 6. The 1.73 ft of the saddle point solution is converted to 370 ft by the updating evader.

Summary

The problems associated with the solution of the TPBVP for very small final ranges is reflected in the instability of the updating scheme for the pursuer. Where he has an open loop final range that is small, nonoptimal play on the part of the evader is difficult to convert to a decrease in the payoff. Where the saddle point solution has a much larger final range, initially, while the pursuer is converting nonoptimal play by the evader into a decrease in the payoff, the TPBVP is amenable to updating within the number of iterations allocated. However as the final range gets smaller the TPBVP becomes more awkward. In one case the pursuer converted a 240 ft final range to .7 ft at some intermediate stage. The updating scheme was able to keep the final predicted range to about 2 ft despite lack of convergence at some update points. However in the last

phase under open loop control the predicted final range of 2 ft became 11 ft.

The updating evader has this aspect in his favor since he is continually increasing the final range. The problem becomes more well behaved and hence easier for him to update. Even if he doesn't update the open loop saddle point strategy provides some small gain against proportional navigation missiles.

In the cases considered no interior controls were found even for proportional navigation. This is probably because for an open loop optimal evasion or even for a rough approximation to optimal evasion the missile is forced into maximum g maneuvers. Hence proportional navigation loses because of its inability to lead or lag its bank angle based on considerations other than the immediate line of sight rate. Many cases in this thesis show bank angle patterns very similar to optimal control with only a constant offset. In other instances, Fig. 3 for example, there is considerable difference in the dynamic behavior, even though at a later stage the bank angle selections are essentially the same. The gain constants for the PN scheme were normally 10. This represents a performance for PN beyond the current capabilities.

V. Conclusions and Recommendations

Conclusions

This thesis compares the principle of proportional navigation to differential game optimal control. But for a few cases presented where launch conditions are very favorable to the missile, proportional navigation normally pays a considerable penalty, in terms of the cost function, in that the missile has the energy and the maneuverability to greatly improve the probability of kill under optimal control. The realistic dynamics used in this thesis are unlikely to provide the basis for a pseudo-closed loop optimal control scheme as suggested in Refs 1, 2, and 4. However the considerable gains that can be made suggest that simpler models may be used so as to compromise between gains in the payoff and in achieving a real time capability.

It appears that the optimal evader has most to gain using this scheme since the numerical problems improve as the final range increases. The open loop control is effective against proportional navigation so that any failure to update the control does not relinquish existing gains. Whereas any failure to update the missile control increases the final range.

Lastly I conclude that the subroutine NSOlA is a powerful means of solving the TPBVP's associated with saddle point solutions. Considerable care should be used in selecting the parameters that control NSOlA's performance

and in this respect NSOIA remains in the same class as most other schemes in that a good understanding of the nature of the solution is essential to obtaining a solution, no matter how powerful a numerical method is used.

Recommendations

It is recommended that further work in this subject should concentrate on finding simpler game models that behave in the same characteristic manner as the nonlinear model of this thesis. Since interior controls have not been found it may be possible to fix load factor at its maximum value and reduce the problem to a single unconstrained control in bank angle for each player. Under these conditions a simpler drag model may well prove sufficiently accurate. If a simpler model produces similar behavior then a pseudo-closed loop real time optimal guidance scheme may well prove to be possible for simulation purposes if not eventually for missile guidance.

Bibliography

1. Anderson, G. M. "A Transition Matrix Method for Generating New Optimal Closed-Loop Solutions to Nonlinear Differential Games". Preprint of International Federation of Automatic Control - International Federation of Operational Research Symposium on Optimization Methods, Applied Aspects, October 8-11, 1974, pp 27-35.

2. Anderson, G. M. "A Real-Time Closed-Loop Solution Method for a Class of Nonlinear Differential Games", IEEE Transactions on Automatic Control. AC-17:576.

3. Anderson, G. M. "Minimax Range/Barrier Trajectories and Their Application to Pursuit-Evasion Combat Problems". Proceedings of IEEE on Decision and Control Theory, Phoenix, Nov 1974.

4. Anderson, G. M. "A Near-Optimal Closed-Loop Solution Method for Nonsingular Zero-Sum Differential Games". Journal of Optimization Theory and Applications, 13:303-318 (March 1974).

5. Asher, R. B. and J. P. Matuszewski. "Optimal Guidance with Maneuvering Targets". Journal of Spacecraft, Vol. 11, No. 3:204-206 (March 1974).

6. Bryson, A. E. and Y. C. Ho. Applied Optimal Control. Waltham, Massachusetts: Blaisdell Company, 1969.

7. Garber, V. "Optimal Intercept Laws for Accelerating Targets". AIAA Journal, Vol. 6, pp 2196-2198 (November 1968).

8. Isaacs, R. Differential Games, New York, New York: John Wiley and Sons, 1965.

9. Leatham, A. L. and U. H. D. Lynch. "Two Numerical Methods to Solve Realistic Air-to-Air Combat Differential Games". 12th Aerospace Science Meeting of AIAA Washington, Feb 1974.

10. Powell, M. J. D. "A Fortran Subroutine for Solving Systems of Nonlinear Algebraic Equations", Numerical Methods for Nonlinear Algebraic Equations, edited by Philip Rabinowitz, New York: Gordon and Breach Science Publishers, 1970.

Appendix A

Tables and Figures

OPT EVASION-OPT PURSUIT

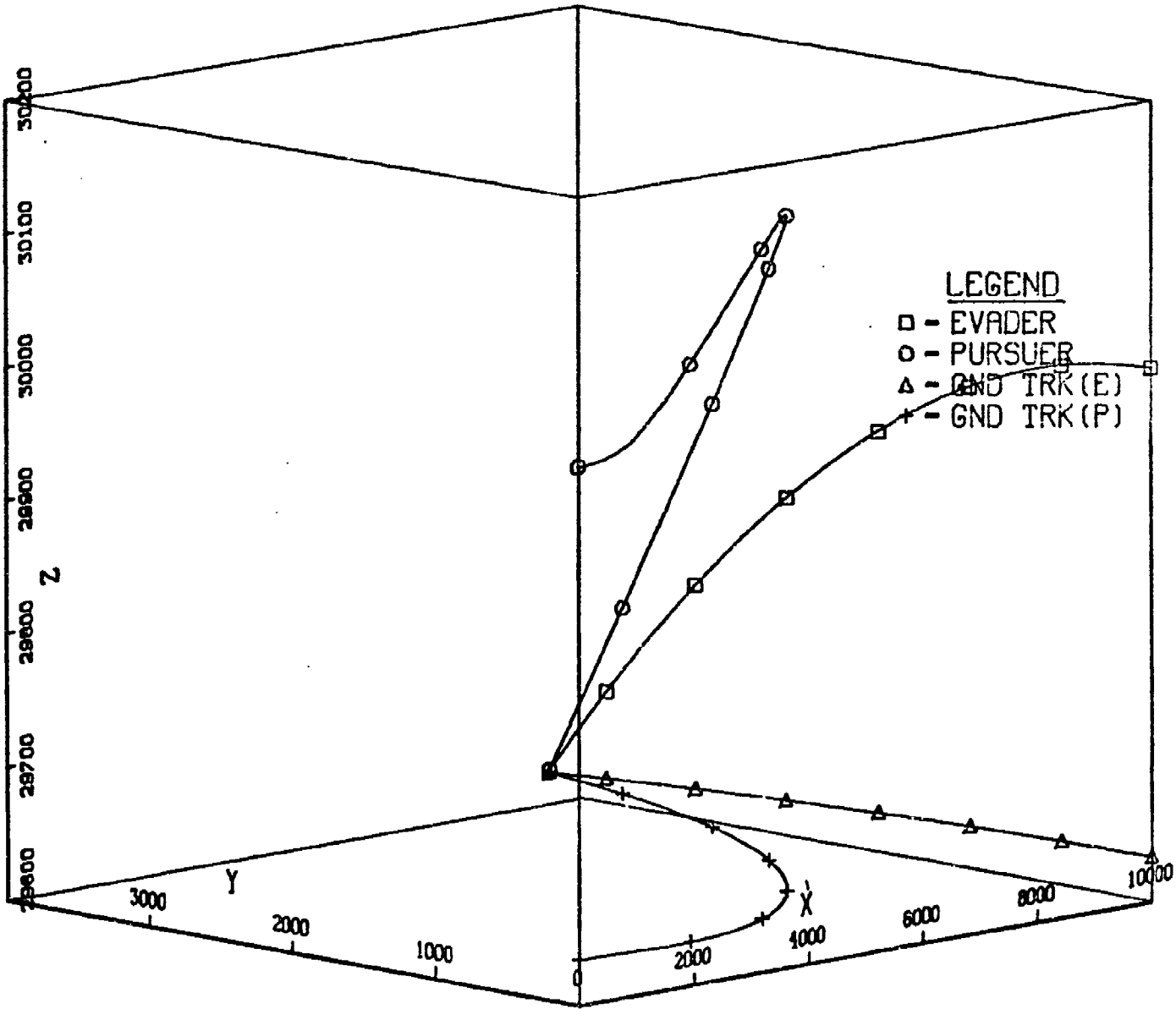

Fig. 2.

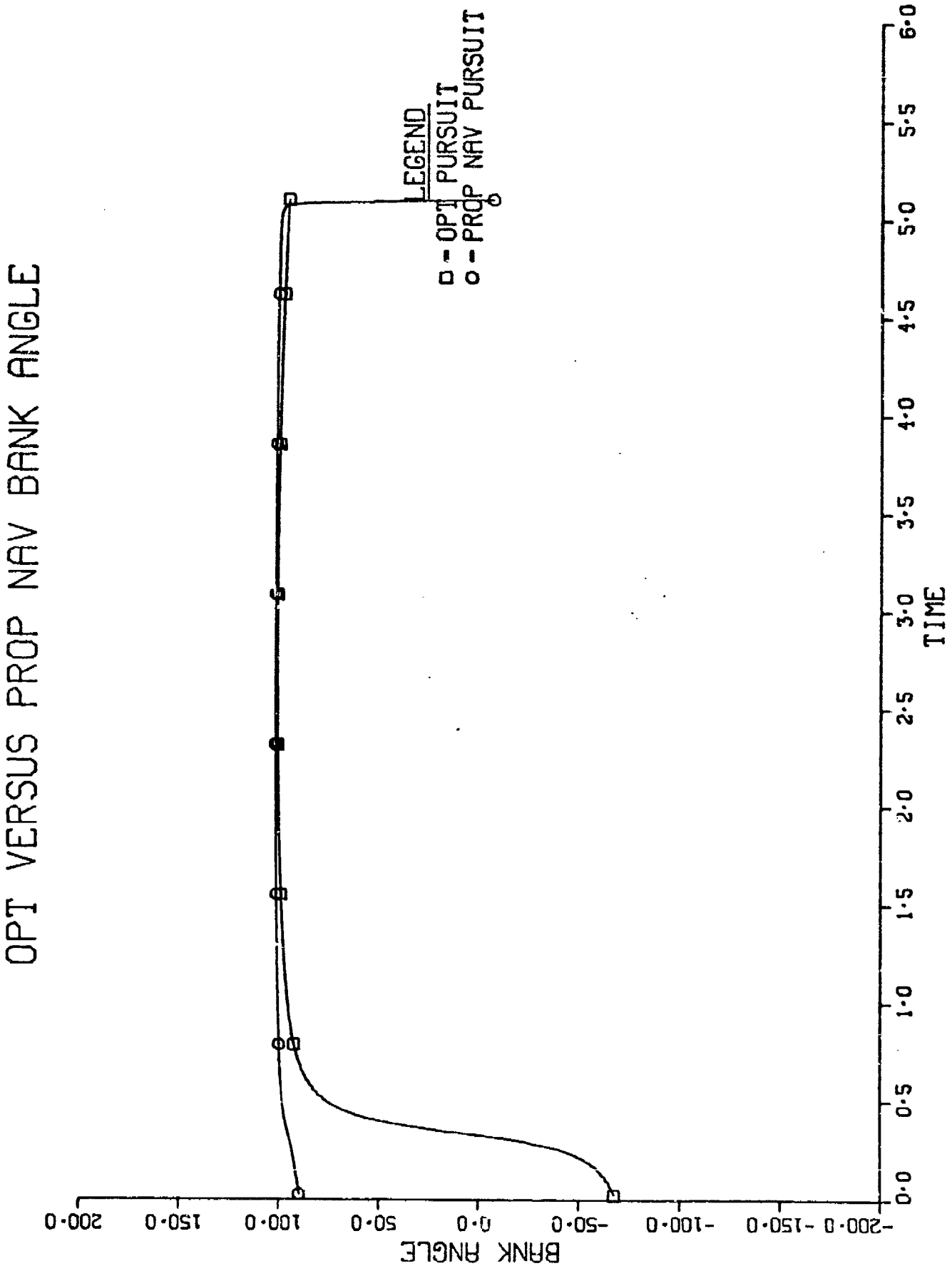
OPT VERSUS PROP NAV BANK ANGLE
LEGEND
□ - OPT PURSUIT
o - PROP NAV PURSUIT
BANK ANGLE
200·0
150·0
100·0
50·0
0·0
-50·0
-100·0
-150·0
-200·0
TIME
0·0
0·5
1·0
1·5
2·0
2·5
3·0
3·5
4·0
4·5
5·0
5·5
6·0

Fig. 3

OPT EVASION-OPT PURSUIT

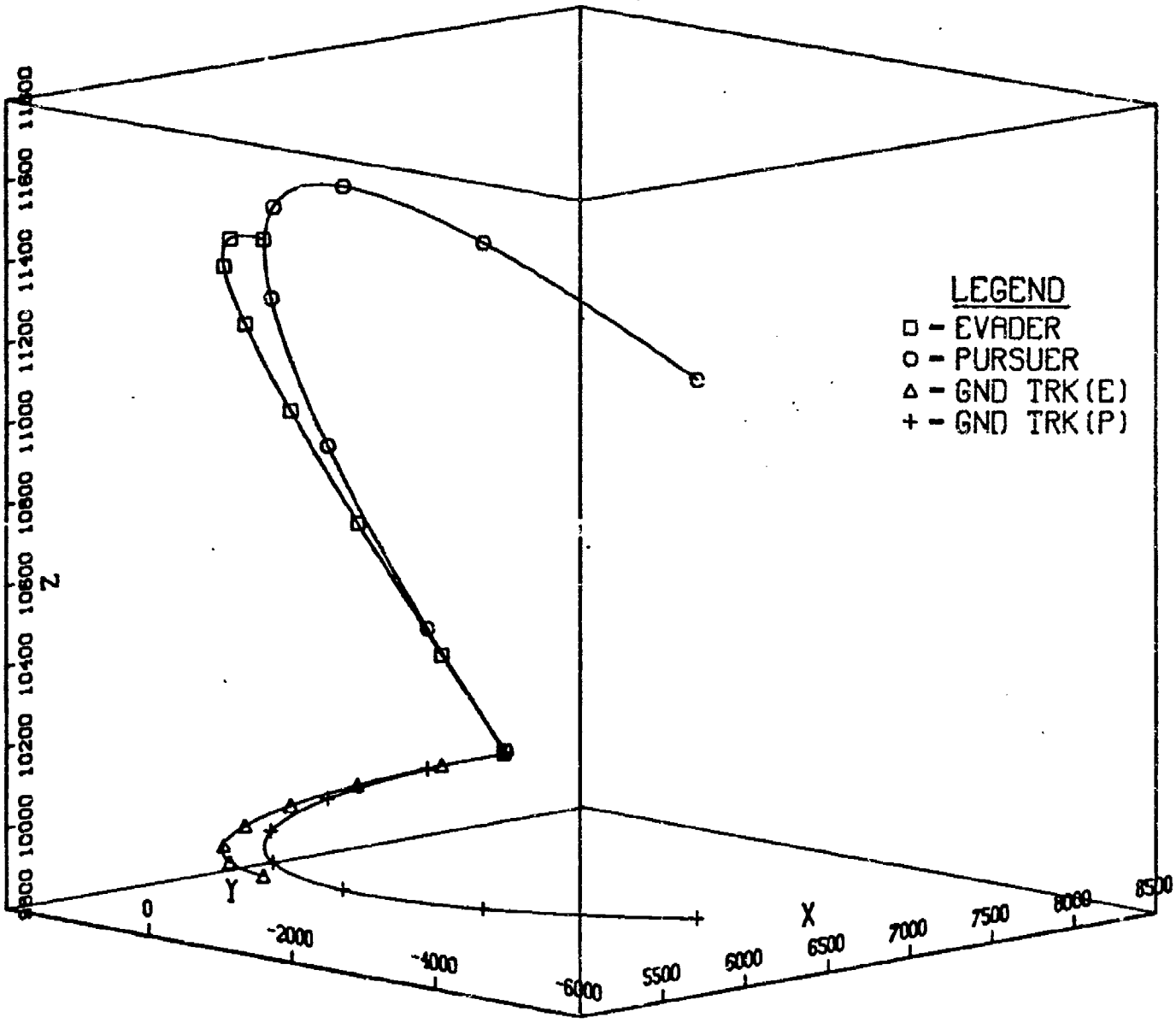

Fig. 4.

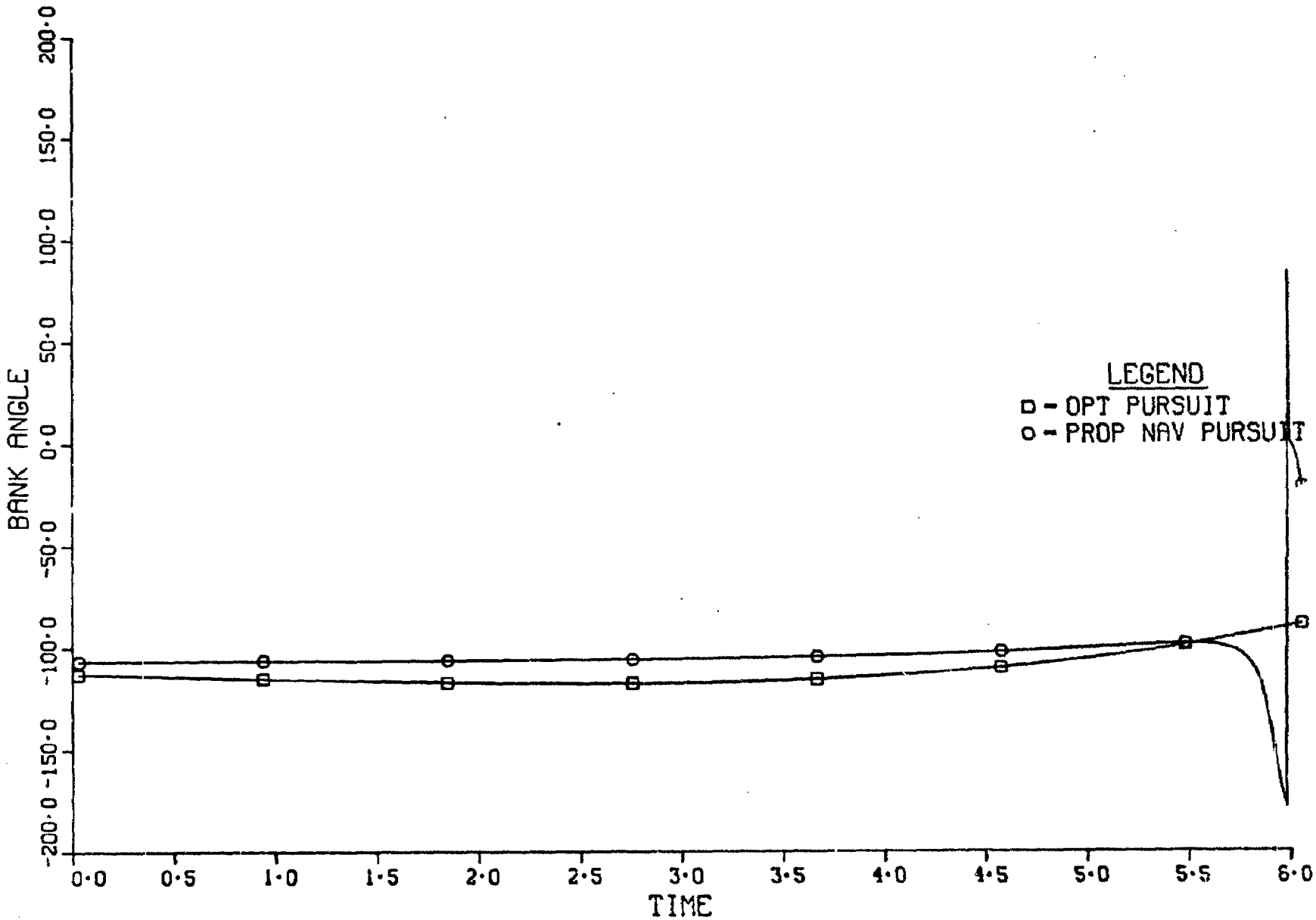
OPT VERSUS PROP NAV BANK ANGLE
BANK ANGLE
200·0
150·0
100·0
50·0
0·0
-50·0
-100·0
-150·0
-200·0
0·0
0·5
1·0
1·5
2·0
2·5
3·0
3·5
4·0
4·5
5·0
5·5
6·0
TIME
LEGEND
□ - OPT PURSUIT
○ - PROP NAV PURSUIT

Fig. 5

OPT EVASION-OPT PURSUIT

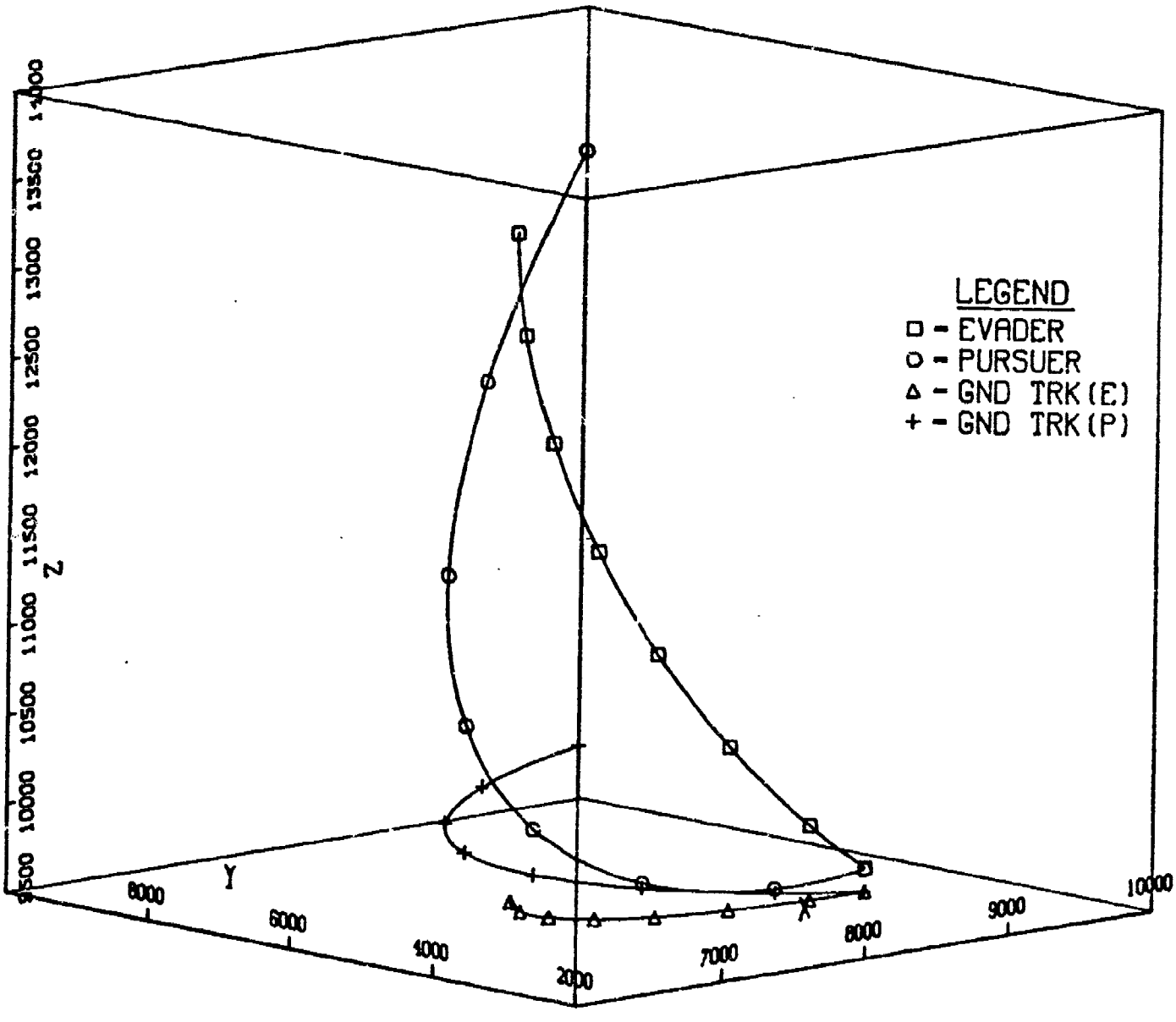

Fig. 6

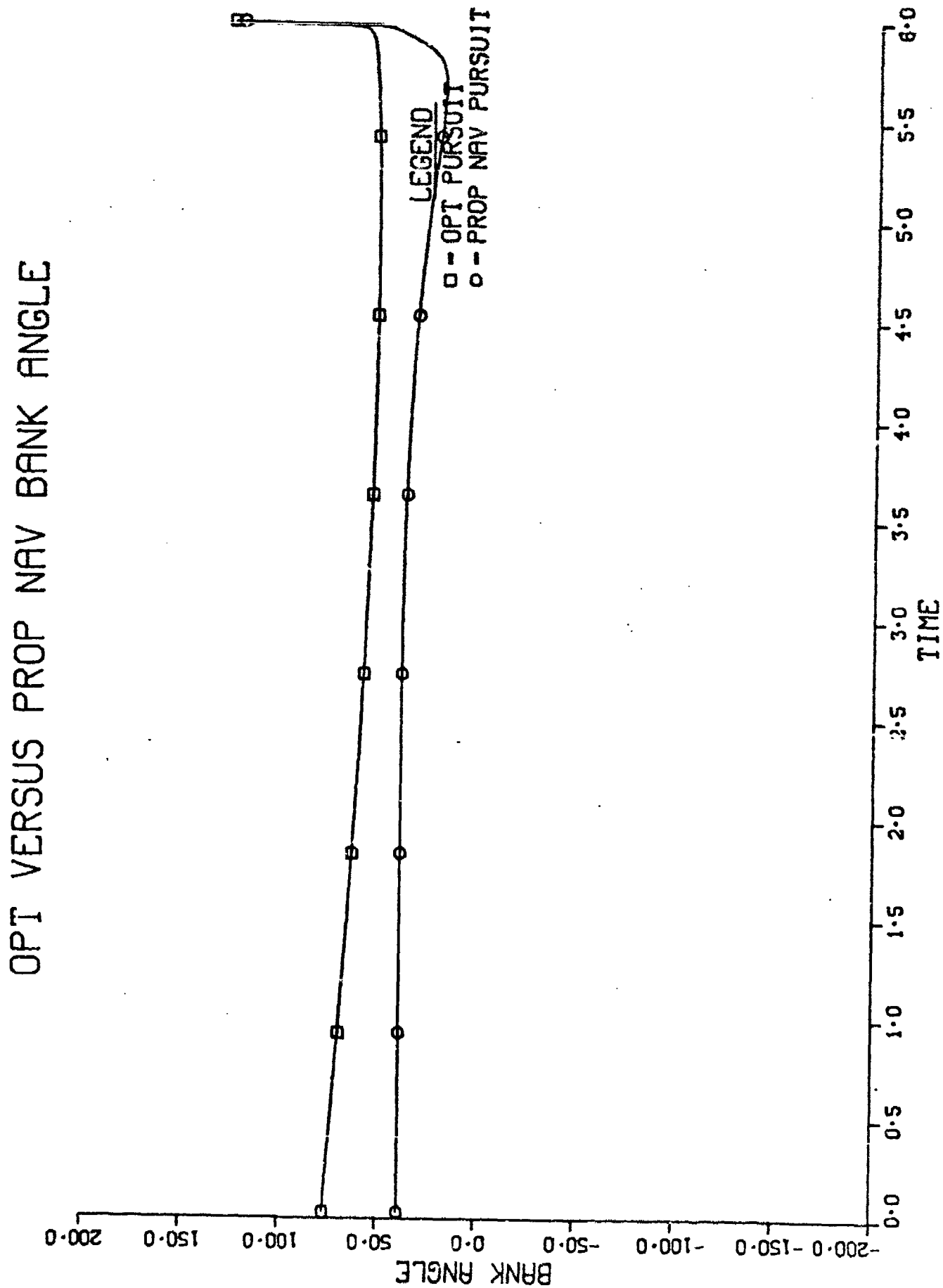
OPT VERSUS PROP NAV BANK ANGLE
LEGEND
□ - OPT PURSUIT
o - PROP NAV PURSUIT
BANK ANGLE
200·0
150·0
100·0
50·0
0·0
-50·0
-100·0
-150·0 -200·0
TIME
0·0
0·5
1·0
1·5
2·0
2·5
3·0
3·5
4·0
4·5
5·0
5·5
6·0

Fig. 7

OPT EVASION-OPT PURSUIT

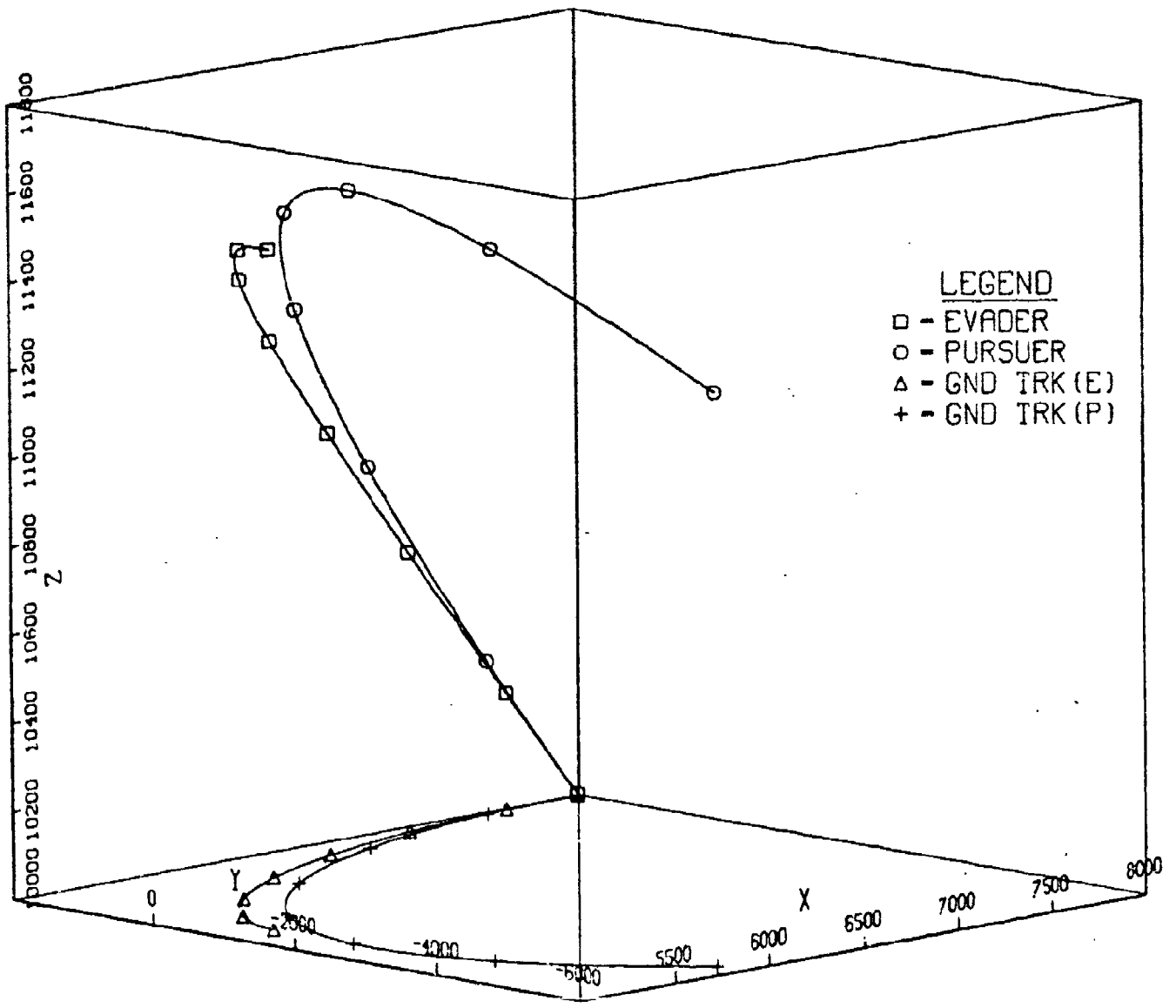

Fig. 8

OPT VERSUS PROP NAV BANK ANGLE

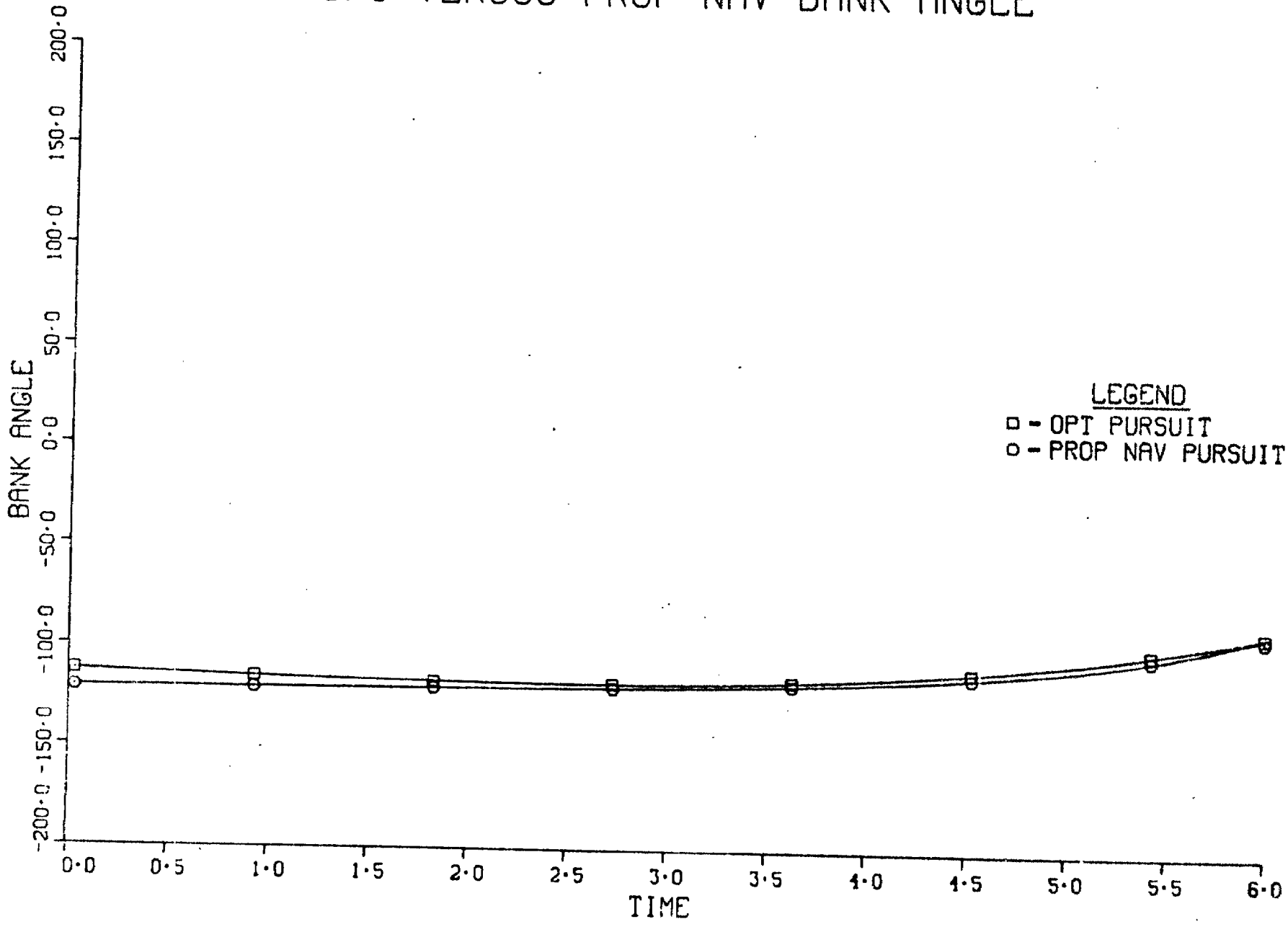

Fig. 9

OPT EVASION-OPT PURSUIT

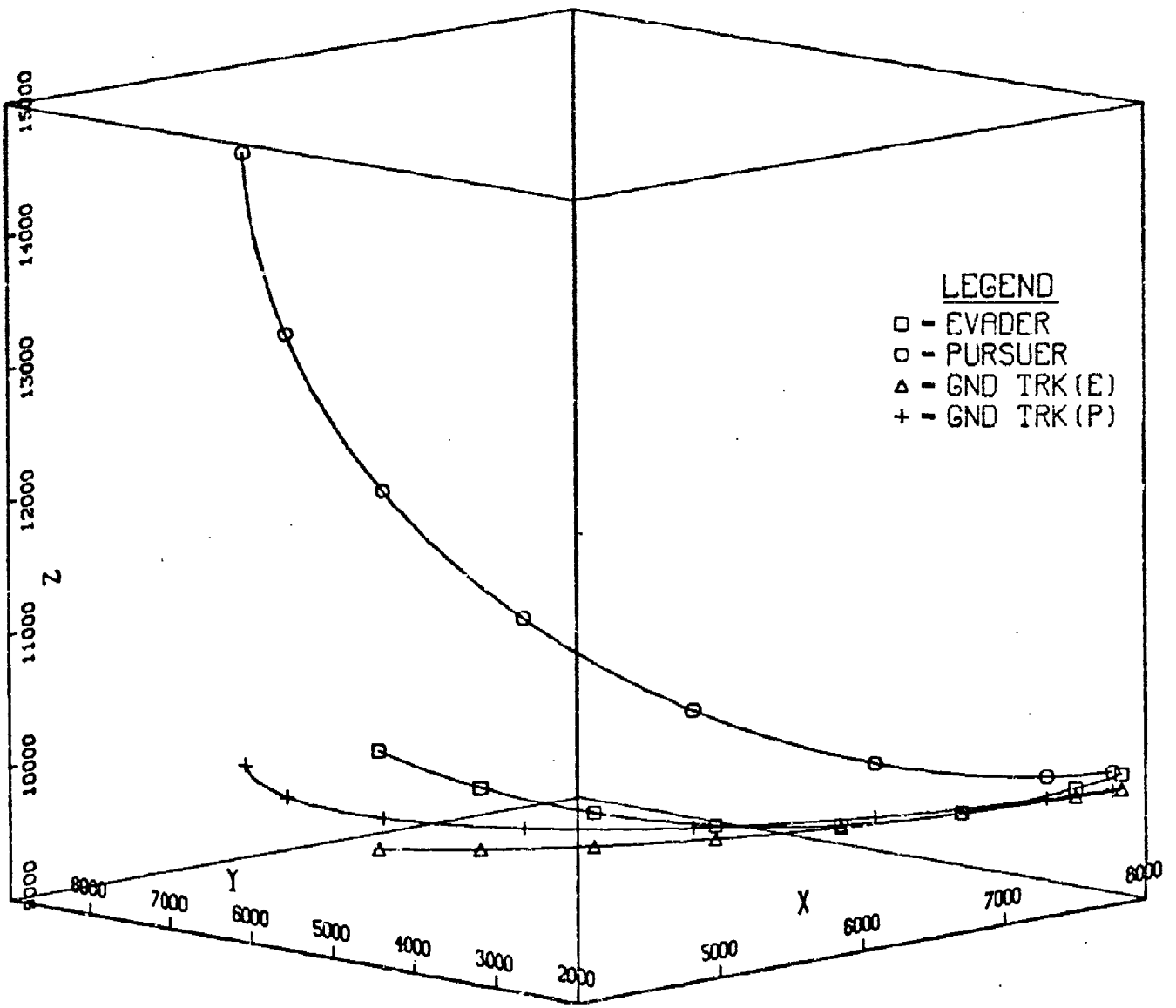

Fig. 10

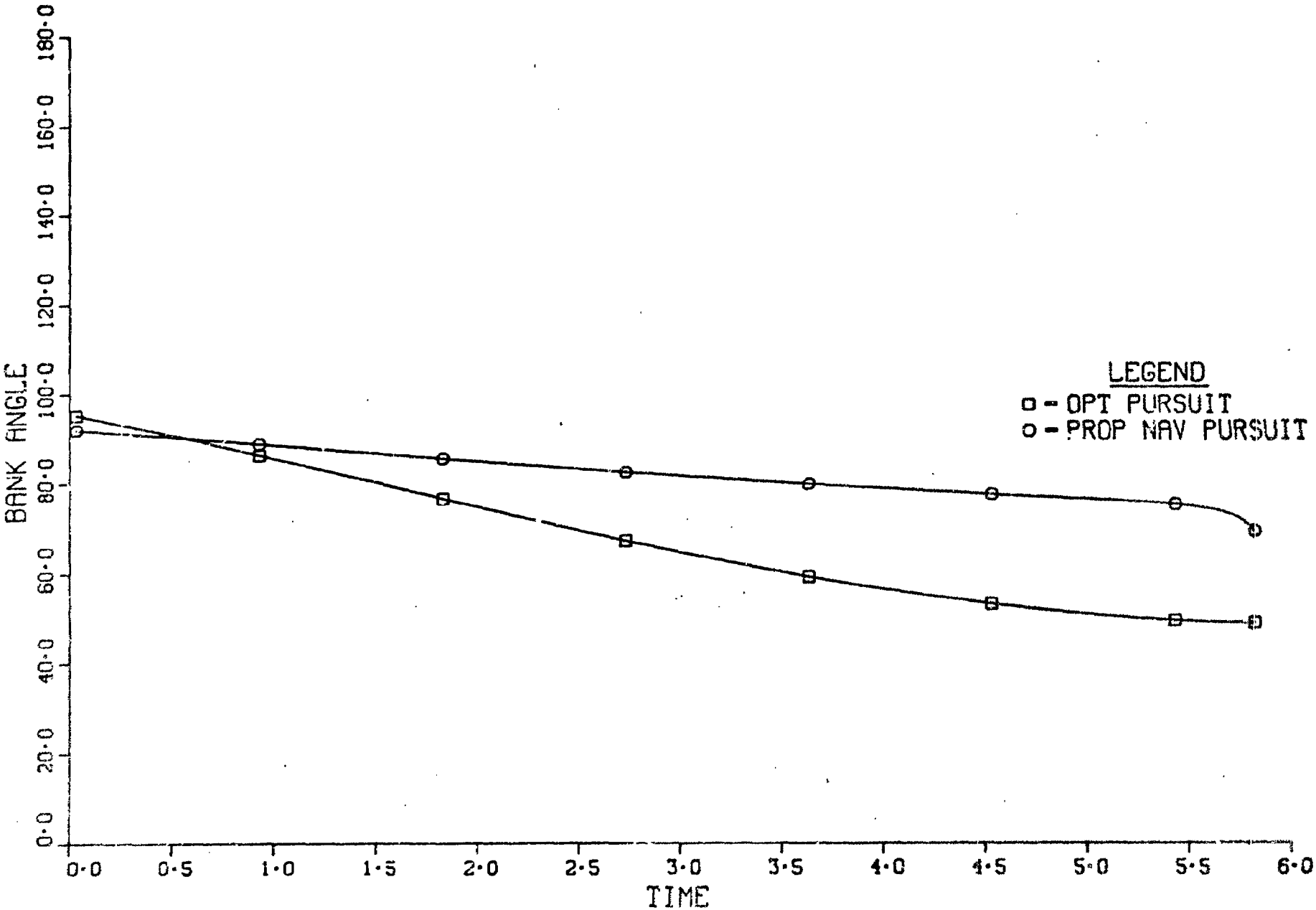
OPT VERSUS PROP NAV BANK ANGLE
BANK ANGLE
0·0
20·0
40·0
60·0
80·0
100·0
120·0
140·0
160·0
180·0
0·0
0·5
1·0
1·5
2·0
2·5
3·0
3·5
4·0
4·5
5·0
5·5
6·0
TIME
LEGEND
□ - OPT PURSUIT
○ - PROP NAV PURSUIT

Fig. 11

OPT EVASION-OPT PURSUIT

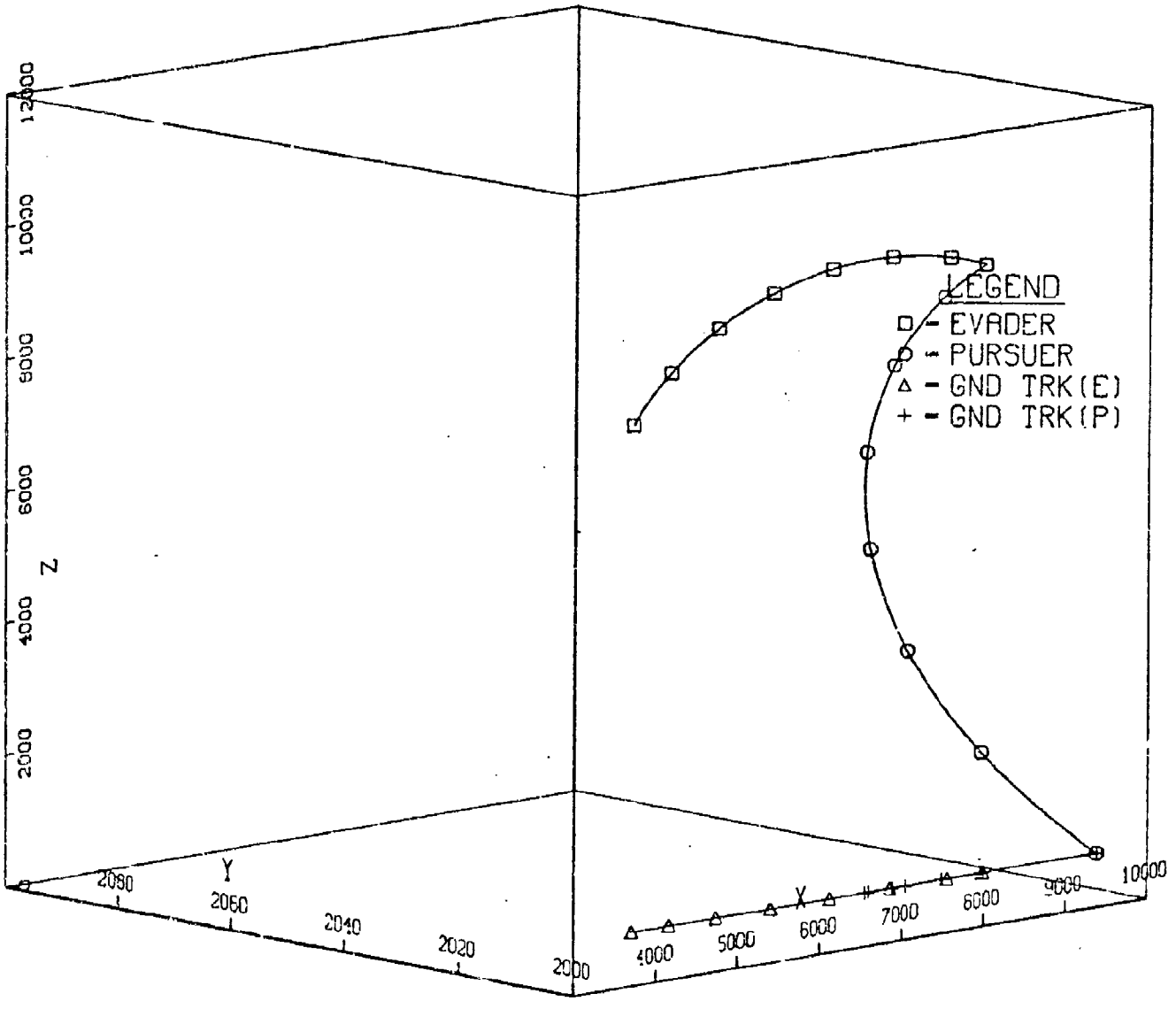

Fig. 12

OPT EVASION-OPT PURSUIT

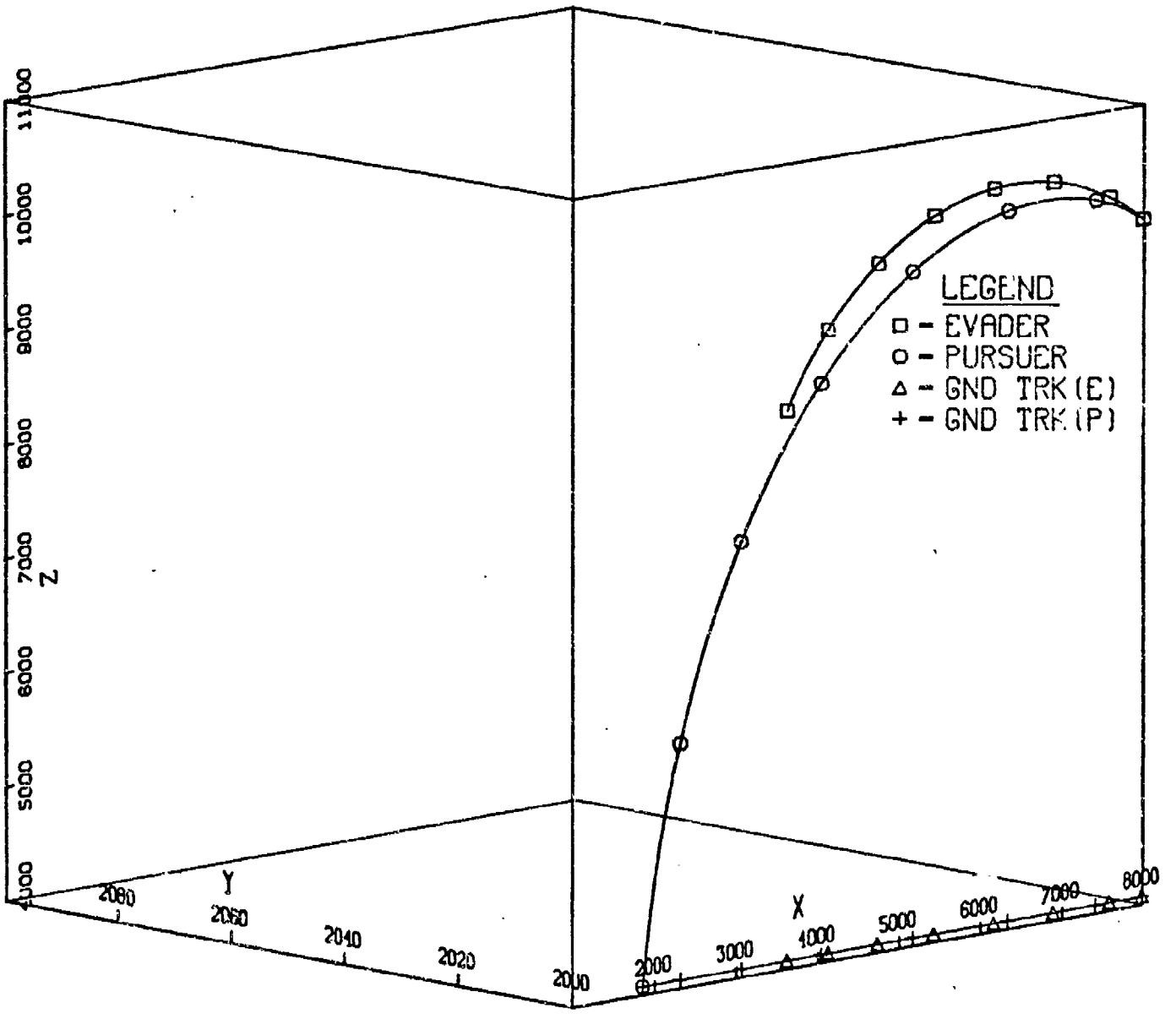

Fig. 13

OPT EVASION-OPT PURSUIT

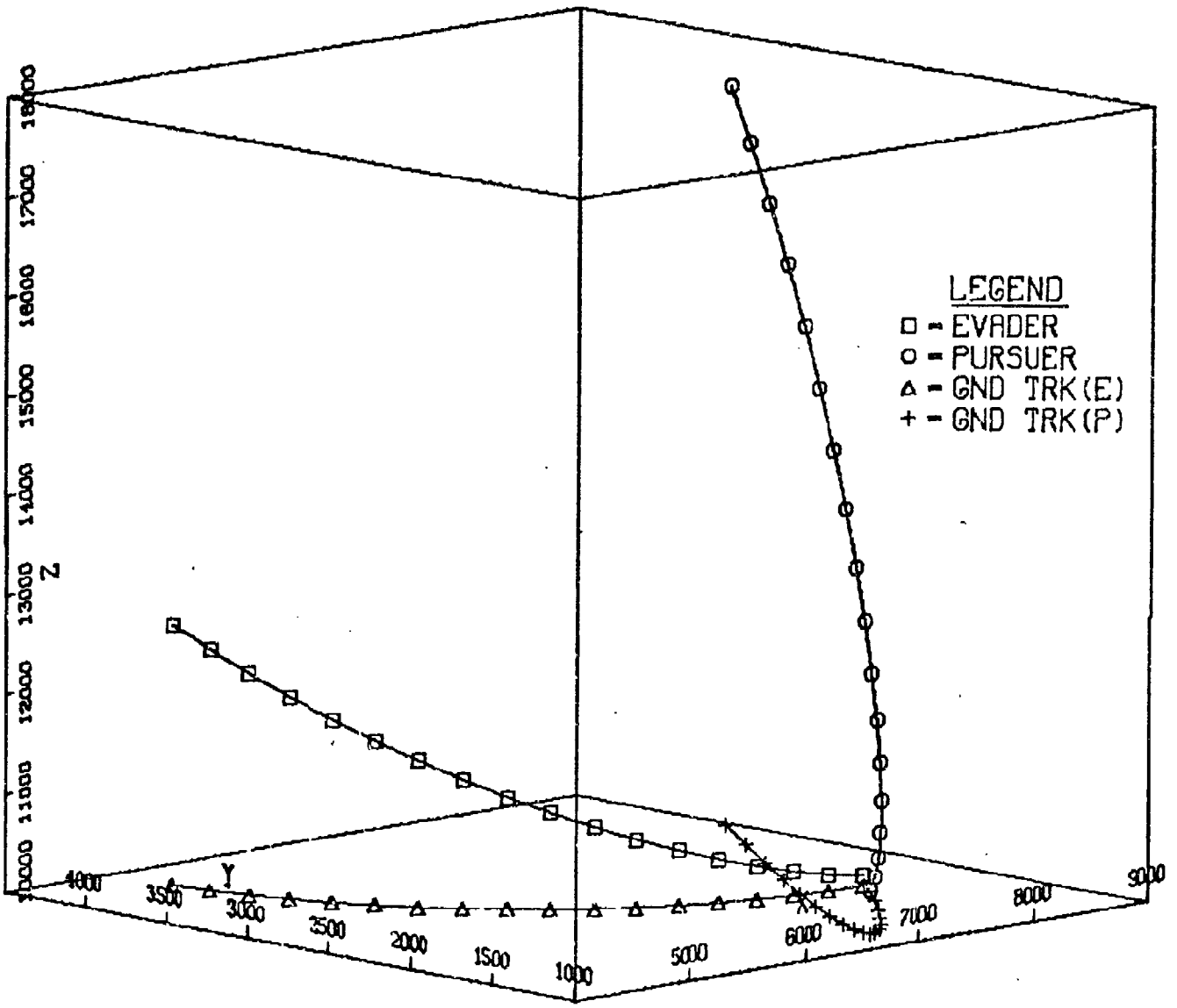

Fig. 14

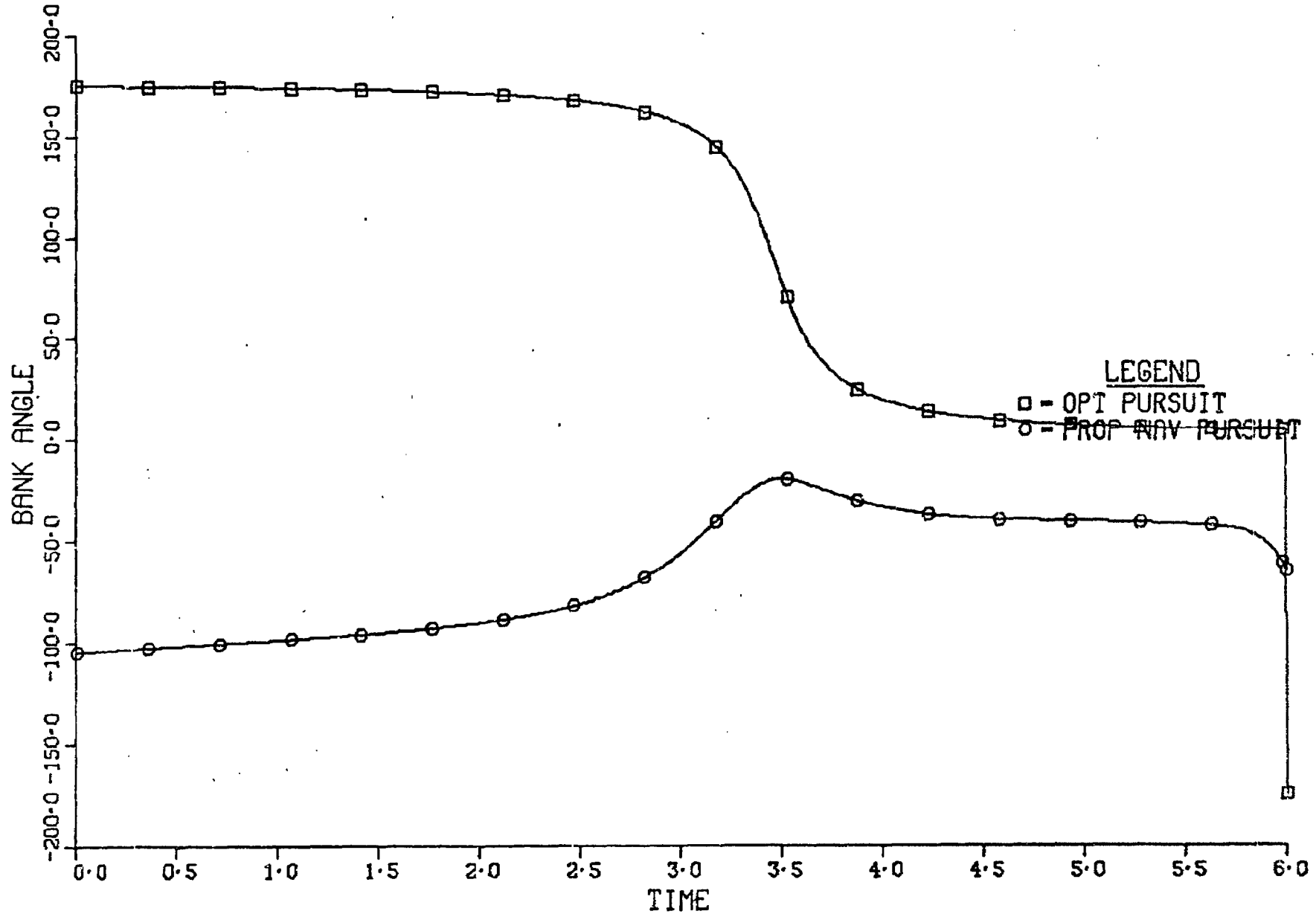
OPT VERSUS PROP NAV BANK ANGLE
BANK ANGLE
200·0
150·0
100·0
50·0
0·0
-50·0
-100·0
-150·0
-200·0
0·0
0·5
1·0
1·5
2·0
2·5
3·0
3·5
4·0
4·5
5·0
5·5
6·0
TIME
LEGEND
□ = OPT PURSUIT
○ = PROP NAV PURSUIT

Fig. 15

Table II

Saddle Point Solution

State	Evader	Pursuer
x	4972 ft	9199 ft
y	2986 ft	10260 ft
z	33150 ft	33170 ft
v	706 ft/sec	2219 ft/sec
γ	- 846 rads	-.619 rads
σ	-.632 rads	-2.41 rads
λ_x	209	-209
λ_y	211	-211
λ_z	180	-211
λ_v	179	2563
λ_γ	681248	-607926
λ_σ	847488	-1478936

OPT EVASION-OPT PURSUIT

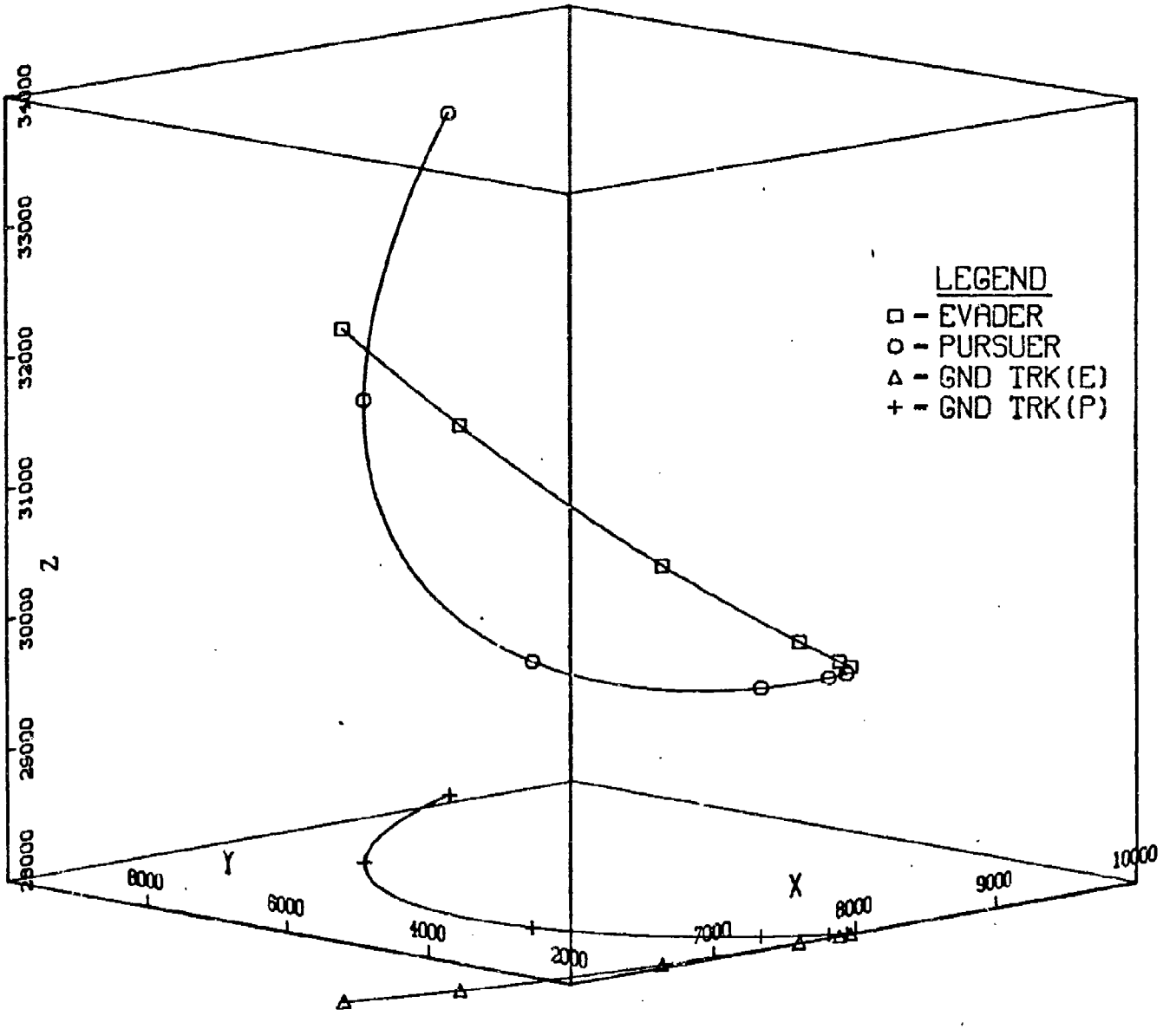

Fig. 16

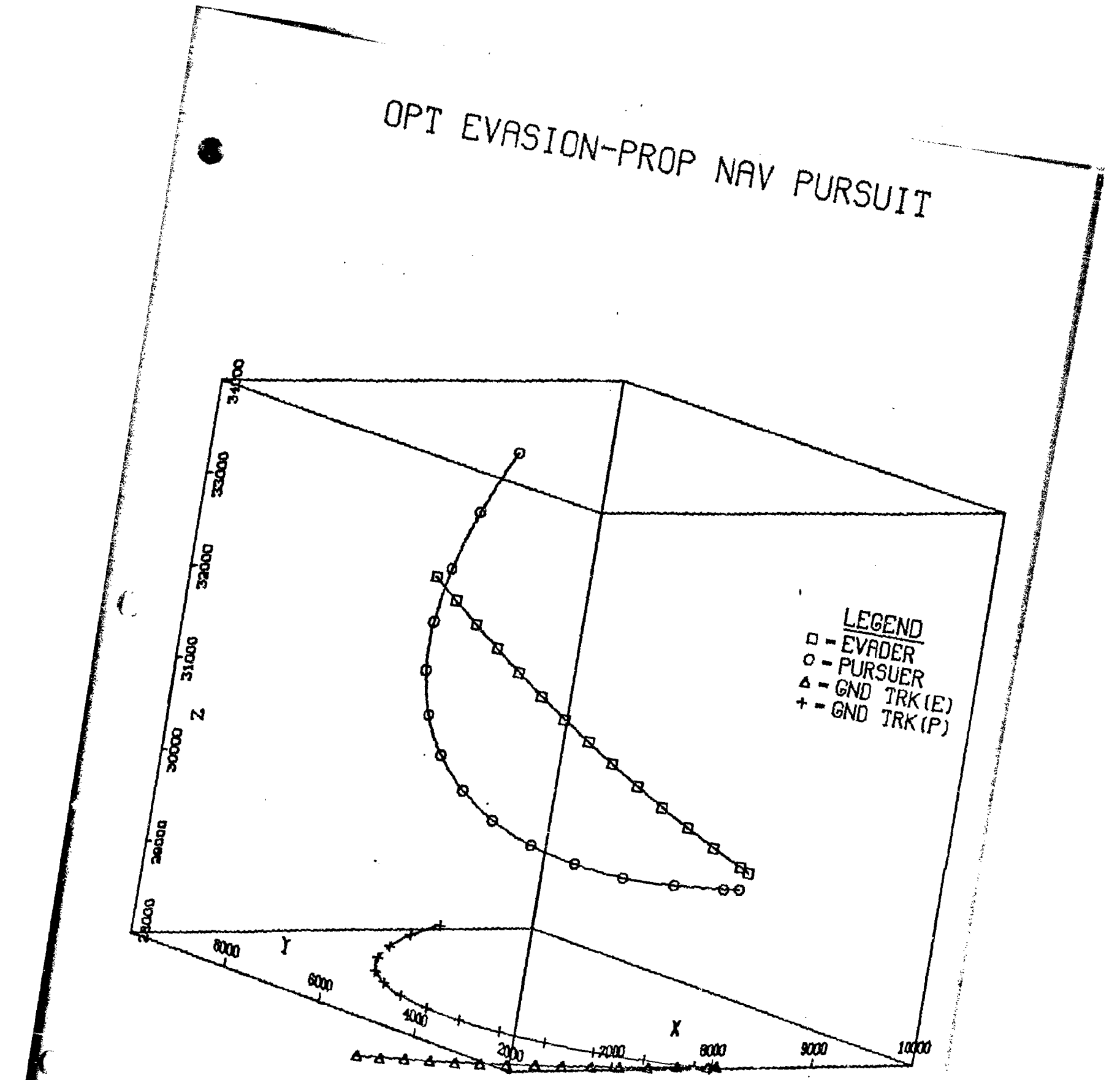
OPT EVASION-PROP NAV PURSUIT
34000
33000
32000
31000
30000
29000
28000
Z
8000
Y
6000
4000
2000
X
+2000
8000
9000
10000
LEGEND
□ - EVADER
○ - PURSUER
△ - GND TRK(E)
+ - GND TRK(P)

Fig. 17

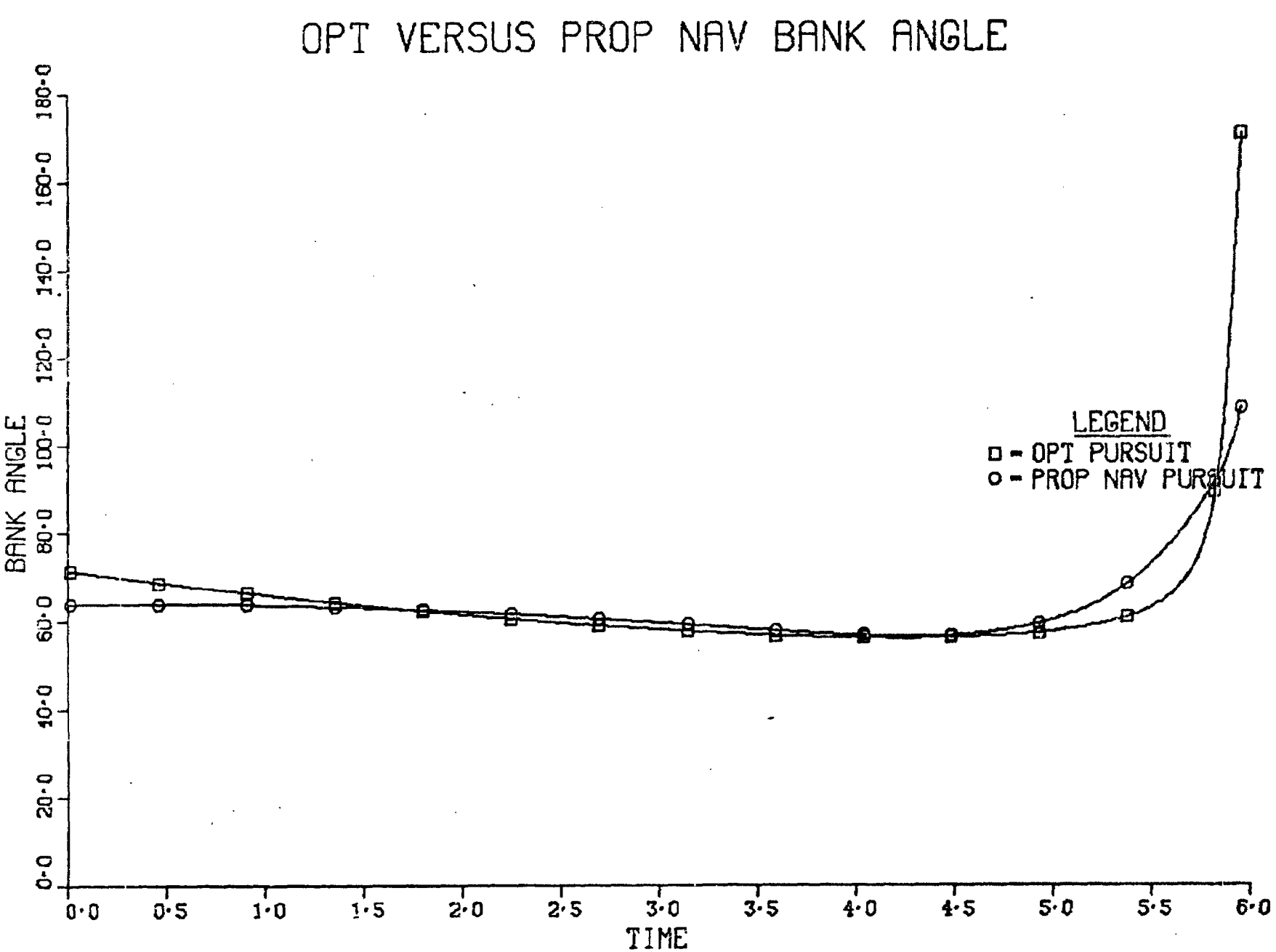
OPT VERSUS PROP NAV BANK ANGLE
BANK ANGLE
0·0
20·0
40·0
60·0
80·0
100·0
120·0
140·0
160·0
180·0
0·0
0·5
1·0
1·5
2·0
2·5
3·0
3·5
4·0
4·5
5·0
5·5
6·0
TIME
LEGEND
□ - OPT PURSUIT
○ - PROP NAV PURSUIT

FIF. 18

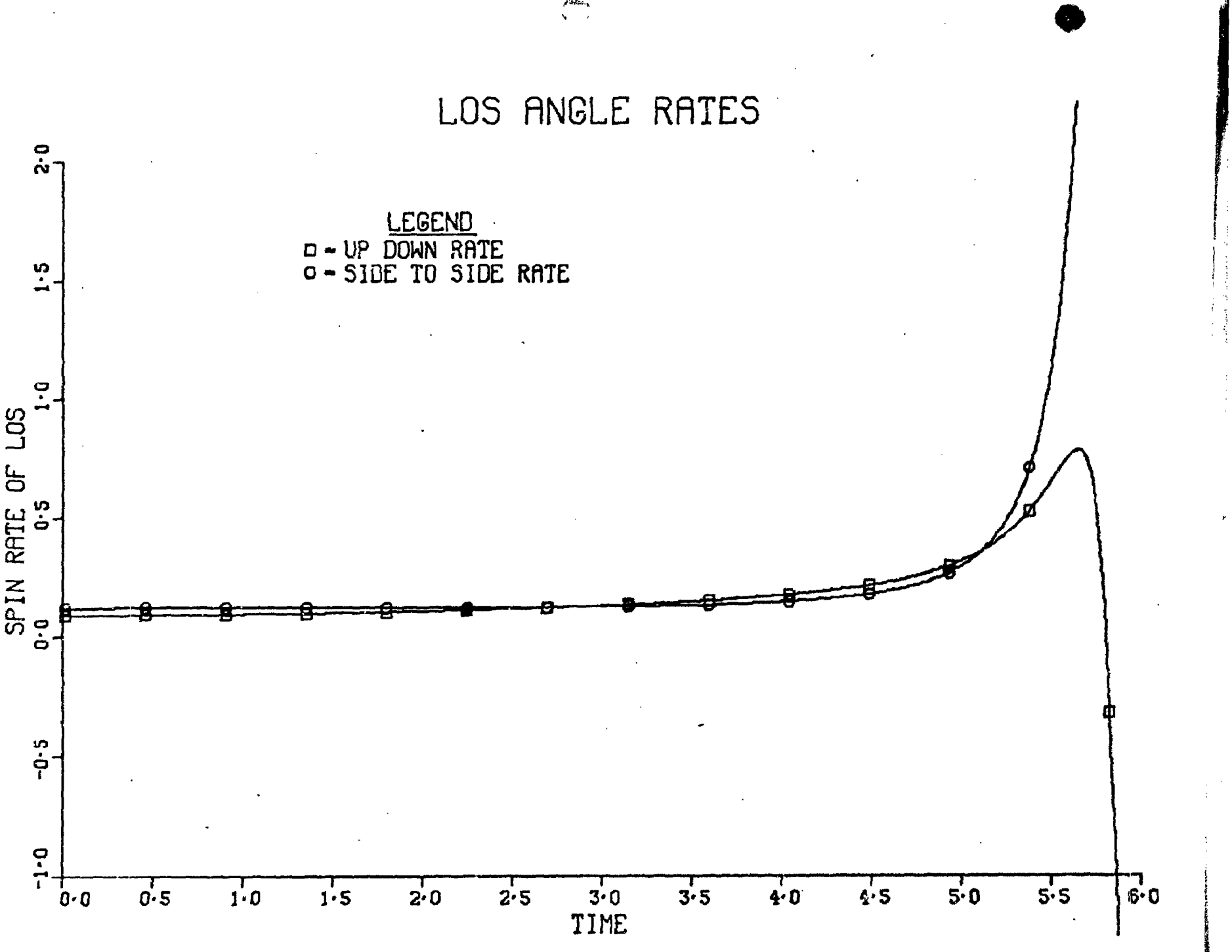
LOS ANGLE RATES
LEGEND
□ - UP DOWN RATE
○ - SIDE TO SIDE RATE
SPIN RATE OF LOS
2·0
1·5
1·0
0·5
0·0
-0·5
-1·0
0·0
0·5
1·0
1·5
2·0
2·5
3·0
3·5
4·0
4·5
5·0
5·5
6·0
TIME

Fig. 19

Table III

Saddle Point Solution

State	Evader	Pursuer
x	6457 ft	9249 ft
y	3807 ft	6667 ft
z	13625 ft	16112 ft
v	773 ft/sec	2065 ft/sec
γ	-078 rads	-.38 rads
σ	-2.03 rads	-2.57 rads
λ_x	2.02	-2.02
λ_y	2.02	-2.02
λ_z	1.78	-1.88
λ_v	-7.8	20.8
λ_γ	-5698	8178
λ_σ	6796	-6959

OPT EVASION-OPT PURSUIT

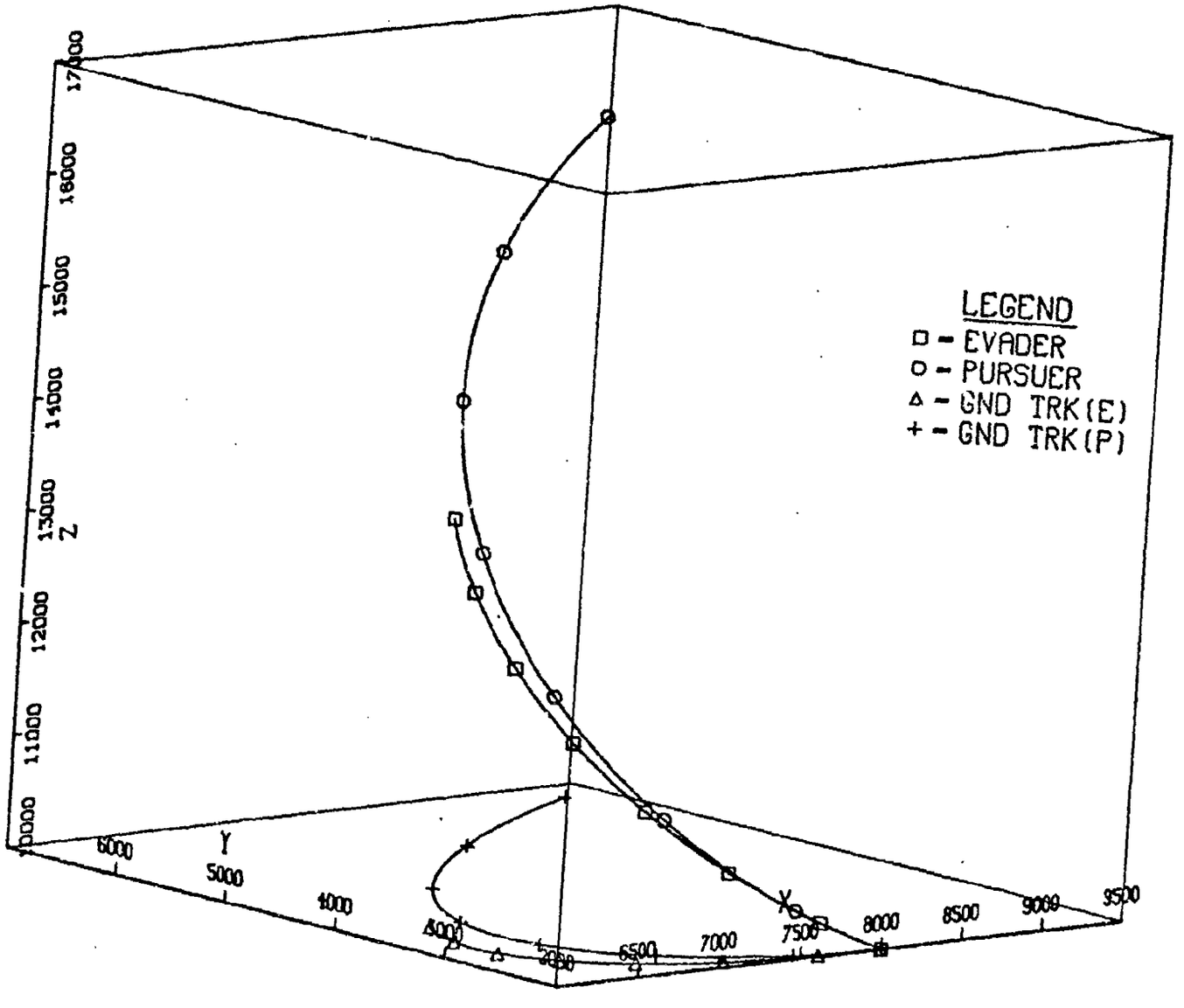

Fig. 20

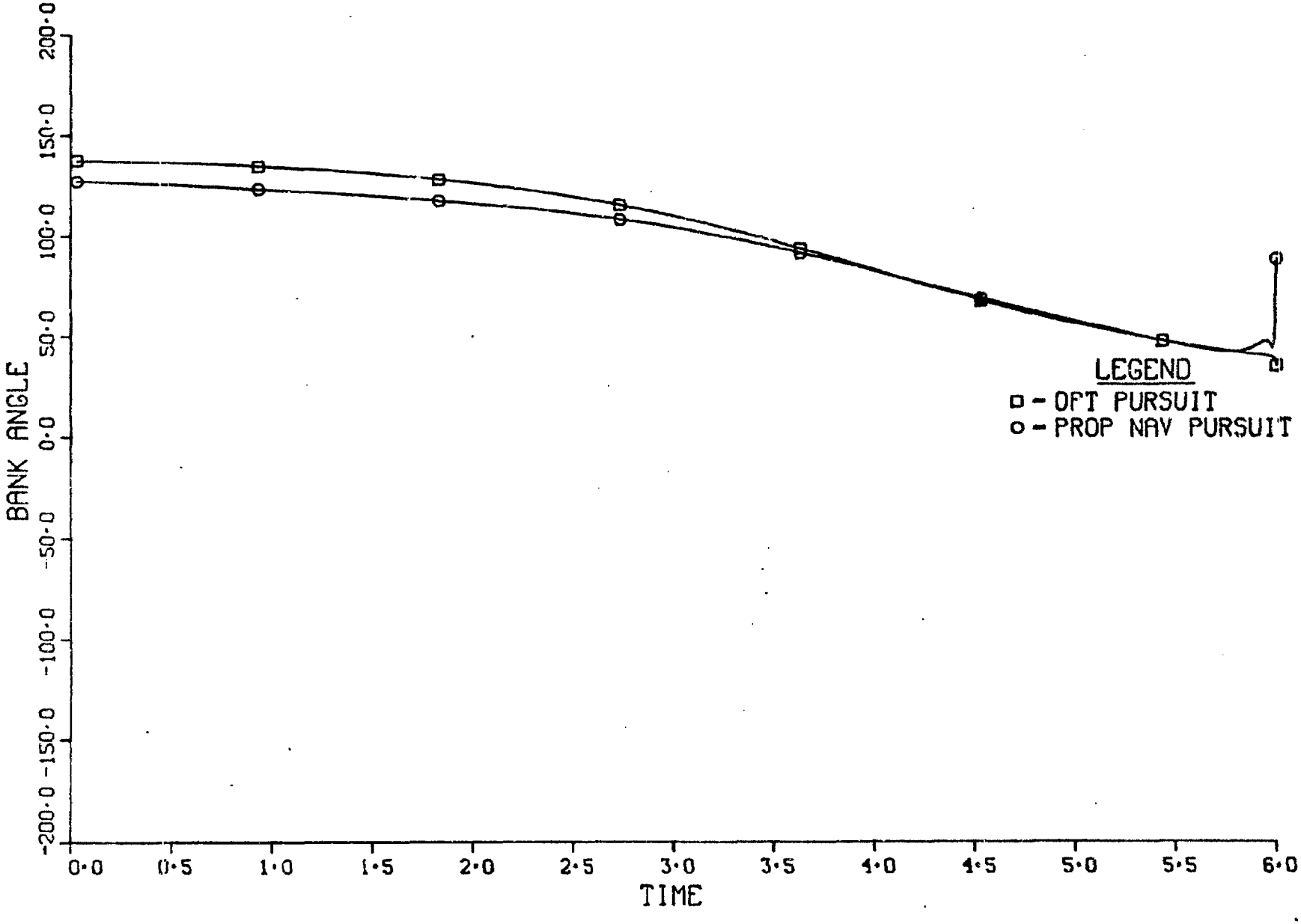
OPT VERSUS PROP NAV BANK ANGLE
BANK ANGLE
200·0
150·0
100·0
50·0
0·0
-50·0
-100·0
-150·0
-200·0
0·0
0·5
1·0
1·5
2·0
2·5
3·0
3·5
4·0
4·5
5·0
5·5
6·0
TIME
LEGEND
□ - OPT PURSUIT
○ - PROP NAV PURSUIT

Fig. 21

OPT EVASION-PROP NAV PURSUIT

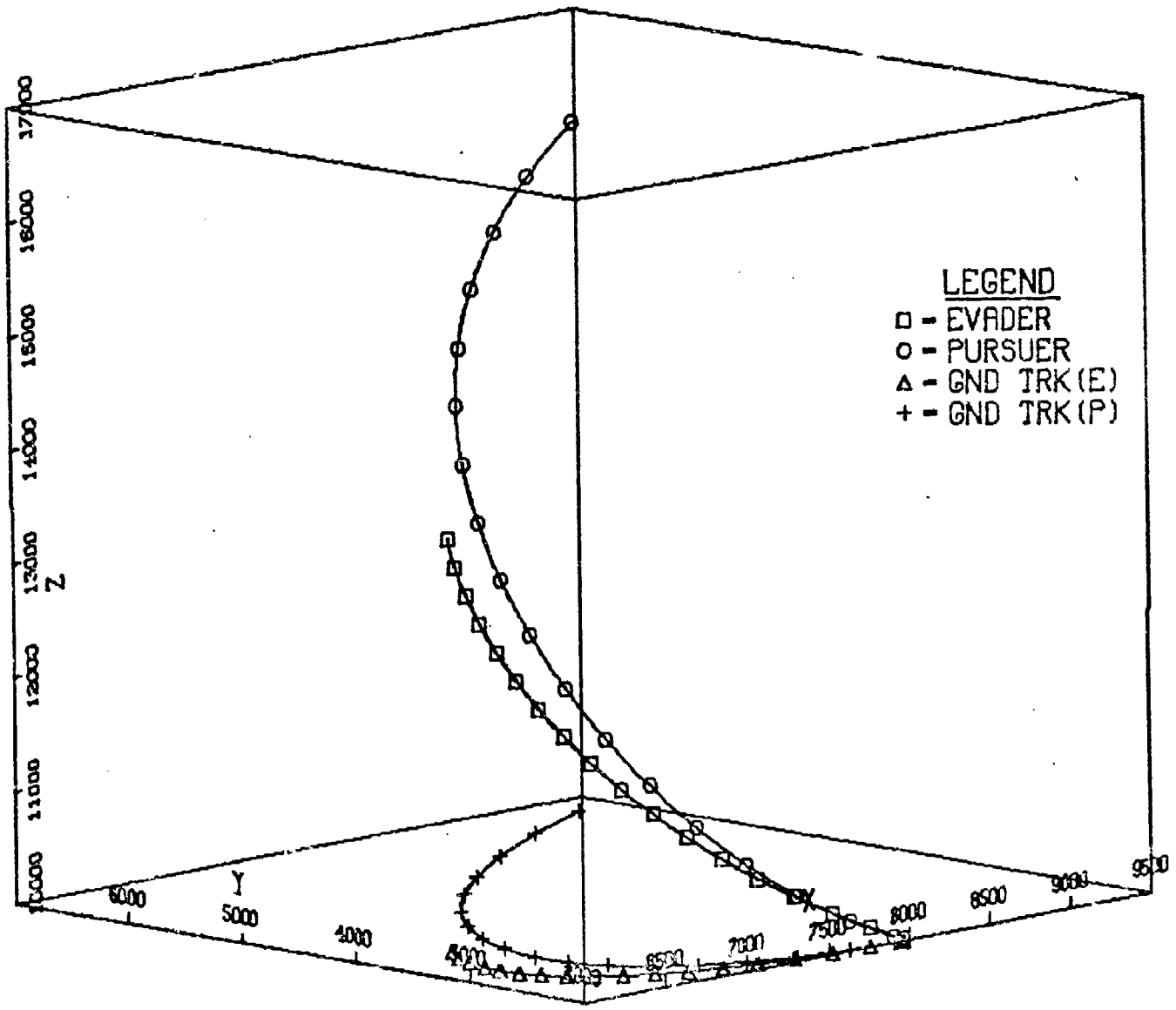

Fig. 22

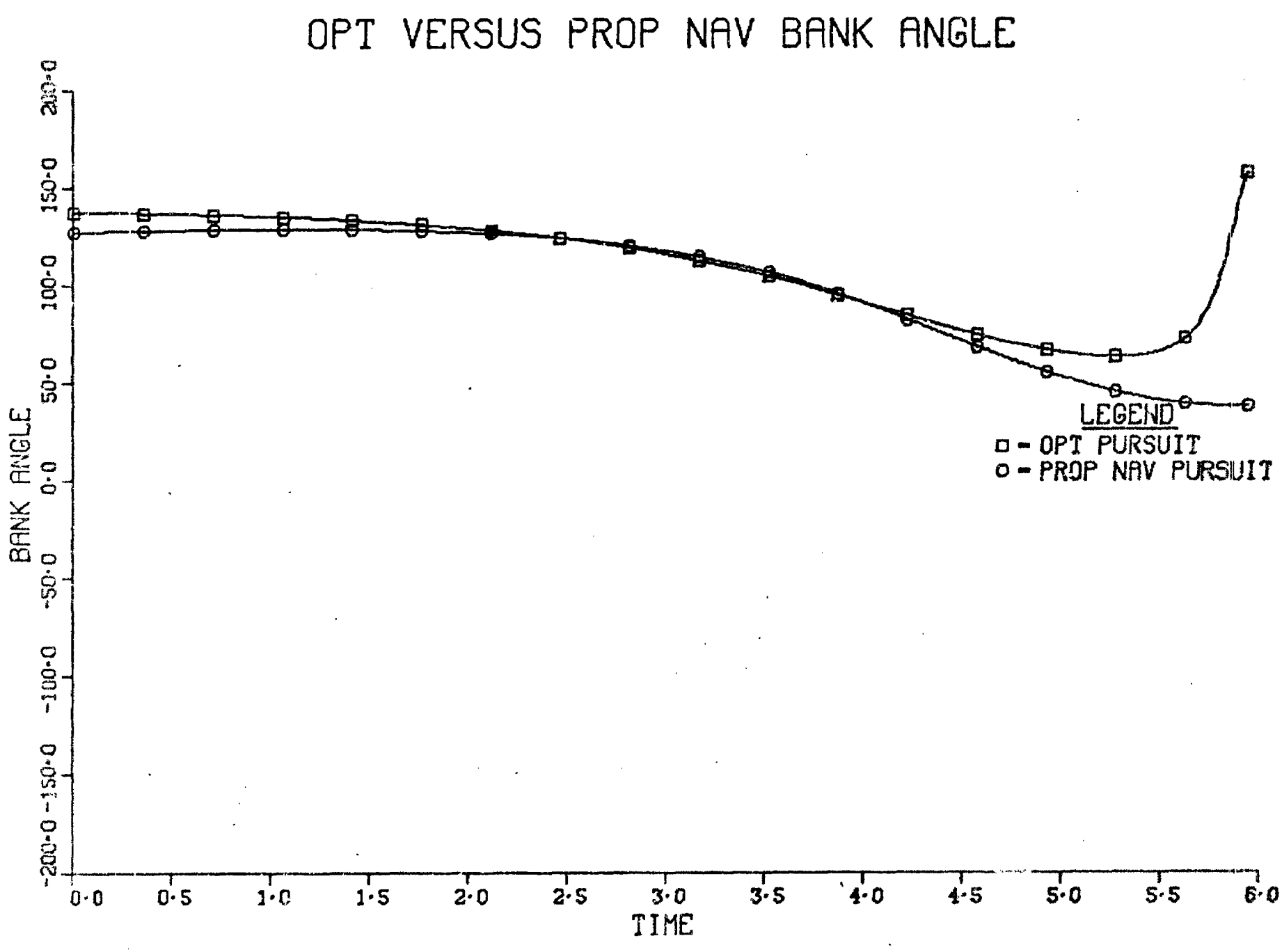
OPT VERSUS PROP NAV BANK ANGLE
BANK ANGLE
-200·0
-150·0
-100·0
-50·0
0·0
50·0
100·0
150·0
200·0
0·0
0·5
1·0
1·5
2·0
2·5
3·0
3·5
4·0
4·5
5·0
5·5
6·0
TIME
LEGEND
□ - OPT PURSUIT
○ - PROP NAV PURSUIT

Fig. 23

Table IV

Saddle Point Solution

State	Evader	Pursuer
x	4936 ft	9341 ft
y	3013 ft	10358 ft
z	33198 ft	33326 ft
v	703 ft/sec	2235 ft/sec
γ	-.84 rads	-.62 rads
σ	-.64 rads	-2.43 rads
λ_x	200	-200
λ_y	199	-199
λ_z	171	-201
λ_v	174	2473
λ_γ	650585	-554617
λ_σ	814617	-1409966

OPT EVASION-OPT PURSUIT

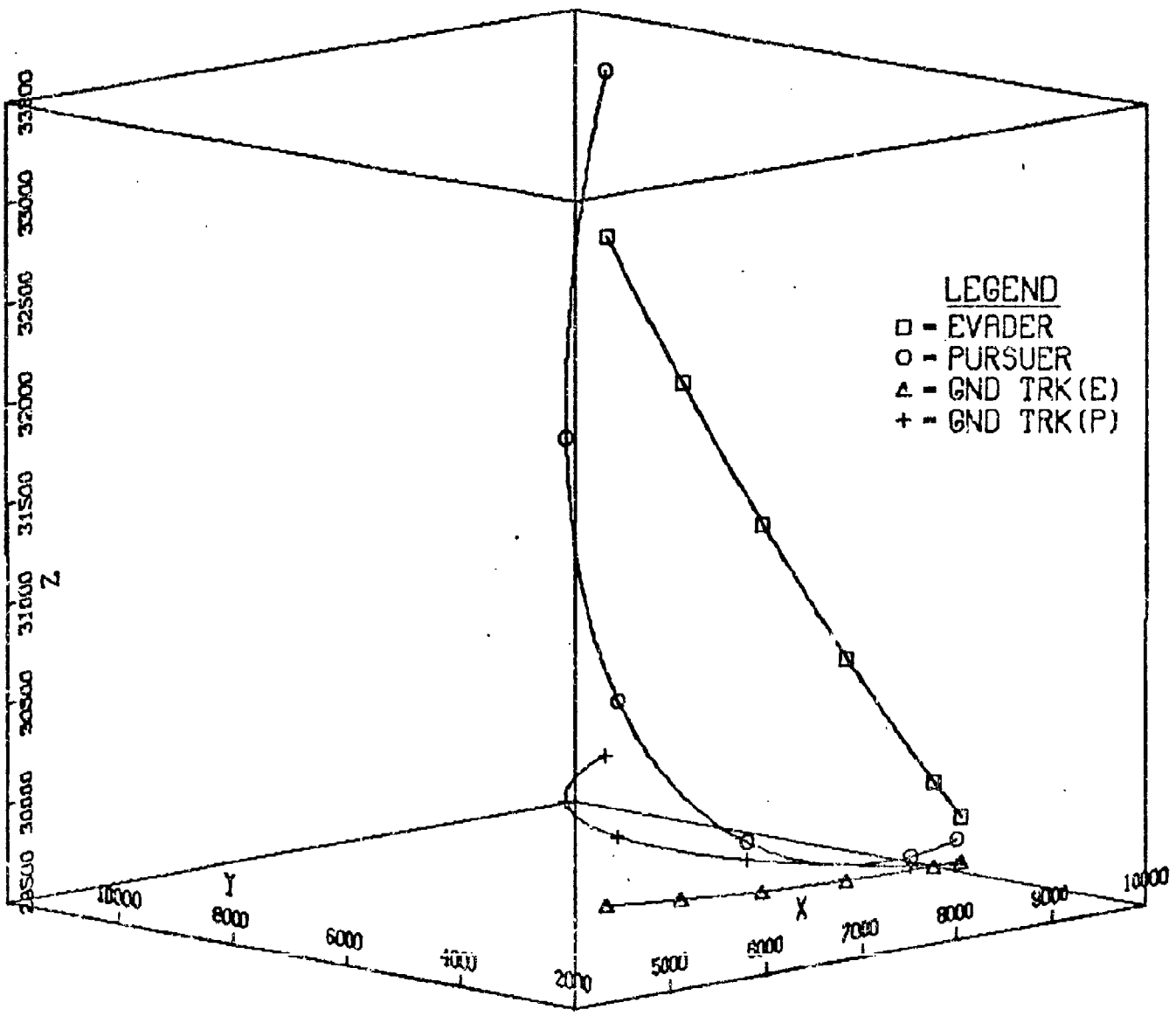

Fig. 24

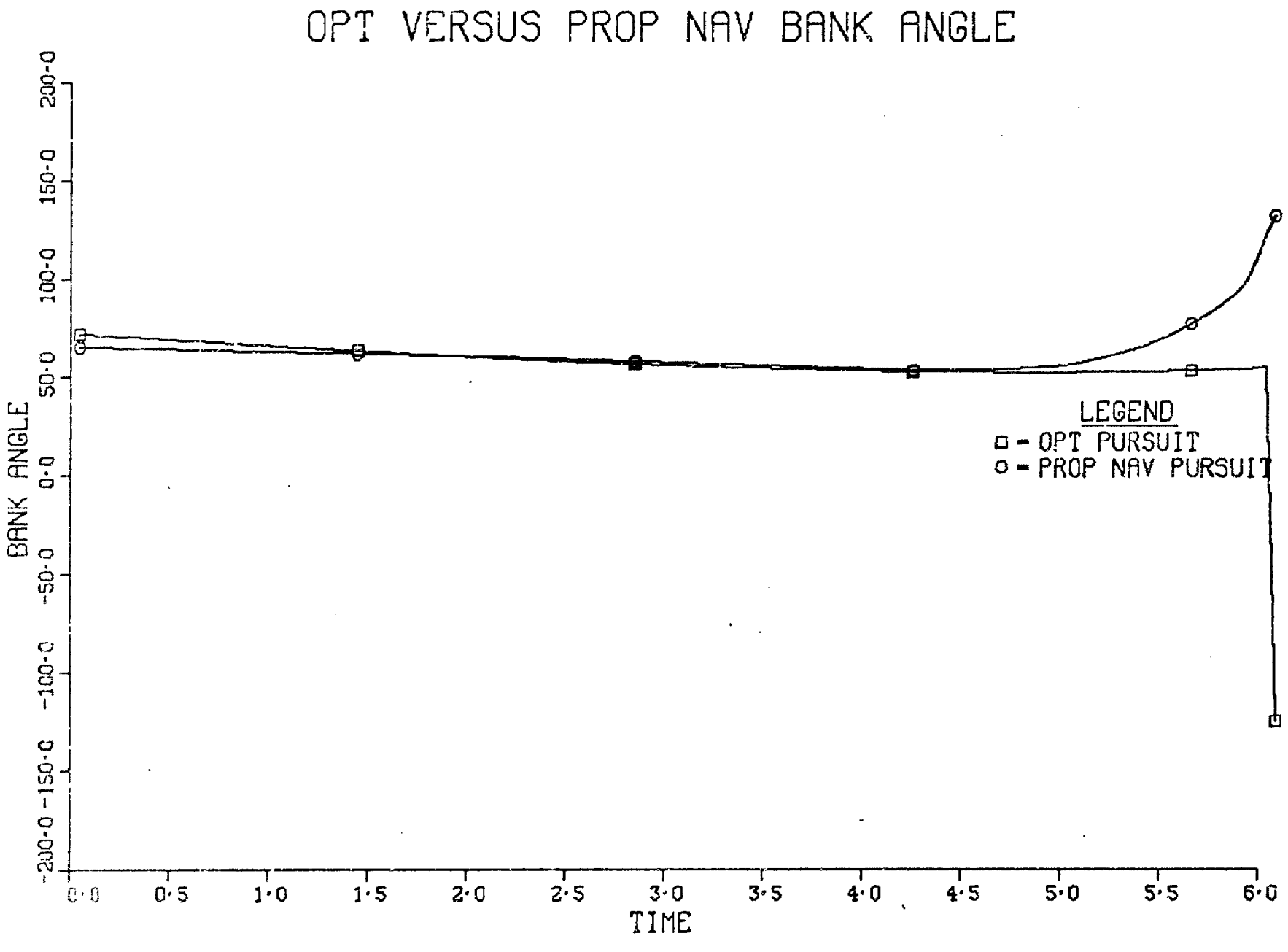
OPT VERSUS PROP NAV BANK ANGLE
BANK ANGLE
200·0
150·0
100·0
50·0
0·0
-50·0
-100·0
-150·0
-200·0
0·0
0·5
1·0
1·5
2·0
2·5
3·0
3·5
4·0
4·5
5·0
5·5
6·0
TIME
LEGEND
□ - OPT PURSUIT
○ - PROP NAV PURSUIT

OPT EVASION-PROP NAV PURSUIT

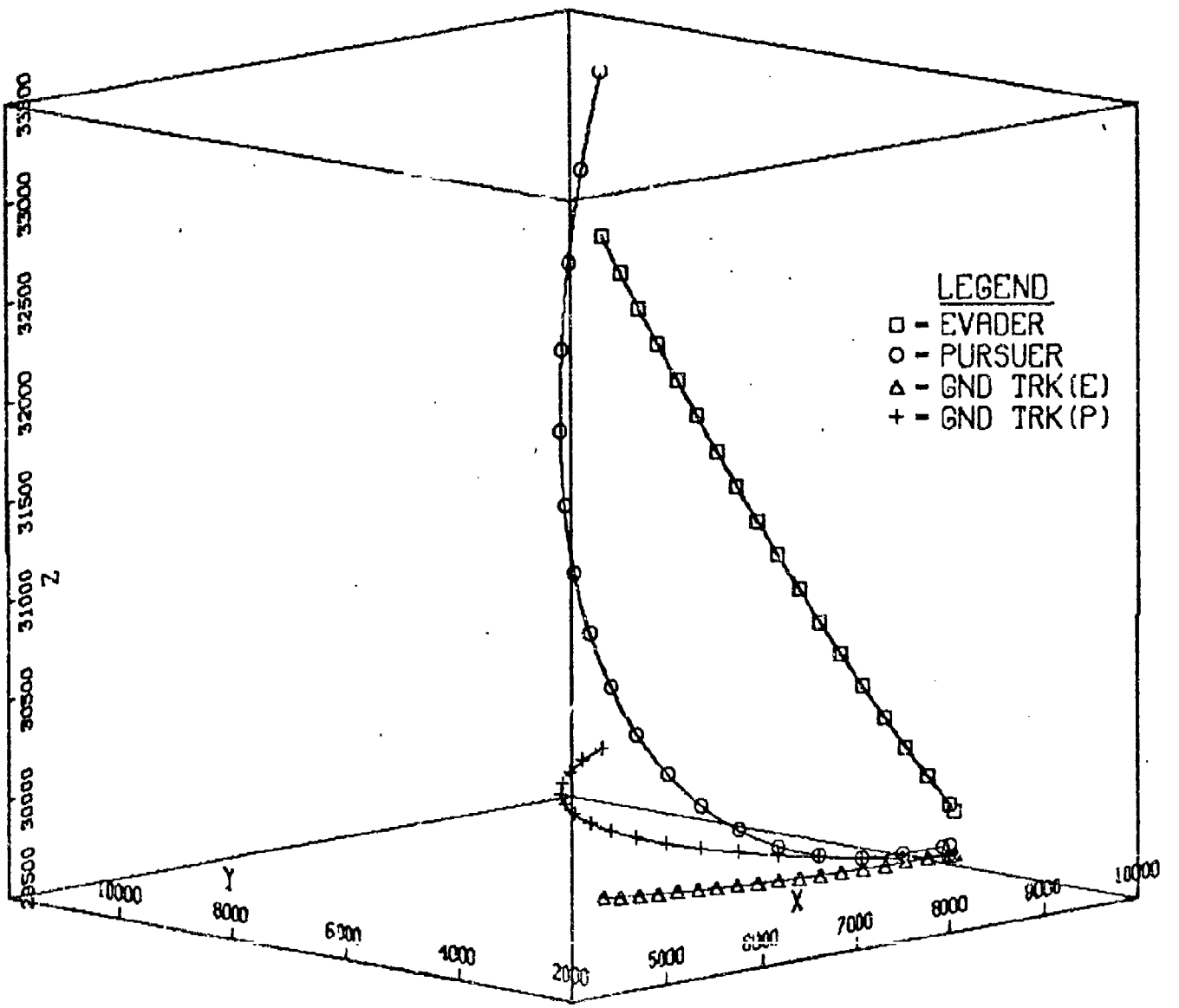

Fig. 26

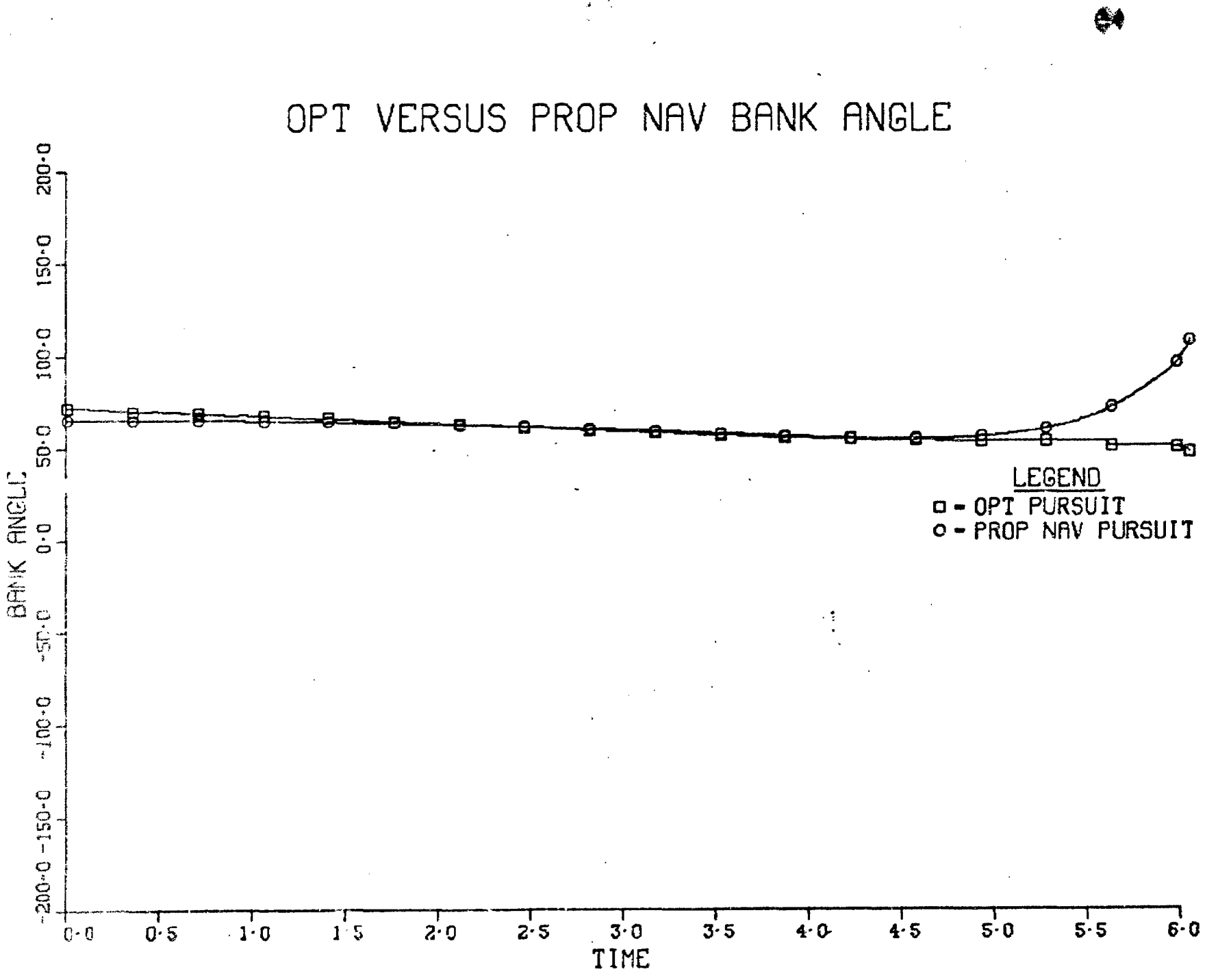
OPT VERSUS PROP NAV BANK ANGLE
BANK ANGLE
200·0
150·0
100·0
50·0
0·0
-50·0
-100·0
-150·0
-200·0
0·0
0·5
1·0
1·5
2·0
2·5
3·0
3·5
4·0
4·5
5·0
5·5
6·0
TIME
LEGEND
□ - OPT PURSUIT
○ - PROP NAV PURSUIT

Table V

Saddle Point Solution

State	Evader		Pursuer	
	$t_0 = 0$	$t_f = 6$	$t_0 = 0$	$t_f = 6$
x ft	4178	8003	10920	8002
y ft	4435	1999	10242	1998
z ft	11123	10003	7782	10002
v ft/sec	849	799	2491	999
γ rads	-.5	.1	-.29	1.08
σ rads	-1.2	.0	-2.18	.79
Costate				
λ_x	2.	2.	-2.	-2.
λ_y	2.	2.	-2.	-2.
λ_z	2.02	2.	-1.77	-2.
λ_v	-2.3	0.	13.	0
λ_γ	5533.	-8.4	-23734.	5.6
λ_σ	12518.	3.4	-10647.	-304

OPT EVASION-OPT PURSUIT

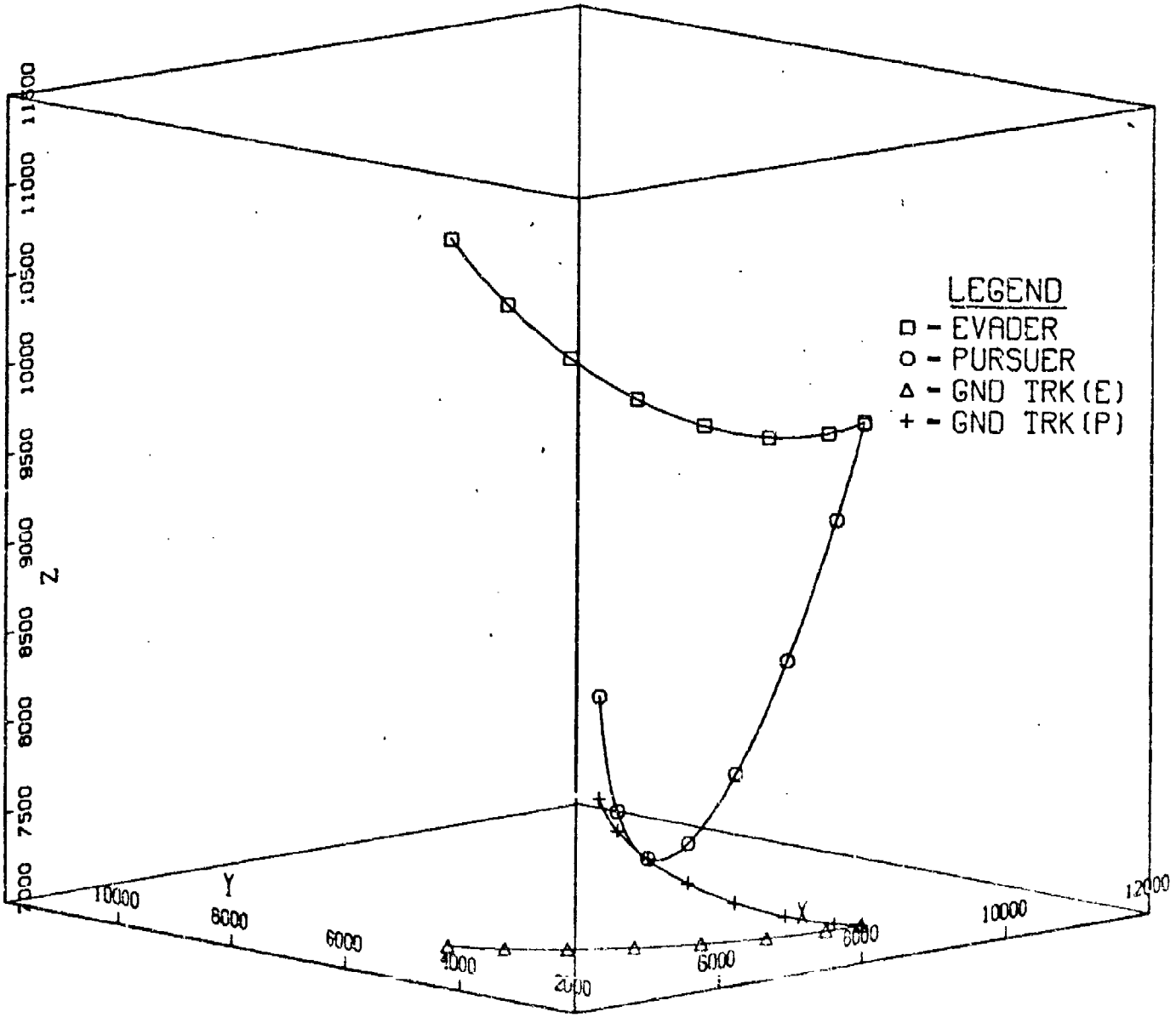

Fig. 28

OPT VERSUS PROP NAV BANK ANGLE

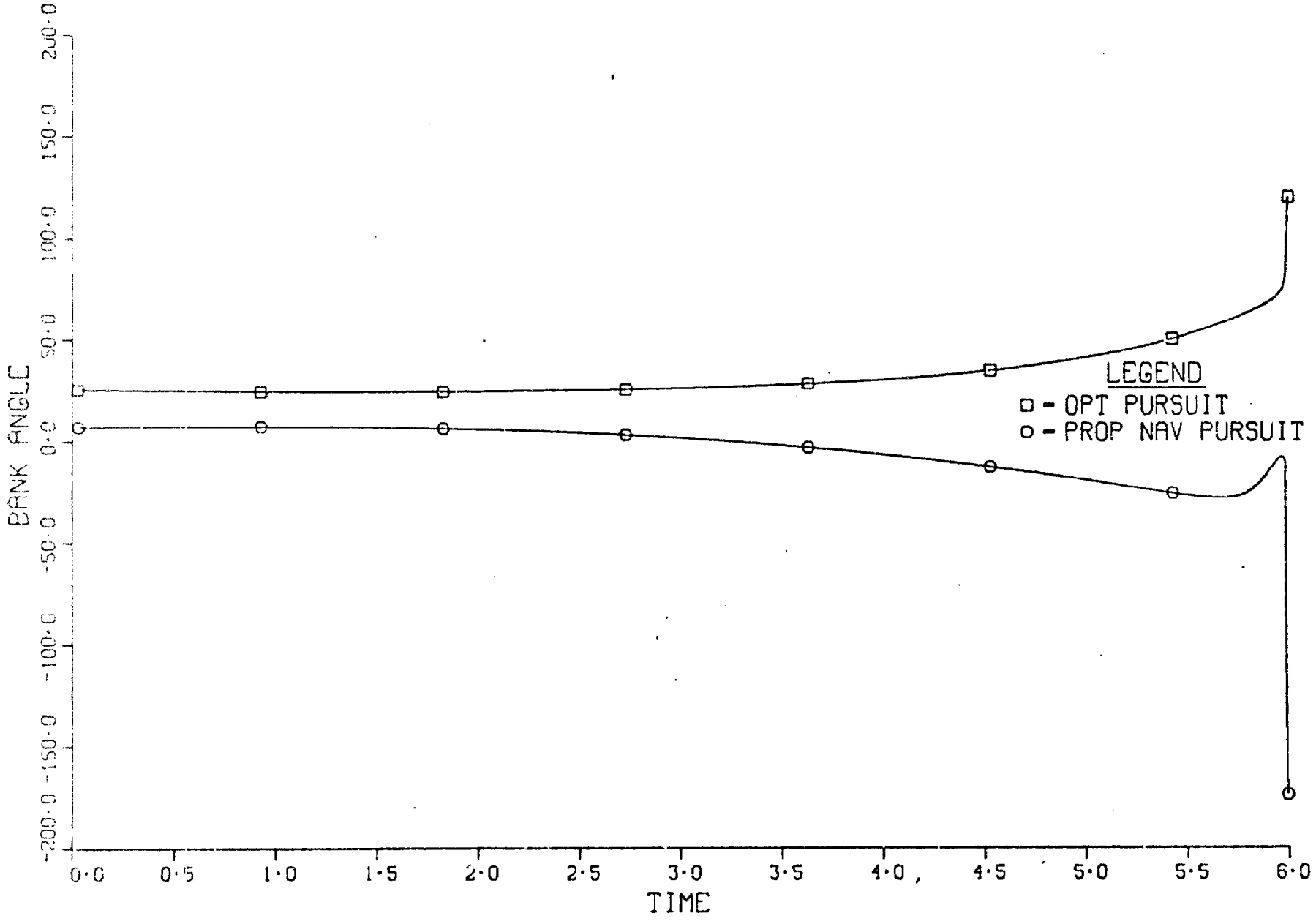

FIG. 29

OPT EVASION-PROP NAV PURSUIT

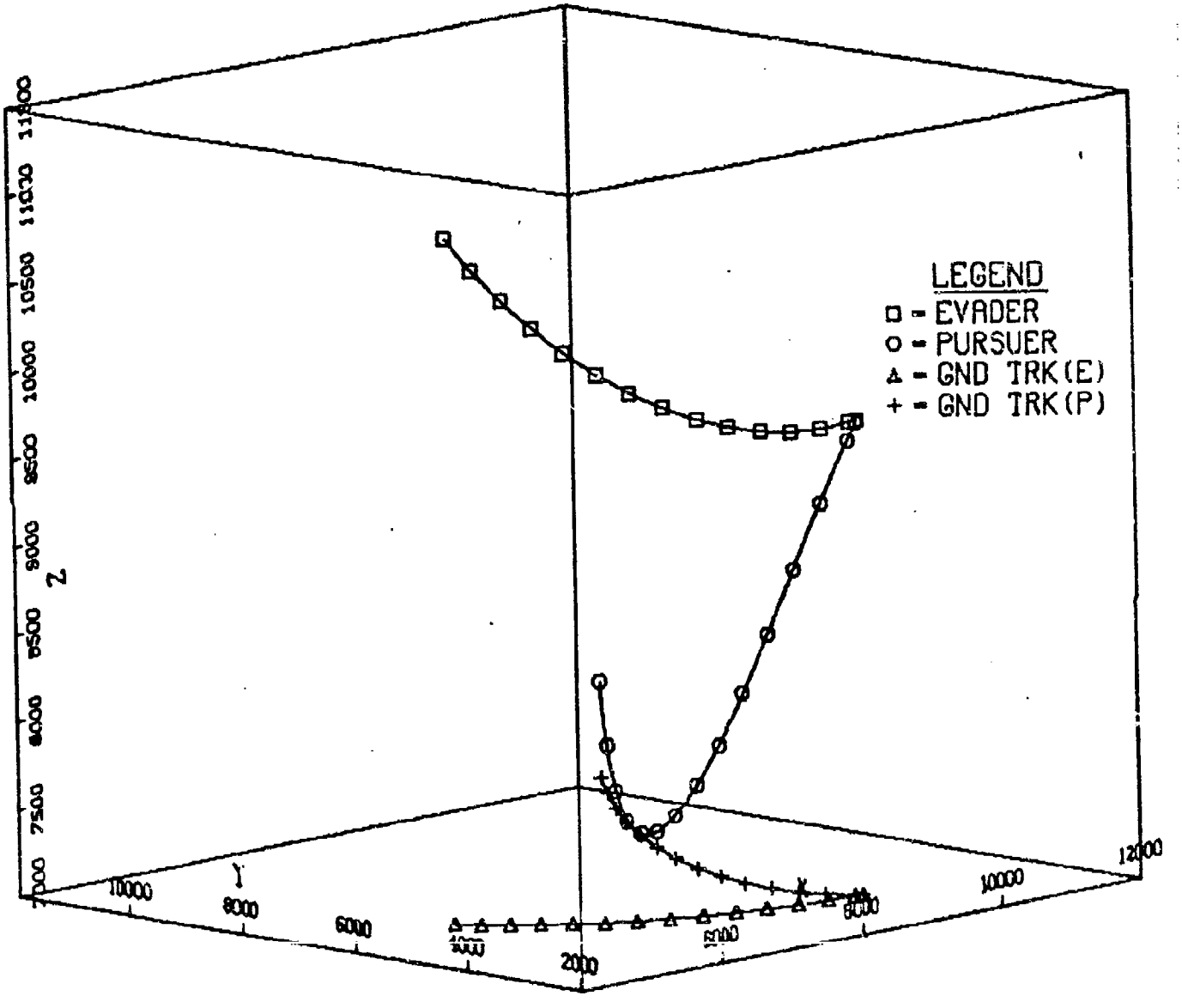

Fig. 30

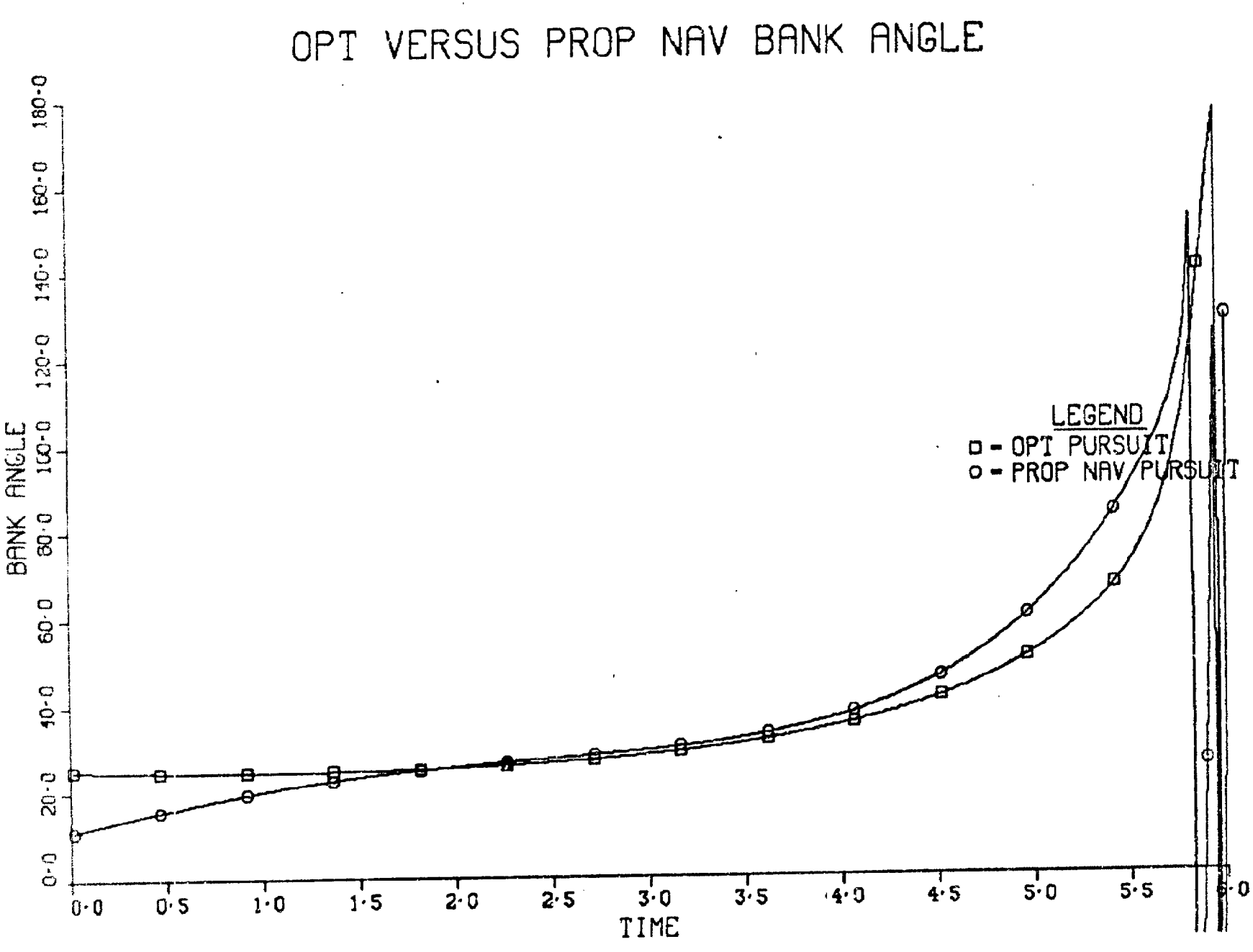
OPT VERSUS PROP NAV BANK ANGLE
BANK ANGLE
0·0
20·0
40·0
60·0
80·0
100·0
120·0
140·0
160·0
180·0
0·0
0·5
1·0
1·5
2·0
2·5
3·0
3·5
4·0
4·5
5·0
5·5
6·0
TIME
LEGEND
□ = OPT PURSUIT
○ = PROP NAV PURSUIT

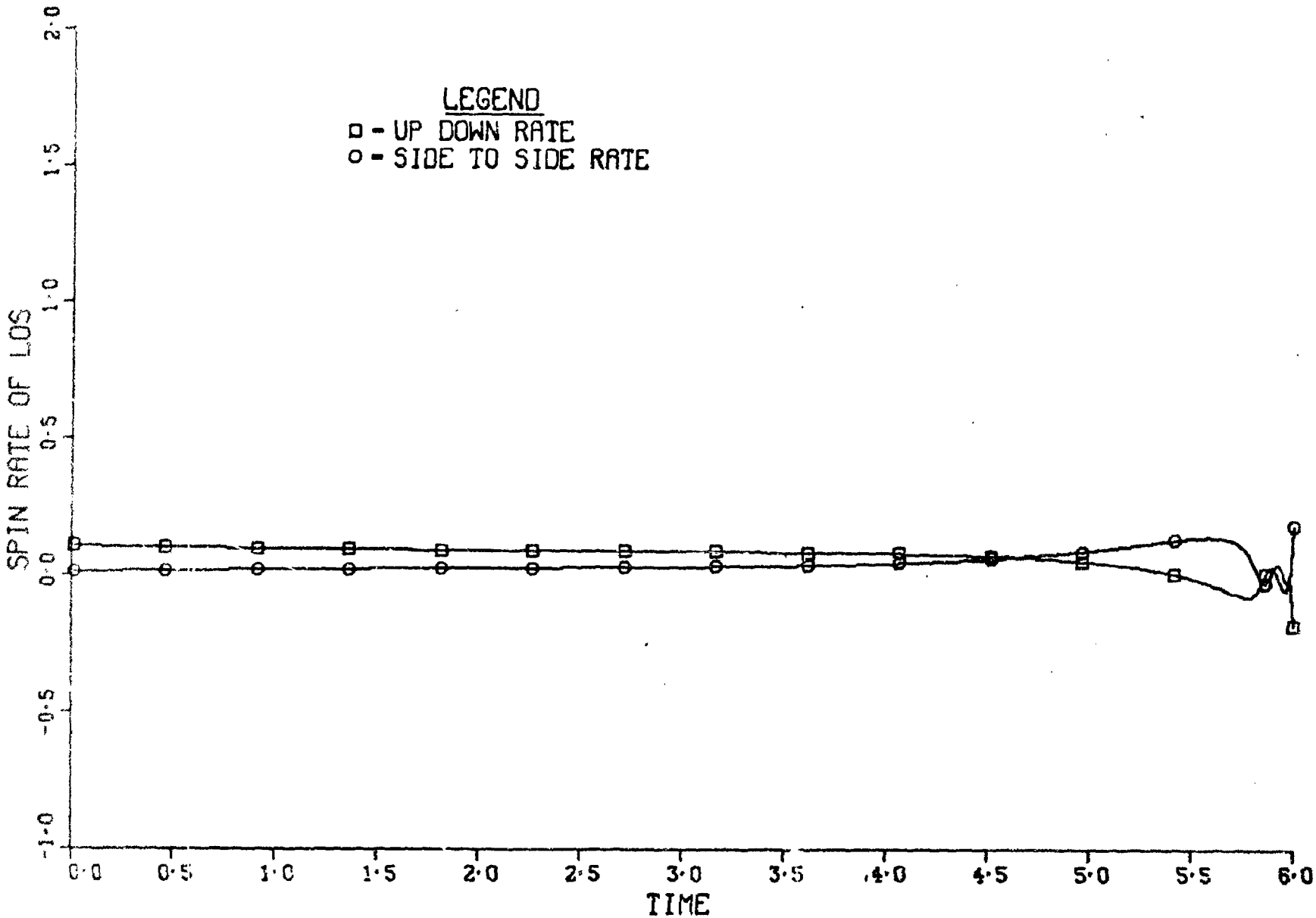
LOS ANGLE RATES
LEGEND
□ - UP DOWN RATE
○ - SIDE TO SIDE RATE
SPIN RATE OF LOS
2·0
1·5
1·0
0·5
0·0
-0·5
-1·0
0·0
0·5
1·0
1·5
2·0
2·5
3·0
3·5
4·0
4·5
5·0
5·5
6·0
TIME

Fig 32

Table VI

"OPT" Evasion

	R	TCA	Cost	Error	τ	$\tau_0 - t$
0	4.39	1.14	15	239	6	6
1	31.45	1.10	985	2767	5.74	5.707
2	58.12	1.05	3374	16541	5.49	5.414
3	56	1.00	3131	129	5.24	5.121
4	68.9	.97	4747	196	4.97	4.828
5	79.5	.94	6329	259	4.70	4.535
6	88.3	.90	7795	304	4.43	4.242
7	95.5	.88	9125	268	4.16	3.949
8	101.7	.85	10337	25	3.88	3.656
9	107.1	.82	11467	48	3.61	3.363
10	112.1	.80	12560	55	3.327	3.070
11	116.9	.77	13661	31	3.04	2.777
12	121.7	.75	14811	22	2.76	2.484
13	126.6	.73	16039	21	2.47	2.191
14	131.7	.70	17363	7	2.19	1.898
15	137.1	.68	18748	33	1.90	1.605
16	142.7	.66	20362	386	1.62	1.313
17	150.3	.63	22584	228	1.33	1.019
18	160.8	.63	25860	24	1.02	.726
19	171.1	.65	29289	226	.71	.433
20	178.3	.66	31791	80	.41	.140
21	180.1	.66	32442	2	.11	-.152
22	180.2	.65	32464		0	-.445

OPT EVASION-PROP NAV PURSUIT

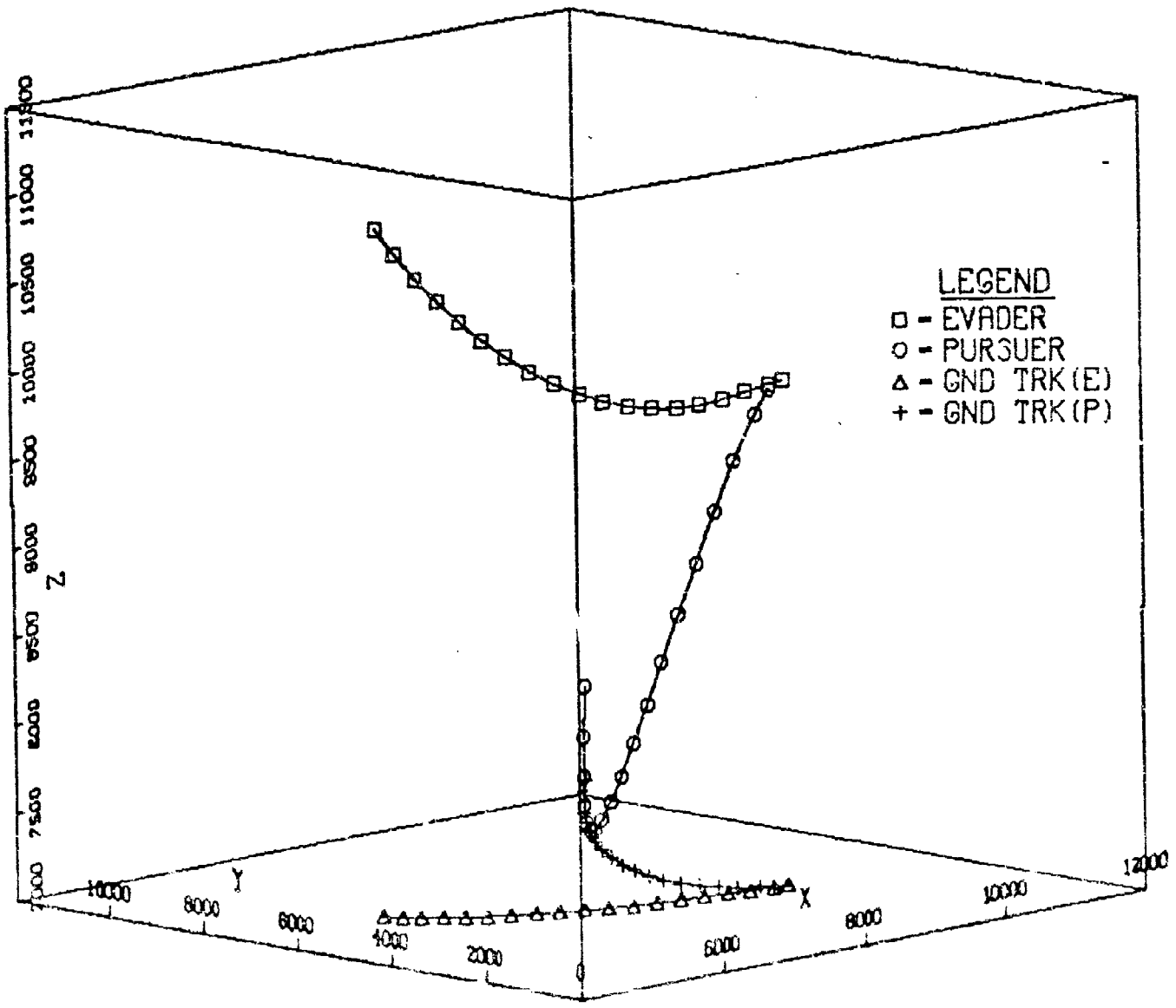

Fig. 33

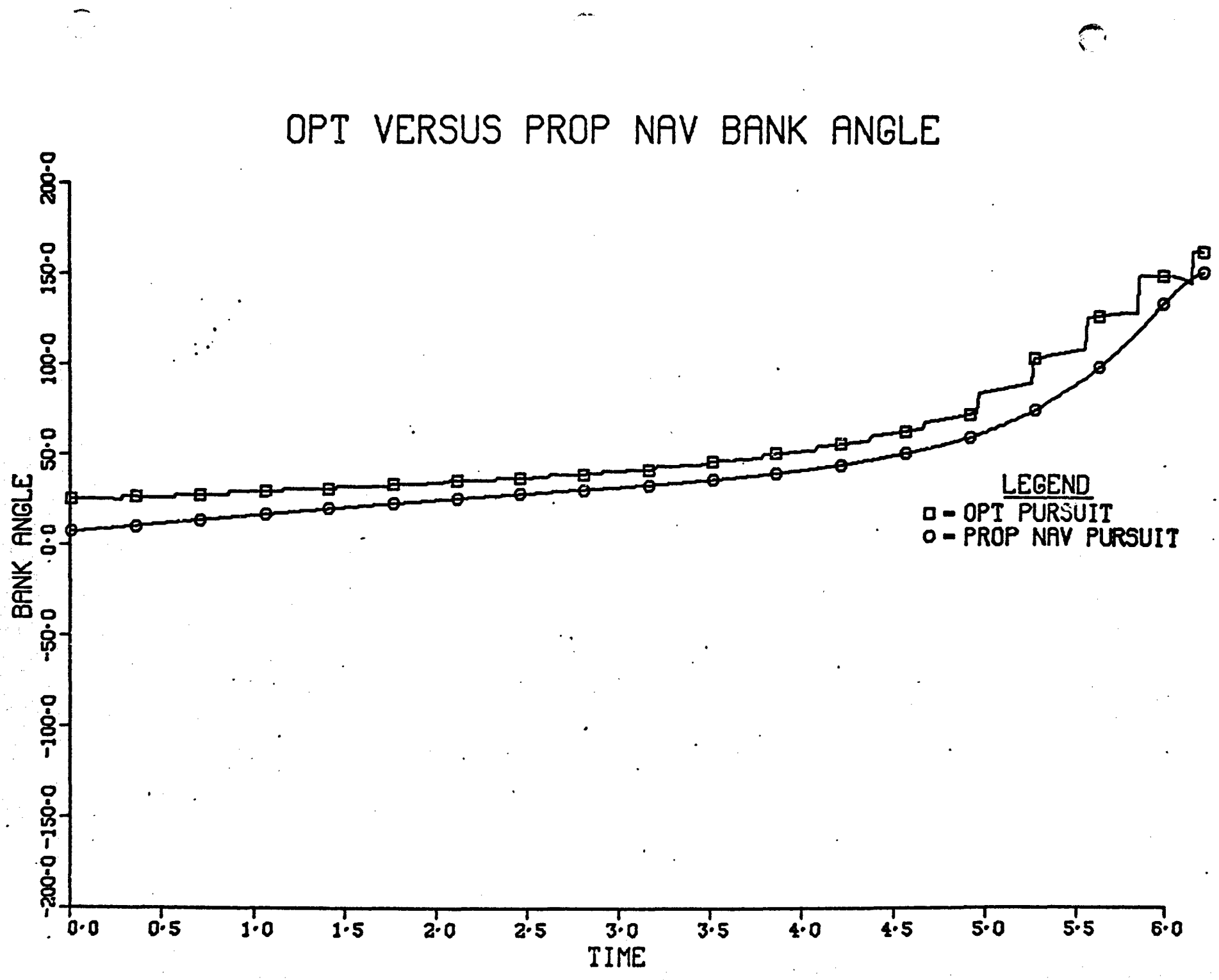
OPT VERSUS PROP NAV BANK ANGLE
BANK ANGLE
200·0
150·0
100·0
50·0
0·0
-50·0
-100·0
-150·0
-200·0
0·0
0·5
1·0
1·5
2·0
2·5
3·0
3·5
4·0
4·5
5·0
5·5
6·0
TIME
LEGEND
□ = OPT PURSUIT
○ = PROP NAV PURSUIT

Fig. 34

Table VII

Evader's Costate History

	λ_x		λ_y		λ_z	
	In	Out	In	Out	In	Out
0	1.99	1.99	1.98	1.98	2.00	2.00
1	1.99	13	1.98	12	2.00	12
2	13	42	12	36	12	30
3	42	71	36	57	39	63
4	71	90	57	67	63	77
5	90	108	67	74	77	89
6	108	123	74	78	89	98
7	123	136	78	80	98	105
8	136	148	80	81	105	111
9	148	160	81	80	111	115
10	160	171	80	78	115	119
11	171	183	78	75	119	122
12	183	195	75	70	122	125
13	195	208	70	64	125	127
14	208	222	64	56	127	128
15	222	237	56	46	128	128
16	237	252	46	31	128	126
17	252	279	31	-14	126	109
18	279	302	-14	-65	109	88
19	309	314	-65	-121	88	61
20	314	311	-121	-169	61	37
21	311	305	-169	-189	37	27

Table VIII

Evader's Costate History

	λ_v		λ_γ		λ_σ	
	In	Out	In	Out	In	Out
0	-12	-12	6518	6518	12453	12453
1	-10	-60	6596	42452	11881	75319
2	-48	-136	42496	134076	71511	223344
3	-104	-140	132856	217525	210976	341921
4	-95	-87	213396	262847	321156	391233
5	-40	-14	255299	294299	365283	416446
6	30	66	283010	313289	386311	422942
7	106	146	298234	320259	389568	413679
8	178	221	301699	318129	378058	394004
9	245	286	296411	308454	356930	366781
10	299	342	384018	292586	328969	334146
11	343	387	265927	271695	296262	297838
12	377	420	243345	246556	260503	258884
13	398	441	217102	217828	222745	218235
14	408	449	187930	186023	183983	176725
15	403	442	156455	151907	145141	135257
16	384	416	123596	117086	107267	95047
17	346	386	91235	77421	71922	41846
18	302	326	57999	42076	30068	515
19	233	241	29536	25017	339	-24454
20	141	141	9261	1491	-13174	-26901
21	39	39	696	-168	-6844	-8703

Table IX

"OPT" Pursuit

Update	$R(t_f)$	TCA	Cost	Error	τ	$\tau_0 - t$
0	4.4	1.14	151	239	6	6
1	27	1.22	780	4931	5.64	5.707
2	44	1.4	2003	11645	5.2	5.414
3	8.6	1.55	73	3752	4.8	5.121
4	17.4	1.55	303	2086	4.41	4.828
5	1.19	1.49	.64	2109	4.07	4.535
6	4.18	1.46	16.49	1995	3.72	4.242
7	1.40	1.6	2.67	825	3.17	3.949
8	2.5	1.87	9.26	254	2.69	3.656
9	.95	2.01	5.17	65	2.31	3.363
10	9.04	2.01	85.9	390	2.02	3.070
11	6.942	2.06	52.9	37[illegible]	1.70	2.777
12	4.8	2.06	27.9	195	1.41	2.484
13	1.91	2.06	8.39	36	1.12	2.191
14	5.66	2.06	36.8	191	.828	1.898
15	6.19	2.07	43.2	202	.532	1.605
16	6.33	2.08	45.	220	.239	1.313
17	13.03	2.08	164	-	0	1.019

NON OPT EVASION-OPT PURSUIT

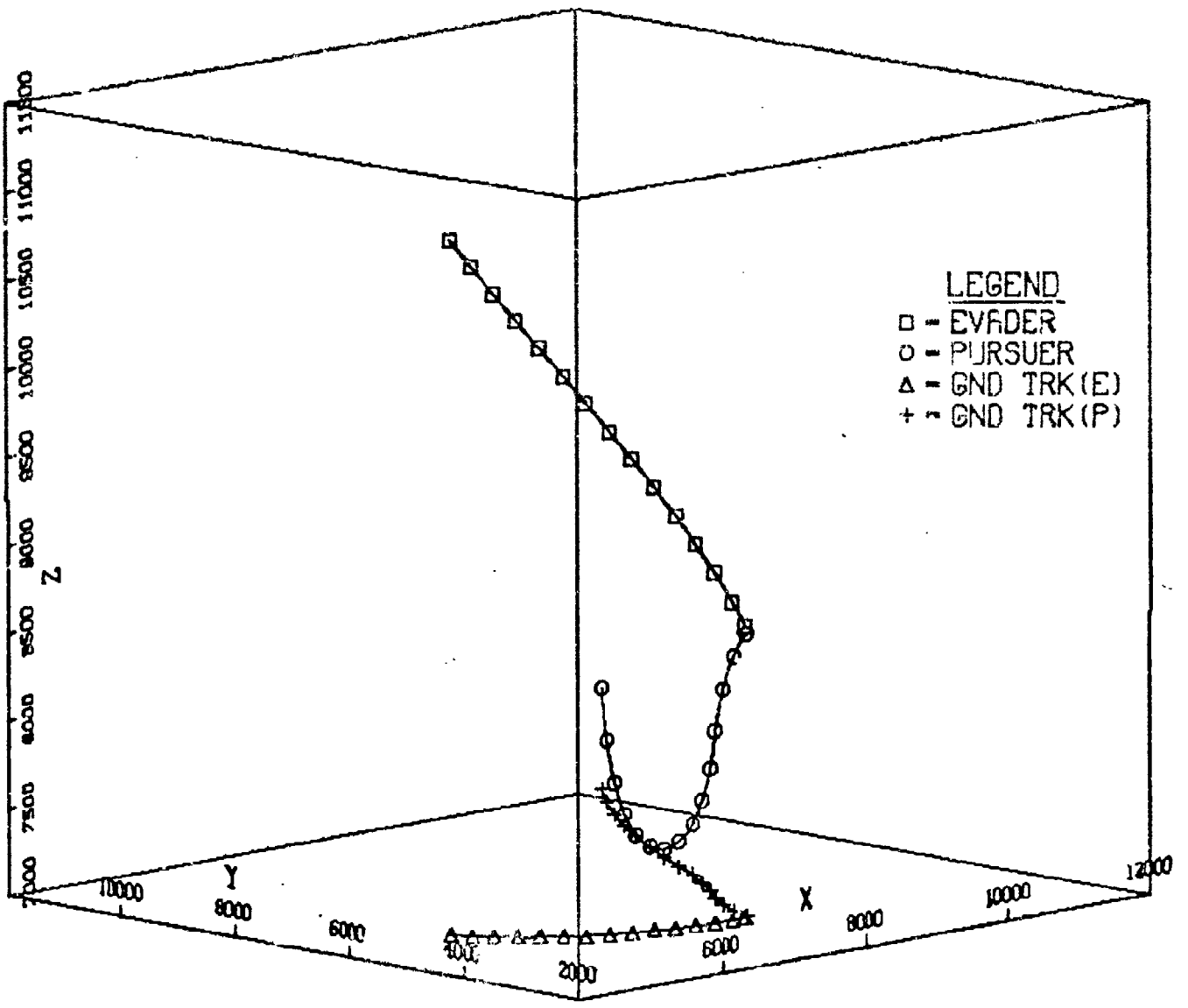

Fig. 35

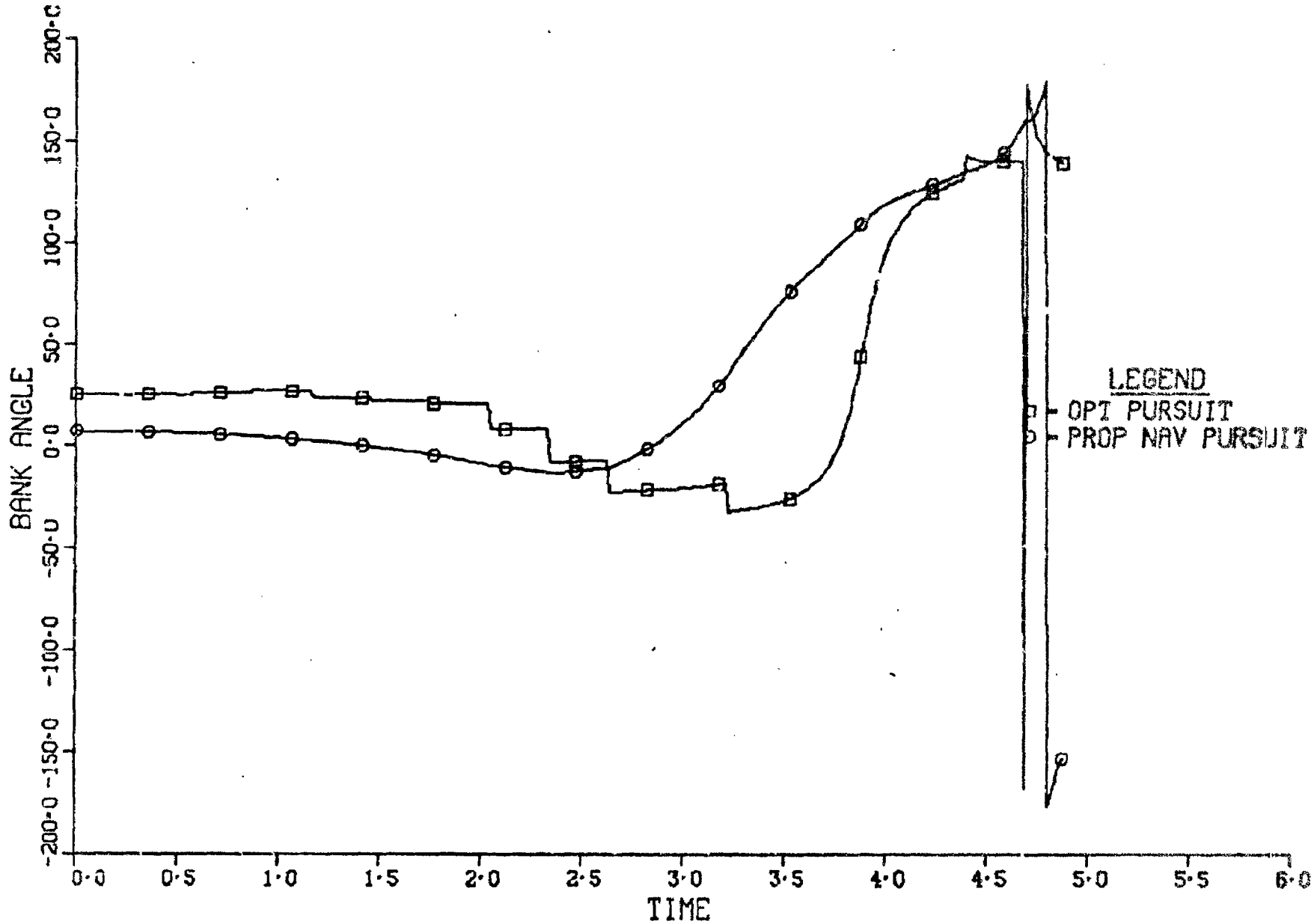
OPT VERSUS PROP NAV BANK ANGLE
BANK ANGLE
200·0
150·0
100·0
50·0
0·0
-50·0
-100·0
-150·0
-200·0
0·0
0·5
1·0
1·5
2·0
2·5
3·0
3·5
4·0
4·5
5·0
5·5
6·0
TIME
LEGEND
OPT PURSUIT
PROP NAV PURSUIT

Fig. 36

NON OPT EVASION-PROP NAV PURSUIT

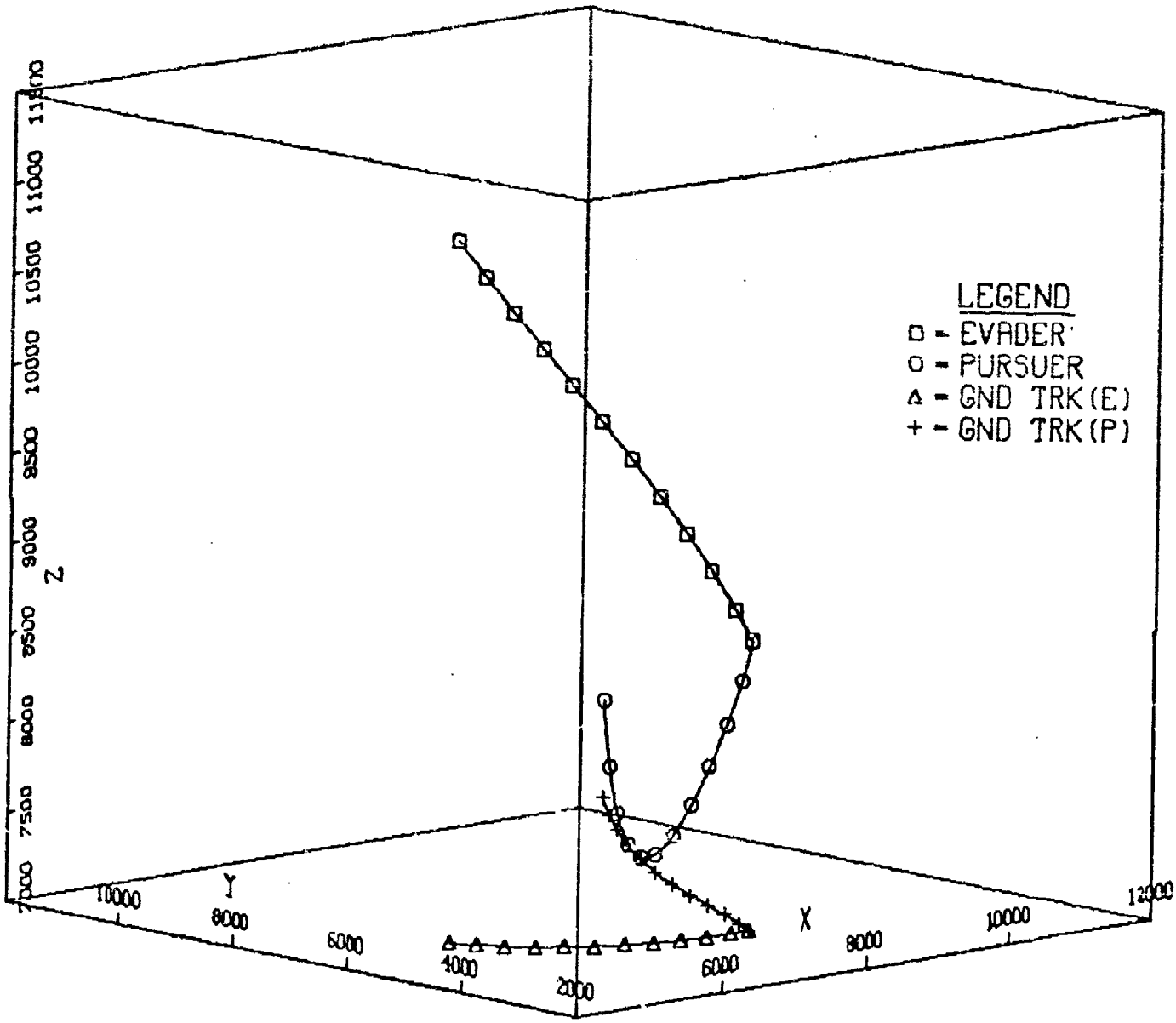

Fig. 37

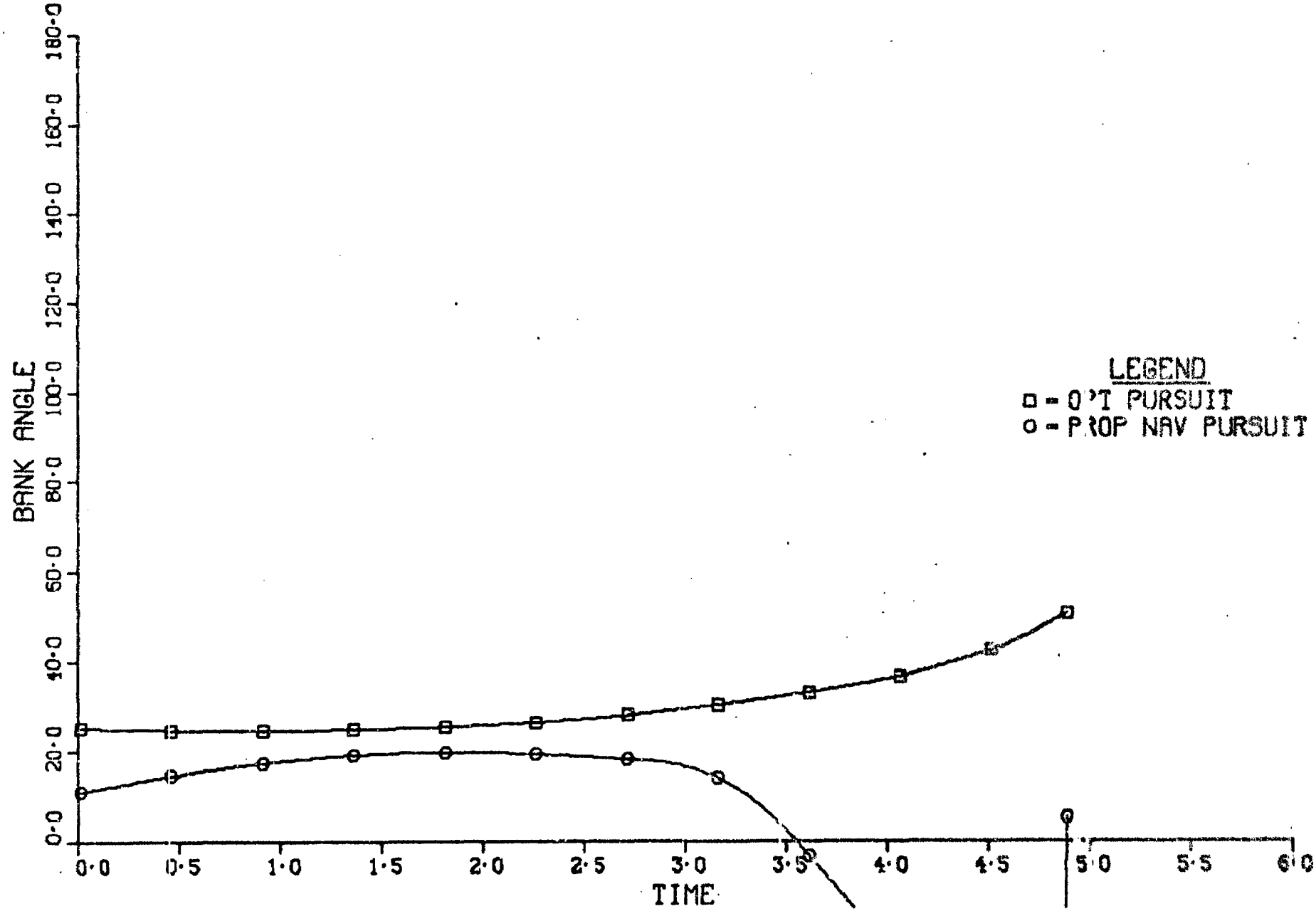
OPT VERSUS PROP NAV BANK ANGLE
BANK ANGLE
0·0
20·0
40·0
60·0
80·0
100·0
120·0
140·0
160·0
180·0
0·0
0·5
1·0
1·5
2·0
2·5
3·0
3·5
4·0
4·5
5·0
5·5
6·0
TIME
LEGEND
□ = O'T PURSUIT
o = PROP NAV PURSUIT

Fig. 38

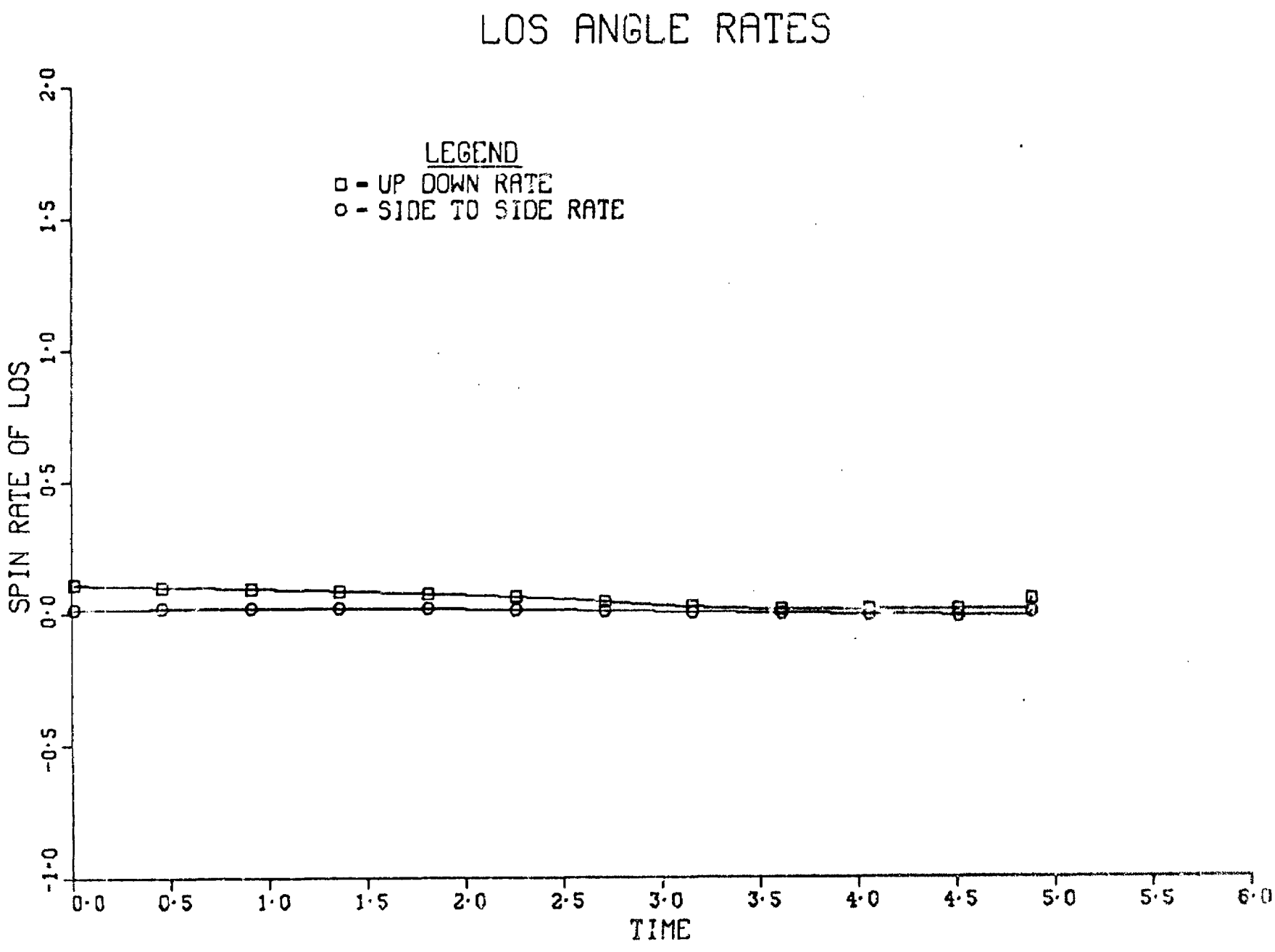
LOS ANGLE RATES
LEGEND
□ - UP DOWN RATE
○ - SIDE TO SIDE RATE
SPIN RATE OF LOS
2·0
1·5
1·0
0·5
0·0
-0·5
-1·0
0·0
0·5
1·0
1·5
2·0
2·5
3·0
3·5
4·0
4·5
5·0
5·5
6·0
TIME

Fig. 39

Table X

"OPT" Evasion

	R	TCA	Cost	Error	τ	$\tau_0 - t$
0	1.76	.086	-6.85	18	6	6
1	11.8	.04	131	2205	5.77	5.765
2	12.7	.06	151	1357	5.56	5.531
3	10.0	.06	90	295	5.38	5.296
4	11.6	.05	124	105	5.2	5.063
5	15.5	.05	232	421	4.99	4.828
6	15.0	.05	216	176	4.81	4.593
7	15.9	.04	245	184	4.61	4.359
8	16.9	.04	277	141	4.41	4.125
9	17.2	.05	287	112	4.21	3.891
10	17.5	.05	297	141	4.00	3.656
11	17.6	.05	302	219	3.78	3.422
12	17.7	.06	304	15	3.56	3.188
13	17.7	.05	304	249	3.32	2.953
14	17.7	.06	304	136	3.09	2.719
15	17.8	.06	307	6	2.86	2.484
16	18.0	.06	315	291	2.62	2.250
17	18.3	.06	3256	17	2.39	2.016
18	18.7	.06	340	68	2.16	1.781
19	19.1	.06	353	200	1.92	1.547
20	19.3	.07	362	257	1.69	1.313
21	19.8	.07	382	265	1.46	1.078
22	19.4	.07	368	176	1.23	.844
23	19.8	.07	381	242	1.00	.609
24	21.	.07	432	287	.76	.375
25	21.4	.07	448	281	.52	.141
26	21.9	.06	472	235	.29	-.094

Table XI

"OPT" Evasion

	R	TCA	Cost	Error	τ	$\tau_0 - t$
0	1.73	1.12	-1.3	.5	6	6
1	86.8	1.06	7529	34742	5.82	5.765
2	164	1.03	27127	104577	5.65	5.531
3	125	.968	15677	329	5.53	5.296
4	159	.917	25455	369	5.37	5.063
5	190	.868	36282	30	5.20	4.828
6	218	.820	47579	86	5.02	4.593
7	242	.775	58881	84	4.83	4.359
8	264.2	.732	69819	148	4.64	4.125
9	283	.693	80106	297	4.44	3.891
10	299	.657	89522	75	4.23	3.656
11	312	.625	97911	130	4.02	3.422
12	324	.598	105179	67	3.80	3.188
13	333	.577	111295	260	3.56	2.953
14	341	.56	116291	120	3.31	2.719
15	346	.55	120242	8	3.07	2.484
16	351	.54	123256	117	2.82	2.250
17	354	.54	125443	28	2.57	2.016
18	356	.53	126920	189	2.32	1.781
19	357	.53	127806	172	2.07	1.547
20	358	.53	128231	157	1.82	1.313
21	358	.53	128350	43	1.59	1.078
22	358	.53	128362	7	1.35	.844
23	359	.53	128540	104	1.12	.609
24	359	.52	129242	25	.91	.375
25	361	.51	130932	1	.69	.141
26	366	.48	133954	39	.48	-.094
27	371	.45	137871	204	25	-.328

Appendix B

Numerical Aspects

TPBVP Solution Method

A saddle point solution to a differential game formulation is defined by a two point boundary value problem in the form

$$\begin{aligned} \dot{x} &= f(x,\lambda,t) \qquad x(t_0) = x_0 \\ \dot{\lambda} &= g(x, \ ,t) \qquad (t_f) = \phi_x\Big|_{t_f} \\ t_f &= \text{free} \qquad\quad H(t_f) = -\phi_t\Big|_{t_f} \end{aligned} \tag{B-1}$$

where there are n+1 unknowns at t_0, namely $\lambda(t_0)$ and t_f and at some time t_f there are n+1 relationships that must hold. The problem could be more generally stated as follows

$$F(x) = 0 \tag{B-2}$$

where x = estimates of n+1 unknowns in Eqs (B-1) and the vector function F represents the relationships that must hold to some acceptable degree of accuracy at time t_f. The solution of Eq (B-2) provides the appropriate unknowns at time t_0 such that if both players play optimally throughout, the terminal conditions for the game will be met. Evalpation of F requires integration of the system dynamics using some present estimate of the $\lambda(t_0)$ for a period $(t_f - t_0)$, given a current estimate of the final time t_f. Now consider

the minimization of the scalar cost function

$$\min_{x} F^T(x)F(x) = J^* \tag{B-3}$$

The first order necessary conditions are

$$\frac{\partial J^*}{\partial x} = \underline{0} = 2F^T F_x \tag{B-4}$$

the solution of which is either

$$\begin{aligned} F^T &= 0^T \\ F_x &= [0] \end{aligned} \tag{B-5}$$

Another solution exists when F_x is singular for some $F \neq 0$. Using these three possible solutions together with Eq (B-3) the three solutions can be separately identified as follows

$$\text{(a)} \quad F^T(x)F(x) \leq \varepsilon \tag{B-6}$$

$$\text{(b)} \quad F^T F > kF^T F_x \tag{B-7}$$

$$\text{(c)} \quad |F_x| = 0 \tag{B-8}$$

In (a) the solution of Eq (B-2) has been achieved to within ε. In (b) the gradient of F, F_x is such as to predict a very large step δ in a Newton-Raphson search for the minima of $F^T F$. The constant k allows some control over what is and what is not an acceptably large step. Normally in gradient search techniques a singular matrix F_x precludes finding the gradient direction unless the generalized inverse of F_x is used.

A Fortran subroutine published at Ref 10 searches for a solution to Eq (B-2) until F^TF is less than some ε, which is part of the calling parameters. It initially estimates F_x by numerical differentiation using a user supplied step size and after taking the inverse of F_x thereafter uses approximations of F_x^{-1} based on the steps it takes in the search. Should the gradient scheme define an unacceptably large step, as controlled by k in Eq (B-7), then control is returned to the calling program. By continuously approximating F_x^{-1} then the problems associated with Eq (B-8) are avoided.

Since the scheme uses an approximation to F_x^{-1} it tends to take cautious steps in the search for a solution so that the assumptions in making the approximation are not violated. Changes in this step size are made if the predicted value of $F(x+\delta)$ and the actual value are either very close in which case Δ the step size is increased or wildly different in which case Δ is reduced. In the algorithm the Newton-Raphson step is calculated and if this is less than or equal to Δ it is used directly. If this is not the case the algorithm predicts the optimum step size in the direction of steepest descent assuming that it is searching on a quadratic surface. This step size is compared with Δ as before. Should neither steepest descent nor Newton-Raphson predict a step size less than Δ a combination is used to calculate a step of Δ in a direction somewhere between the two.

Because the scheme has a pseudo cost function F^TF which has a minima at the solution of $F(x) = 0$, it retains the value of x that has produced the smallest value of F^TF and on an error return to the calling program usually returns this "best" value of x no matter how far away the current estimate of x may be.

This then is the algorithm that has been used throughout to solve the two point boundary value problems that represent the saddle point solution.

Numerical Problems

The Hamiltonian in the game formulation was independent of time and hence

$$\frac{dH}{dt} = \frac{\partial H^T}{\partial x}\frac{dx}{dt} + \frac{\partial H^T}{\partial \lambda}\frac{d\lambda}{dt} + \frac{\partial H}{\partial t}$$

$$= \frac{\partial H^T}{\partial x} f + f^T \frac{d\lambda}{dt} + \frac{\partial H}{\partial t}$$

$$= -\dot{\lambda}^T f + f^T \dot{\lambda} = 0 \qquad \text{(B-9)}$$

The Hamiltonian at final time was zero and hence should have remained so. When a set of states, representing the termination of a differential game with a miss of 100 feet in each direction, was integrated backwards in time, the Hamiltonian oscillated rapidly and then gradually settled at some value. The differential game was coded in an unnormalized form, that is positions in feet, velocities in feet per second, etc. Even when the integration step size of 5 μsec was used

and the Hamiltonian oscillated, but to much smaller limits than previously, the trouble seemed to lie in the integration and not the equations being integrated. The integration routine used was a 4th order Runge-Kutta to start and thereafter a 4th order predictor-corrector. The choice of fixed or variable step size could be made in the calling parameters. For a variable step size the routine would increase or decrease the step size as necessary to keep the error bound below some given value. As the step size required changing the scheme would use Runge-Kutta to start afresh before moving to predictor-corrector integration. It was noticed that it was always the Runge-Kutta steps that produced the oscillation which would then settle down considerably during predictor-corrector integration. When, in variable step size mode, the Runge-Kutta scheme was used to start afresh after each change of step size, back came the oscillations. With a miss distance of some 176 feet the values of $\lambda_\gamma(t_f)$ and $\lambda_\sigma(t_f)$ would lie between +10 and -10 but their slopes would be of the order 1.E5. Since the states and costates were being integrated by a single routine the range of slopes that the one routine had to handle was from -1E5 to +1E5. The value of $\dot{\lambda}_\gamma$ was largely determined by such terms as $\lambda_\chi \cdot v$ where λ_x was 200 and v was 800.

The expression for $\dot{\lambda}_\gamma$ contained λ_γ, λ_v and λ_σ. Both $\dot{\lambda}_\sigma$ and $\dot{\lambda}_v$ contained terms in λ_γ so that

$$\dot{\lambda}_\gamma = A\lambda_\gamma + B\lambda_\sigma + C\lambda_v + \ldots \quad \text{(B-10)}$$

$$\dot{\lambda}_\sigma = D\lambda_\gamma + \ldots \quad \text{(B-11)}$$

$$\dot{\lambda}_v = E\lambda_\gamma + \ldots \quad \text{(B-12)}$$

and thus

$$\ddot{\lambda}_\gamma = (A^2+BD+CE)\lambda_\gamma + \ldots \quad \text{(B-13)}$$

and further differentiation would not separate the costates. However it does show that an exponential form of the homogeneous solution could contribute the stiffness seen in integrating the costate equations.

That the trouble was largely independent of the large value of the slopes could be seen later in the integration where the slopes were still in the range 1E5 but the Hamiltonian had more or less stabilized and despite the error generated initially was stable to 3 or 4 significant digits.

By splitting the integration of the state equations into two phases good results were achieved and if the integration procedure was reversed the original states could be returned to, within about 6 or 7 significant digits on a 15 digit machine. The total time was divided into 256 steps and the last 6 steps were further subdivided into 200.

This gave a very fine step size around the final time and an acceptably coarse step size away from t_f which kept the time spent on integration as small as possible without

sacrificing accuracy. When integrating forward into t_f the points in time at which Runge-Kutta steps were taken would be different from the points when integrating away from t_f thus causing differences. The values of the states and costates achieved by integrating away from t_f were therefore used as an initial guess for the two point boundary value problem, and when subroutine NS01A had reduced the errors in the transversality conditions to some prespecified level it was found that the terminal state had changed slightly.

For the situation where the missile hit the aircraft the values of the terms A, B, C, D and E in Eq (B-13) were such that the Hamiltonian remained at 2.E-14 throughout the integration.

Vita

Robin Poulter was born in Sunderland, C° Durham, England, on 9 February 1946. He was educated at the Duke of York School, Nairobi, Kenya, and Drax Grammar School, Selby, Yorkshire, before entering the Royal Air Force in September 1964. He graduated from the Royal Air Force College with a B.Sc.(Hons) in Aeronautical Engineering in April 1969. Prior to attending AFIT he served as a project officer for the Royal Air Force on Secondary Radar Systems at the Royal Radar Establishment, Malvern, Worcestershire, England.